Russian Original Vol. 41, No. 6, December, 1976

June, 1977

SATEAZ 41(6) 1037-1136 (1976)

SOVIET ATOMIC ENERGY

АТОМНАЯ ЭНЕРГИЯ
(ATOMNAYA ÉNERGIYA)

TRANSLATED FROM RUSSIAN

CONSULTANTS BUREAU, NEW YORK

SOVIET ATOMIC ENERGY

Soviet Atomic Energy is a cover-to-cover translation of *Atomnaya Énergiya*, a publication of the Academy of Sciences of the USSR.

An agreement with the Copyright Agency of the USSR (VAAP) makes available both advance copies of the Russian journal and original glossy photographs and artwork. This serves to decrease the necessary time lag between publication of the original and publication of the translation and helps to improve the quality of the latter. The translation began with the first issue of the Russian journal.

Consultants Bureau journals appear about six months after the publication of the original Russian issue. For bibliographic accuracy, the English issue published by Consultants Bureau carries the same number and date as the original Russian from which it was translated. For example, a Russian issue published in December will appear in a Consultants Bureau English translation about the following June, but the translation issue will carry the December date. When ordering any volume or particular issue of a Consultants Bureau journal, please specify the date and, where applicable, the volume and issue numbers of the original Russian. The material you will receive will be a translation of that Russian volume or issue.

Subscription
$117.50 per volume (6 Issues)
2 volumes per year

Single Issue: $50
Single Article: $7.50

Prices somewhat higher outside the United States.

CONSULTANTS BUREAU, NEW YORK AND LONDON

227 West 17th Street
New York, New York 10011

Published monthly. Second-class postage paid at Jamaica, New York 11431.

Soviet Atomic Energy is abstracted or indexed in *Applied Mechanics Reviews, Chemical Abstracts, Engineering Index, INSPEC—Physics Abstracts and Electrical and Electronics Abstracts, Current Contents,* and *Nuclear Science Abstracts.*

SOVIET ATOMIC ENERGY

A translation of *Atomnaya Énergiya*

June, 1977

Volume 41, Number 6 December, 1976

CONTENTS

CONTENTS

(continued)

CONTENTS

(continued)

Engl./Russ.

The Russian press date (podpisano k pechati) of this issue was 11/23/1976. Publication therefore did not occur prior to this date, but must be assumed to have taken place reasonably soon thereafter.

ARTICLES

AN INVESTIGATION OF RESONANCE ABSORPTION OF NEUTRONS IN RBMK-TYPE GRID

L. N. Yuroba, A. V. Bushuev, A. F. Kozhin, M. B. Egiazarov, and P. M. Kamanin

UDC 539.125.5.173.162.3

The object of the present work is to obtain experimental data that would characterize the absorption of resonance neutrons in grids of RBMK type of the Leningrad Atomic Power Station.

The computation of resonance absorption in such strongly hetrogeneous grids is a very complicated problem. The difficulties are associated with the consideration of not only energy but also the spatial distribution of the flux of retarded neutrons. The presence of strong intrachannel retardation leads to a noticeable spatial inhomogenity of the field of resonance neutrons in the cell. One of the possible directions in searching for the solution of this problem is an experimental measurement of these dependences on the models of the active zone of a reactor. The variation of the concentration of hydrogen in a hetrogeneous water film may have an effect on the physical process in the intermediate thermal region of the neutron energy. Therefore, the integral parameters ρ^{28}, $\langle \sigma_c^{28} \rangle / \langle \sigma_f^{25} \rangle$, which are sensitive to this region of the neutron spectrum and also the effective resonance absorption integral I_{eff}^{28} were measured.

In the present work we describe the experiments carried out by two experimental groups on RBMK-type grids and present their results. The dimensions of the experimental assemblies, parameters of the fuel cassettes, and the procedures of measurements somewhat differ but the results were close, which permitted us to arrive at consistent conclusions.

The height of one of the experimental assemblies of 25 cells in an RBMK-type reactor was 2 m. Cassettes of cylindrical form were placed in graphite stack with 25-cm steps. The fuel elements were prepared from aluminum tubes (13.5 × 0.65 mm), and filled with tablets of natural uranium dioxide with a density of 10.2 g/cm^3 and diameter 12.15 mm (see Fig. 1).

A neutron beam from the horizontal experimental channel of the IRT-2000 reactor served as the source for the subcritical assembly. The beam was directed along the hollow channel into the depth of a 1-m-high graphite prism, which served as the base of the assembly and was used for forming spatial–energy distribution of neutrons entering into the assembly.

The axial distribution of neutrons in the assembly was measured by copper foils and Si – ^{235}U semiconductor detectors with cadmium coating and without it. The upper and lower boundaries of the region of asymptotic spectrum of neutrons were determined and the location for subsequent experiments along the height was determined. The cadmium ratios for reaction ^{238}U (n, γ) in cassettes placed at the center of the assembly in the second and the end rows were determined at this height. The values of cadmium ratios coincided within the errors of measurements (± 1.5%). This permitted the conclusion that the leakage of neutrons does not effect the results of measurements of R_{Cd}^{28}, ρ^{28}, I_{eff}^{28} at the center of the assembly and the obtained values correspond to the parameters of an infinite array within the indicated errors.

The parameters were measured with the use of indicators of about 1 mm in thickness prepared from standard UO_2 tablets filling the fuel elements. During the experiments, the indicators were placed in detachable fuel elements, which were mounted in an experimental cassette in the place of the ordinary fuel elements. In the measurements of the rate of reaction ^{238}U(n,γ) for resonance neutrons, a cadmium screen of 0.5 mm thick-

Translated from Atomnaya Énergiya, Vol. 41, No. 6, pp. 387-391, December, 1976. Original article submitted July 16, 1975; revision submitted April 30, 1976.

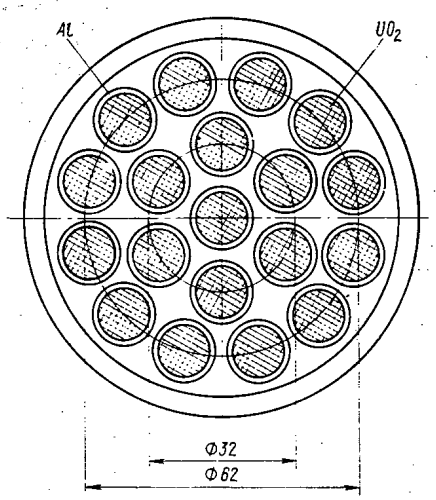

Fig. 1. The transverse cross section of the channel with cassette.

TABLE 1. Values of the Parameters Occurring in Formulas (2) and (3).

Parameter	Value	Source of information
I_{∞}^{28}, b	275±5	[5]
K_{st}^{bl}	0,3150±0,0054	[3]
S_i (d = 1mm)	1,335±0,005	Experiment
S_{st} (d = 0.1mm)	1,045±0,004 0,993±0,003 (w/o water) 0,996±0,003 (with water)	[3]
Φ_{st}/Φ_i		Experiment
$f(E)$	9,983 (w/o water) 0,995 (with water)	Computed by N. I. Belousov MIFI

TABLE 2. Results of Experiments

Medium around fuel element	Arrangement of fuel elements	$K_i \cdot 10^2$	I_{eff}^{28}, b	$K_{e_i} = \frac{K_i}{K_0}$	$\frac{K_{e_i}\text{ (with water)}}{K_{e_i}\text{ (w/o water)}}$
Graphite	Single fuel element	7,50±0,22	20,6±0,7	1,0	—
Air	Row 1	5,52±0,16	15,2±0,5	0,736±0,007	—
	Row 2	4,51±0,13	12,4±0,4	0,601±0,014	
	Row 3	4,60±0,12	12,7±0,4	0,613±0,020	
	Value average for cassette	5,16±0,15	14,2±0,5	0,688±0,010	—
Water	Row 1	5,65±0,13	15,5±0,5	0,753±0,028	1,02±0,04
	Row 2	4,90±0,13	13,5±0,4	0,653±0,026	1,09±0,04
	Row 3	4,93±0,12	13,5±0,4	0,657±0,025	1,07±0,04
	Value average for cassette	5,37±0,13	14,8±0,4	0,716±0,027	1,04±0,04

ness was used. The results of [1, 2], in which means of decreasing the effect of cadmium on the results of measurement are indicated, were taken into consideration in choosing the scheme for arranging the indicator.

The standard method was used for determining I_{eff}^{28}. The desired quantity was obtained by comparing the rates of reaction in the indicator irradiated in the fuel elements of the cassette and in a uranium metallic foil standard irradiated in the retarder at the distance of 10 cm from the cassette where the spectrum of epicad-

TABLE 3. Results of Measurements with the Second Assembly

Medium around fuel element	Arrangement of fuel elements	$I^{28}_{eff\,i}/I^{28}_{eff_{st}}$	I_{eff}, b
Air	Row 1	0,770±0,015	16,2±0,7
	Row 2	0,667±0,015	14,1±0,6
	Row 3	0,648±0,014	13,7±0,6
	Av. value for cassette	0,731±0,015	15,4±0,7
Water	Row 1	0,828±0,016	17,5±0,7
	Row 2	0,717±0,014	15,1±0,7
	Row 3	0,703±0,015	14,8±0,7
	Av. value for cassette	0,786±0,016	16,6±0,7

TABLE 4. Values of Some Parameters in Formula (7)

Parameter	Value	Source of information
$\sigma^{28}_{c_{th}}$, б	2,72±0,02	[5]
$\sigma^{25}_{f_{th}}$, б	582,2±1,3	[5]
g_{25}	0,976±0,002	[7]
$Y^{28}_{Ce}\,Y^{25}_{Ce}$	0,816±0,010	[8]
δ^{28} *	0,034±0,02 (with water) 0,045±0,02 (w/o water)	Expt.

*Ratio of number of fissions in ^{238}U to ^{235}U.

TABLE 5. Values of $\langle \sigma^{28}_c \rangle / \langle \sigma^{25}_f \rangle$ and ρ^{28}

Parameter	Experimental system	Without water	With water
$\langle \sigma^{28}_c \rangle / \langle \sigma^{25}_f \rangle$	Assembly in IRT	$(7,50\pm0,13)\cdot10^{-3}$	$(6,16\pm0,04)\cdot10^{-3}$
	Assembly in F-1	$(7,23\pm0,16)\cdot10^{-3}$	$(6,04\pm0,16)\cdot10^{-3}$
ρ^{28}	Assembly in IRT	0,670±0,025	0,441±0,009

mium neutrons is close to 1/E. The self-blocking coefficients for the standard K^{bl}_{st} were determined experimentally in [3]. The method of determination is based on the measurements of cadmium ratios for the standard R_{st} and a thin uranium sample R_0:

$$K^{bl}_{st} = (R_0 - 1)/(R_{st} - 1). \quad (1)$$

The thin samples were prepared from aluminum foil of 0.1 mm thickness with a layer of natural uranium of 0.25 mg/cm^2 thickness. The corrections for the self-blocking of thin samples and for the difference of the neutron spectrum in the retarder from 1/E spectrum were determined computationally.

The measurements of the intensity of reaction ^{238}U (n, γ) are based on recording of γ radiation of ^{239}Np with an energy of 277 keV. A measuring system with a Ge(Li) detector was used for this purpose. The energy resolution of the system at 277 keV was 2.4 keV.

Due to the unequal distribution of the radioactive nuclei in the sources, i.e., the indicators and the standards, errors may arise due to the different efficiency of recording of γ quanta emitted from different segments of the source. In order to eliminate this effect an absorbing filter of variable thickness was placed between the source and the detector so that the efficiency of recording of γ quanta with an energy of 277 keV was equalized.

From the measurements of the activity of irradiated foil we obtain a_i/a_{st}, the ratio of activities of the indicator irradiated in one of the fuel elements of the cassette and the standard. The effective resonance integral of the fuel element of the i-th row of the cassette was determined from the formula

$$I^{28}_{eff\,i} = I^{28}_{\infty} K_i, \quad (2)$$

where I^{28}_{∞} is the true resonance absorption integral of ^{238}U; K_i are coefficients that take account of the self-blocking of the fuel element and the mutual screening of the fuel elements in the cassette, which were computed from the formula

$$K_i = K^{bl}_{st} \frac{a_i}{a_{st}} \frac{S_i}{S_{ст}} \frac{\Phi_{st}}{\Phi_i} \frac{N_{st}}{N_i} f(E). \quad (3)$$

Here K^{bl}_{st} is the coefficient of self-blocking of the standard; Φ_{st}/Φ_i is the correction taking account of the difference of the neutron fluxes at the locations of the i-th fuel element and the standard caused by the macrodis-

tribution of neutron flux in the assembly; N_{st}/N_i is the ratio of the number of nuclei ^{238}U in the standard and in the indicator; f(E) is the computed correction for the departure of the spectrum of epicadmium neutrons in the retarder from 1/E; S_i and S_{st} are the correction for the self-absorption of γ quanta with an energy of 277 keV in the indicator and the standard. The absorption coefficient of such γ quanta in UO_2 for the given geometry of the measurements was determined experimentally and was 0.60 mm^{-1}. The correction coefficient for the self-absorption was computed from the formula given in [4]. The values of the parameters occurring in formulas (2) and (3) are given in Table 1.

The values of $I^{28}_{eff_i}$ were determined for fuel elements of all the rows of the cassette, and $I^{28}_{eff_0}$ was determined for single fuel element placed at the boundary of the cell. The ratios of $I^{28}_{eff_0}$ and I^{28}_{∞} determine the coefficient of resonance blocking of the capture cross section of ^{238}U in the fuel; K_i and K_0 are, respectively, the coefficients of mutual screening for the fuel elements in the fuel cassette. The effective resonance integral of the fuel cassette was determined from the formula

$$I^{28}_{eff} = \frac{\sum_i n_i I^{28}_{eff_i}}{\sum_i n_i}, \qquad (4)$$

where n_i is the number of fuel elements in the i-th row of the cassette; $I^{28}_{eff_i}$ is the effective resonance integral of the fuel element of the i-th row of the cassette. The results are given in Table 2.

Another series of experiments were conducted on a subcritical assembly of 49 cells mounted in a wide neutron beam (150 × 150 cm) of the F-1 reactor. The height of the assembly was 1.8 m. Cassettes with diameter of the fuel core of the fuel elements equal to 11.0 mm (casing 13.5 × 1.0 mm) were investigated. The region of the asymptotic spectrum was determined by axial and radial measurements with indicators made of ^{238}U, ^{115}In, ^{55}Mn, ^{239}Pu, and ^{235}U in cadmium filters and without them. The experiments showed that within the assembly a region with 120 × 120 × 100 cm dimensions has the asymptotic spectrum of neutrons that is characteristic for this grid. In these experiments the resonance integral was determined from measurement of the relative rate of absorption of epicadmium neutrons in the rods of the cassette and in a single rod placed in the retarder at the boundary of the cell. The value of the resonance integral for the single rod was calculated from the Hellstrand formula. Metallic foil of 10-fold depleted uranium of 0.09 mm thickness were used for the measurements. The rate of capture reaction in ^{238}U was measured on a NaI(Tl) spectrometer from the γ radiation of ^{239}U with an energy of 74 keV. In the analysis of the results corrections were introduced to take account of the small background from the radiation of the fission products. The effective resonance integral for different fuel elements of the cassette was determined from a formula similar to (3):

$$\frac{I^{28}_{eff_i}}{I^{28}_{eff_{st}}} = \frac{a_i}{a_{st}} \frac{\Phi_{st}}{\Phi_i}, \qquad (5)$$

where $I^{28}_{eff_{st}} = 21.1 \pm 0.8$b for a rod of 11 mm diameter (computed from Hellstrand formula).

The resonance integral of the cassette was determined from formula (4). The results are shown in Table 3.

Thus, the following conclusions can be made:

1. The effective resonance integrals for the two investigated types of cassettes differ insignificantly. The somewhat larger value of the resonance integral in Table 3 is due to the smaller diameter of the uranium cores of the fuel elements.

2. The filling of the fuel channels by water has a weak effect on the effective resonance integral of the cassette.

In the experiments for the determination of ρ^{28} and $\langle \sigma_c^{28} \rangle / \langle \sigma_f^{25} \rangle$ in the assembly on IRT reactor the above-mentioned indicators made of uranium dioxide and Ge(Li) spectrometer were used. The value of ρ^{28} was determined from the measurements of the cadmium ratio R^{28}_{Cd} for the reaction ^{238}U (n, γ) in the fuel elements:

$$\rho^{28} = 1/(1 - R^{28}_{Cd}). \qquad (6)$$

The determination of R^{28}_{Cd} is based on the measurement of γ radiation of ^{239}Np with an energy of 277 keV from the indicators irradiated in a cadmium screen and without cadmium. The irradiation was carried out in two diametrically opposite experimental fuel elements of the cassette.

The parameter $\langle\sigma_c^{28}\rangle/\langle\sigma_f^{25}\rangle$ was determined from the measurements of γ radiation of ^{239}Np with an energy of 277 keV and the decay products of ^{143}Ce with an energy of 293 keV (the procedure is described in [6]).

$$\frac{\langle\sigma_c^{28}\rangle}{\langle\sigma_f^{25}\rangle}=\frac{\sigma_{c_{th}}^{28}}{\sigma_{f_{th}}^{25}g_{25}}\frac{a_{Np}}{a_{Ce}C_{28}}\frac{a_{Ce}^{T.K}}{a_{Np}^{T.K}}, \quad (7)$$

where $\sigma_{c_{th}}^{28}$ and $\sigma_{f_{th}}^{25}$ are the cross sections of radiation capture in ^{238}U and in the fission of ^{235}U for thermal neutrons; g_{25} is the Wescot factor; a_{Np} and a_{Ce} are the radiation intensities of ^{239}Np and ^{143}Ce indicators irradiated in the fuel element; $a_{Np}^{t.c}$ and $a_{Ce}^{t.c}$ are the intensities of emission of ^{239}Np and ^{143}Ce indicators irradiated in the thermal column; $C_{28}=\frac{1}{1+\delta^{28}Y_{Ce}^{28}/Y_{Ce}^{25}}$ is a correction taking into consideration the contribution of the fission of ^{238}U to the activity of ^{143}Ce; Y_{Ce}^{28} and Y_{Ce}^{25} are the yields of ^{143}Ce in the fission of ^{238}U and ^{235}U. The indicators were calibrated in the thermal column of the F-1 reactor of the I. V. Kurchatov Atomic Energy Institute.

The values of the parameters occurring in formula (6) are given in Table 4.

The ratio $\langle\sigma_c^{28}\rangle/\langle\sigma_f^{25}\rangle$ was measured also in the assembly on reactor F-1. The rate of reaction of capture in ^{238}U was measured by depleted metallic uranium foil of 0.09 mm thickness; the γ radiation of ^{239}U with an energy of 74 keV was recorded with a NaI(Tl) spectrometer.

The background of the fission product under the peak of 74 keV was taken into consideration in accordance with [9] and it comprised not more than 2% in the fuel and the thermal column. The rate of fission reaction of ^{235}U was measured by foils of a dispersion alloy of aluminum and uranium enriched to 90% in ^{235}U (mass content of uranium 17%) and having a thickness of 0.07 mm. The integral activity of the fission products was recorded. The mean values of $\langle\sigma_c^{28}\rangle/\langle\sigma_f^{25}\rangle$ for the cassette are shown in Table 5.

The results of the measurements show that the filling of the thermal channels by water leads to a reduction of $\langle\sigma_c^{28}\rangle/\langle\sigma_f^{25}\rangle$ and specially of ρ^{28} due to softening of the neutron spectra.

In conclusion, one should note the increased reliability of the results presented here since they were obtained on systems of different dimensions and with the use of different techniques and instruments.

LITERATURE CITED

1. A. V. Bushuev, L. N. Yurova, At. Energ., 27, No. 4, 334 (1969).
2. Y. Hachya, J. Nucl. Science and Technology, 9, 629 (1973).
3. L. N. Yurova et al., At. Energ., 38, No. 4, 245 (1975).
4. D. Watt and D. Reamsden, High Sensitivity Counting Techniques. Pergamon Press (1964), p. 277.
5. BNL-325, 3 Ed. V. I. N. Y. (1973).
6. L. N. Yurova et al., At. Energ., 32, No. 5, 412 (1972).
7. S. I. Sukhoruchkin, Atomic Technology Abroad, No. 8, 34 (1976).
8. L. N. Yurova et al., At. Energ., 36, No. 1, 51 (1974).
9. L. N. Yurova et al., At. Energ., 31, No. 6, 628 (1971).

TWO-DIMENSIONAL KINETIC CALCULATION OF NUCLEAR REACTOR BY THE FINITE-ELEMENTS METHOD

N. V. Isaev, I. S. Slesarev,
N. E. Gorbatov, and A. P. Ivanov

UDC 621.039.51.12

In theoretical investigations of nuclear reactors, it is often necessary to calculate the neutron-physical characteristics of media consisting of heterogeneous regions of complex spatial configuration. Known calculational models of this type include, in particular, two-dimensional systems comprising an irregular set of hexagonal compartments with different physical properties.

In recent years, methods and procedures for the calculation of nuclear reactors consisting of hexagonal compartments have been developed using both diffusional [1, 2] and kinetic [3] approximations. The use of a compartmental approach is extremely convenient for nuclear-reactor designers, since it allows the necessary information to be obtained for every compartment in the reactor. Natural refinements of the compartmental model of a reactor are to use a more complex function to represent the neutron flux inside the compartments (e.g.), by using series expansion with respect to some system of polynomials) or to adopt a more universal triangular grid, which allows the cells of the grid to be reduced in size.

The present work proposes an approximate method of multigroup kinetic calculation of nuclear reactors using a regular triangular grid. The calculation scheme is based on the finite-elements method [4, 5]. The use of the kinetic equation allows the conditions at the outer boundary of the reactor to be accurately realized. In the present paper, in contrast to [5], the operators of the Boltzmann equation are taken in non-self-conjugate form, which is more convenient for computer realization. The use of a regular triangular grid leads to a simple three-point scheme for the calculation of a reactor consisting of hexagonal compartments. The proposed method allows the solution to be found not only at the nodes of the calculation grid, as is usually the case with numerical methods, but at any point within the compartment, since the function that approximates the neutron flux inside the cell is known. The method is also suitable for precision calculations of nuclear reactors consisting of hexagonal compartments.

Finite-Difference Grid

We consider a two-dimensional kinetic equation in the form [6]

$$\hat{L}\Phi^{(g)}(x, y, \mu, \varphi)=\frac{1}{K_{\text{eff}}}\hat{Q}\Phi^{(g)}(x, y, \mu, \varphi), \tag{1}$$

where

$$\hat{L}\Phi^{(g)}(x, y, \mu, \varphi)=$$

$$=\sqrt{1-\mu^2}\left[\cos\varphi\frac{\partial}{\partial x}+\sin\varphi\frac{\partial}{\partial y}+\Sigma_{\text{tot}}^{(g)}\right]\Phi^{(g)}(x, y, \mu, \varphi)-\frac{1}{4\pi}\sum_{p=1}^{g}\int_{-1}^{+1}d\mu'\int_{0}^{2\pi}d\varphi'\Sigma_d^{p\to g}\times$$

$$\times(x, y, \mu, \varphi)\Phi^{(p)}(x, y, \mu', \varphi');\quad \hat{Q}\Phi^{(g)}(x, y, \mu, \varphi)=\frac{\chi^{(g)}}{4\pi}\sum_{p=1}^{G}\int_{-1}^{+1}d\mu'\int_{0}^{2\pi}d\varphi'\nu_f^{(p)}\Sigma_f^{(p)}\times$$

$$\times(x, y)\Phi^{(p)}(x, y, \mu', \varphi');$$

$\mu=\cos\omega$; $\mu_0=\cos\omega\cos\omega'+\sin\omega\sin\omega'\cos(\varphi-\varphi')$; g=1, 2, ..., G is the number of the energy group; ω and φ are directions of flight of the neutrons; $\Sigma_{\text{tot}}^{(g)}(x, y)$, $\Sigma_{\text{f}}^{(g)}(x, y)$ are the total macroscopic cross section and the

Translated from Atomnaya Énergiya, Vol. 41, No. 6, pp. 391-395, December, 1976. Original article submitted March 4, 1975; revision submitted December 26, 1975.

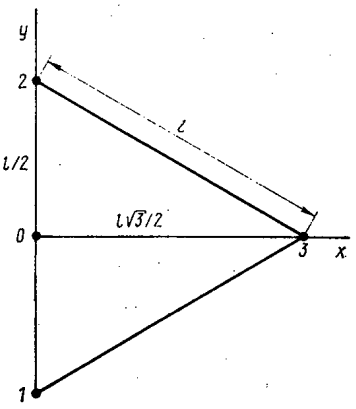

Fig. 1

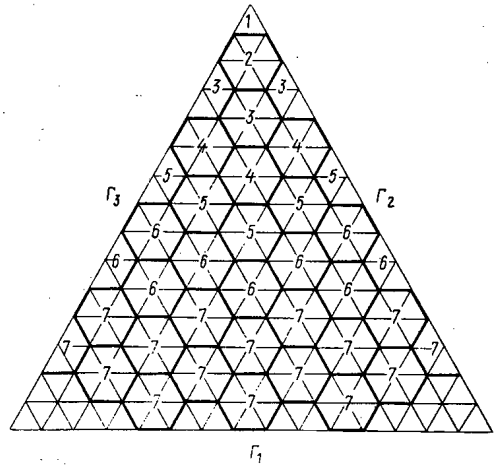

Fig. 2

Fig. 1. Numeration of points in triangular cell.

Fig. 2. Compartmental model of a BFS-16-10 assembly (1/6). Size of hexagonal compartment "under key" 13.5 cm: 1) compensating absorber; 2-5) low-enrichment zones; 6) high-enrichment zone; 7) lateral shield.

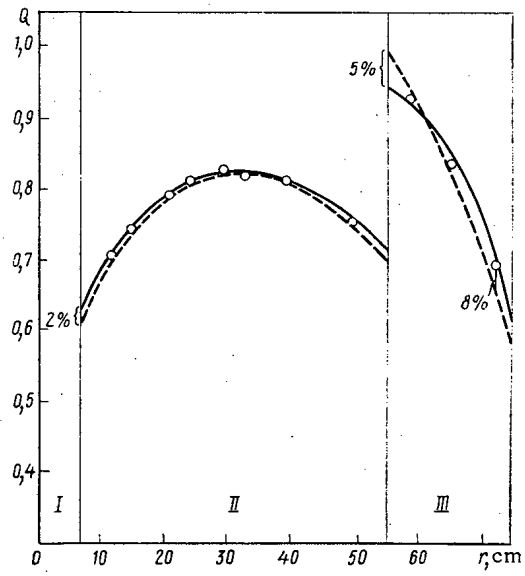

Fig. 3. Radial distribution of heat emission in the BFS-16-10 assembly. The dashed lines show the diffusional calculation; the circles are experimental values; and the continuous curves correspond to the kinetic calculation; I) compensating absorber; II) low-enrichment zone; III) high-enrichment zone.

TABLE 1. Macroconstants of Compartments of BFS-16-10 Assembly

Type of compartment	$\Sigma_{tot}^{(1)}$	$\Sigma_d^{1\to1}$	$\nu_f^{(1)}\Sigma_f^{(1)}$	$\Sigma_{tot}^{(2)}$	$\Sigma_d^{2\to2}$	$\nu_f^{(2)}\Sigma_f^{(2)}$	$\Sigma_d^{1\to2}$
1	0,1913	0,1575	—	0,3359	0,2968	—	0,0266
2	0,1814	0,1683	0,0061	0,2952	0,2877	0,0077	0,00877
3	0,1818	0,1686	0,00608	0,2952	0,2877	0,0077	0,00887
4	0,1818	0,1686	0,00608	0,2950	0,2877	0,0077	0,00887
5	0,1811	0,1680	0,00613	0,2942	0,2868	0,00764	0,0087
6	0,1759	0,1621	0,00843	0,2894	0,2800	0,0118	0,00842
7	0,2126	0,1967	0,00255	0,3324	0,3267	0,00327	0,0128

fission cross section for neutrons of the g-th group; $\Sigma_d^{p\to g}(x, y, \mu_0)$ is the macroscopic cross section for neutron transfer from the p-th to the g-th group; $\nu_f^{(g)}$ is the number of secondary neutrons formed in a single fission episode; $\chi^{(g)}$ is the fraction of the fission spectrum consisting of neutrons of the g-th group; K_{eff} is the effective neutron multiplication factor.

As the boundary condition for Eq. (1) we take the condition of zero input of neutrons to the reactor

$$\Phi^{(g)}(x, y, \mu, \varphi)|_\Gamma = 0; \quad \begin{matrix} -1 \leqslant \mu \leqslant 0; \\ -\frac{\pi}{2} \leqslant \varphi \leqslant \frac{\pi}{2}, \end{matrix} \tag{2a}$$

or the reflection condition

$$\nabla\Phi^{(g)}(x, y, \mu, \varphi)|_\Gamma = 0, \tag{2b}$$

where Γ is the external surface of the reactor.

We consider a reactor of a configuration that can be described by means of regular triangles. The region in which the variables μ and φ are defined is divided into equal intervals $\Delta\mu_j$ and $\Delta\varphi_k$ and Eq. (1) is integrated within these intervals. Then Eq. (1) may be rewritten in the form

$$m[\partial\Psi(x, y)/\partial x] + n[\partial\Psi(x, y)/\partial y] + \Sigma(x, y)\Psi(x, y) = q(x, y), \tag{3}$$

where

$$\Psi(x, y) = \int_{\Delta\mu_j} d\mu' \int_{\Delta\varphi_k} d\varphi' \Phi(x, y, \mu', \varphi');^*$$

$$q(x, y) = \frac{1}{4\pi} \sum_{p=1}^{g} \int_{\Delta\mu_j} d\mu \int_{\Delta\varphi_k} d\varphi \int_{-1}^{+1} d\mu' \int_0^{2\pi} d\varphi' \Sigma_d^{p\to g}(x, y, \mu', \varphi') \Phi^{(p)}(x, y, \mu, \varphi) +$$

$$+ \frac{\chi^{(g)}}{4\pi} \sum_{p=1}^{G} \int_{\Delta\mu_j} d\mu \int_{\Delta\varphi_k} d\varphi \int_{-1}^{+1} d\mu' \int_0^{2\pi} d\varphi' \nu_f^{(p)} \Sigma_f^{(p)}(x, y) \Phi^{(p)}(x, y, \mu', \varphi');$$

$$m = \int_{\Delta\mu_j} d\mu \sqrt{1-\mu^2} \int_{\Delta\varphi_k} \cos\varphi \, d\varphi/d;$$

$$n = \int_{\Delta\mu_j} d\mu \sqrt{1-\mu^2} \int_{\Delta\varphi_k} \sin\varphi \, d\varphi/d;$$

$$d = \int_{\Delta\mu_j} d\mu \int_{\Delta\varphi_k} d\varphi.$$

The solution inside a triangular cell is written in the form of a plane [4]

$$\Psi(x, y) = a + bx + cy. \tag{4}$$

We consider a triangular cell of the grid (Fig. 1). Substituting in Eq. (4) the coordinates of the points 1, 2, and 3 gives

$$\begin{aligned} \Psi_1 &= a - cl/2; \\ \Psi_2 &= a + cl/2; \\ \Psi_3 &= a + bl\sqrt{3}/2. \end{aligned} \tag{5}$$

The solution of Eq. (5) is

$$\begin{aligned} a &= (\Psi_1 + \Psi_2)/2; \\ b &= (2\Psi_3 - \Psi_1 - \Psi_2)/l\sqrt{3}; \\ c &= (\Psi_2 - \Psi_1)\, l. \end{aligned} \tag{6}$$

Here Ψ_1, Ψ_2, and Ψ_3 are the values of the neutron flux at points 1, 2, and 3, respectively. Substituting the coefficients from Eq. (6) into Eq. (4) gives

$$\Psi(x, y) = \Psi_1 A_1(x, y) + \Psi_2 A_2(x, y) + \Psi_3 A_3(x, y), \tag{7}$$

where

$$A_1(x, y) = \frac{1}{2} - \frac{x}{l\sqrt{3}} - \frac{y}{l}; \quad A_2(x, y) = \frac{1}{2} - \frac{x}{l\sqrt{3}} + \frac{y}{l}; \quad A_3(x, y) = \frac{2x}{l\sqrt{3}}.$$

*Here and below the superscript is omitted.

Substituting Eq. (7) into Eq. (3) and integrating over the area of the triangle with weight $A_3(x, y)$ gives

$$\int_0^{l\sqrt{3}/2} dx \int_{-(l/2-\sqrt{3}x/3)}^{l/2-\sqrt{3}x/3} dy A_3(x, y)\{mb+nc + \Sigma_{tot}(x, y)[A_1(x, y)\Psi_1 + A_2(x, y)\Psi_2 + A_3(x, y)\Psi_3] - [q_1A_1(x, y) + q_2A_2(x, y) + q_3A_3(x, y)]\} = 0, \quad (8)$$

where q_1, q_2, and q_3 are the values of the neutron source q at the points 1, 2, and 3, respectively. The result of integration is

$$\Psi_3 = K_1(\Psi_1 + \Psi_2) + K_2(q_1 + q_2) + K_3q_3, \quad (9)$$

where

$$K_1 = (2m/l\sqrt{3} - \Sigma_{tot}/2)/K_4;\ K_2 = 1/(2K_4);\quad K_3 = 1/K_4;\ K_4 = 4m/l\sqrt{3} + \Sigma_{tot}.$$

The range of φ from 0 to 2π is now divided into six equal sections (which is convenient for the construction of the grid and ensures the accuracy required in reactor calculations), giving

$$m = \frac{3}{\pi}\int_{\Delta\mu_j} d\mu\sqrt{1-\mu^2}\int_{\Delta\varphi_k}\cos\varphi\, d\varphi. \quad (10)$$

Thus, it is possible to construct a variational difference scheme such that, given the values of the neutron flux at points 1 and 2, the flux at point 3 can be determined.

To solve Eq. (9) it is convenient to use a scheme of six constraints for the realization of boundary conditions at the outer surface of the reactor. For this purpose, the compartments should be chosen so that in Eq. (9) points 1 and 2 may be assigned values determined from the boundary conditions or from the results of the previous step in the calculation.

Realization of the Method

The method outlined was realized in the form of a TR1 program written in ALGOL 60 (AN GDR translator) for a BÉSM-6 computer. By means of the TR1 program it is possible to calculate K_{eff} for the reactor, the field of neutrons and heat liberation, the coefficient of nonuniformity, and the rates of processes and their integrals. The program realizes boundary conditions as in Eqs. (2a) and (2b) on any of the sides of the triangles. The program may be used for calculations of one half and one sixth of a symmetric reactor; a triangular cell of a nuclear reactor; or a reactor of arbitrary form (boundary conditions are imposed on the external boundaries of the triangle). The number of nodes of the triangular grid may reach 3000, and the number of energy groups 26. The maximum number of energy groups used in the calculation (G_{max}) may be determined from the inequality: $(G_{max}+3) \le 32{,}000$. The TR1 program has a block for macrosection preparation, associated with the BNAB-70 26-group neutron catalog. The time τ required by program TR1 for the reactor calculation on a BÉSM-6 computer is given by the empirical formula: $\tau = 1.3 \cdot 10^{-3} n_{it} n_k$ sec, where n_{it} is the total number of internal iterations over all energy groups; n_k is the number of triangular grid cells.

Results of the Calculation

In investigating the method outlined, attention was concentrated on the dependence of K_{eff} for the reactor on the step size used in the triangular lattice. The results of this investigation were given in detail in [7]. From the analysis of the calculations, it was possible to conclude that saturation of the value of K_{eff} sets in when the lattice dimension l is less than the neutron free path length (which is characteristic of the majority of schemes for the numerical solutions of transfer equations). The order of approximation of the proposed scheme is O (l). The results obtained were used to choose the grid parameters for multigroup calculations of a complex compartmental model of a fast nuclear reactor.

The compartmental model of a BFS-16-10 fast critical assembly, intended for the investigation of a BN-350 reactor, is shown in Fig. 2. Table 1 gives the two-group macroscopic constants of these types of compartment obtained from a multigroup calculation in the P_1 approximation [2]. The calculation for this critical assembly gave $K_{eff} = 1.0023$, in good (to 0.2%) agreement with experimental data. The calculation time for the BFS-16-10 assembly on a BÉSM-6 computer was 4 min.

Calculated values of the energy liberated over the radius of the BFS-16-10 assembly (over the left-hand side of the triangle shown in Fig. 2) are presented in Fig. 3, which also shows, for comparison, experimental values of the energy liberated in the active zone of the assembly obtained using a fission chamber and also a theoretical distribution calculated by the GEKS two-group diffusional program [1]. The energy liberation was

normalized to the fission integral in the active zone of the assembly. The difference in the calculated values of the energy liberated close to the zone boundaries for different properties amounted to 2-8%. The kinetic calculation differed from experiment by not more than 3%.

This example demonstrates the convenience of the proposed method for the analysis of experiments carried out on fast physical assemblies. It should be noted that the method may be used for precision calculations of nuclear reactors in any range but, because of the limitations on the triangular-grid size inherent in the method of numerical solution of the Boltzmann equation, the proposed method is more effective for fast-reactor calculations.

LITERATURE CITED

1. I. S. Akimov, M. E. Minashin, and V. N. Sharapov, At. Energ., 36, No. 6, 427 (1974).
2. V. I. Matveev et al., Preprint 499 of the Physics and Power Institute [in Russian], Obninsk (1974).
3. N. V. Isaev, I. S. Slesarev, and N. E. Gorbatov, At. Energ., 38, No. 3, 164 (1975).
4. L. Semenza, E. Lewis, and E. Rossow, Nucl. Sci. and Engng., 47, 302 (1972).
5. W. Miller, E. Lewis, and E. Rossow, Nucl. Sci. and Engng., 51, 148 (1973).
6. G. I. Marchuk, Methods of Calculating Nuclear Reactors [in Russian], Gosatomizdat, Moscow (1961).
7. N. V. Isaev, Candidate's Dissertation, Moscow Institute of Physical Research, Moscow (1975).

START-UP TESTS ON THE EFFICIENCY OF THE BIOLOGICAL PROTECTION ON NUCLEAR POWER STATIONS EQUIPPED WITH WATER-MODERATED WATER-COOLED POWER REACTORS

A. S. Iz'yurov, A. S. Kuzhil',
V. N. Mironov, A. I. Rymarenko,
and S. G. Tsypin

UDC 621.039.584:621.039.538.7

The basic sources of nuclear radiation on nuclear power stations equipped with water-cooled water-moderated power reactors are the active zone of the reactor, the spent fuel store, the pipelines of the primary circuit carrying active coolant, and the special water treatment plant. A system of biological protection (Fig. 1) has been developed and introduced for the purpose of protecting personnel from the effects of radiation. As a rule, the shielding is made from relatively cheap structural materials: concrete and particularly heavy concrete. Neverthless, the cost of the protective structure comprizes a significant proportion of the capital cost of building a nuclear power station. It is therefore important to clarify to what extent the real biological protection satisfies its basic purpose: that of ensuring a normal radiation situation, and also of determining ways of reducing the expenditure on protection structures. Investigations have therefore been carried out both now and previously in the vicinity of an operating reactor and other sources of ionizing radiation on nuclear power stations [1, 2] with the purpose of determining the safety of power station personnel. Also, as a way of improving the design of the biological protection, more detailed and wide-ranging investigations of the radiation field in all the departments of nuclear power stations have been conducted, including the unmanned areas, the approach to which is impossible after the reactor has been run up to full power.

A particular problem is created by the need to measure γ radiation and neutron fields in locations which are inaccessible with large reactor powers, such as the steam generator cell, etc. This is connected with the fact that at these levels (0.01-0.1% rated) the reactor power can only be determined very approximately (with an error of up to 200-300%). To determine the power of the reactor during studies of the biological protection in the third and fourth units of the Novovoronezh nuclear power station and the first unit of the Kola nuclear

Translated from Atomnaya Énergiya, Vol. 41, No. 6, pp. 395-399, December, 1976. Original article submitted January 7, 1976.

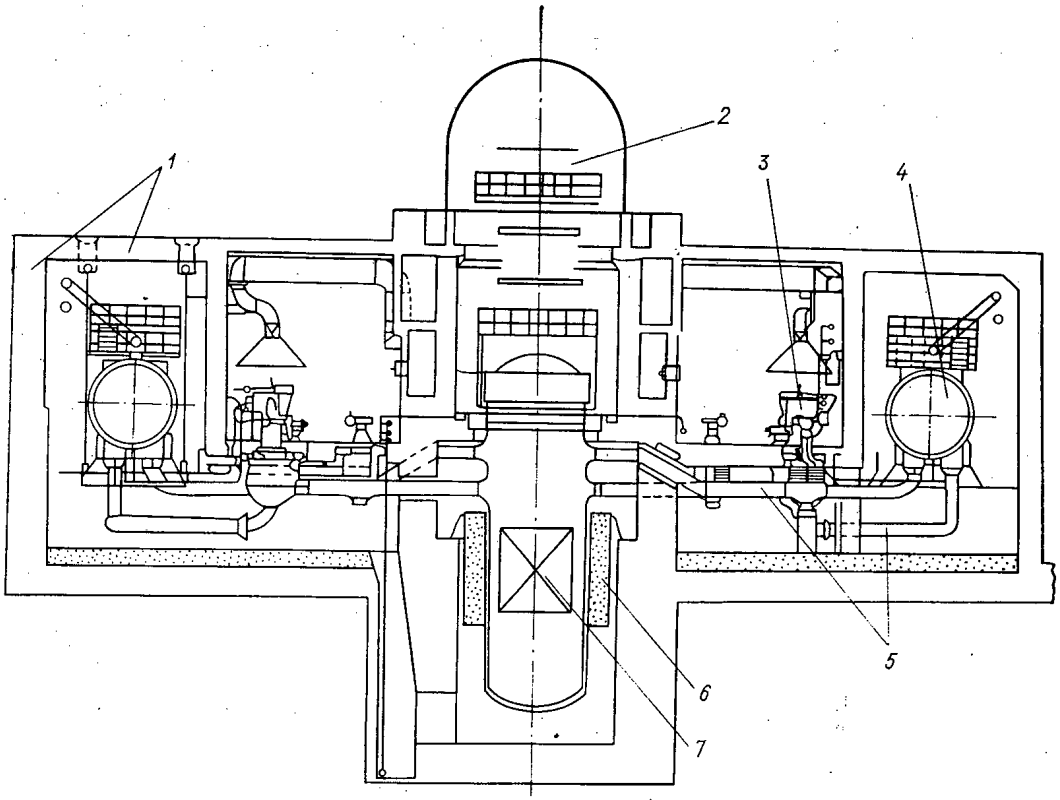

Fig. 1. Biological protection for reactor type VVÉR-440. 1) Concrete protection; 2) protective cowl; 3) main circulating pump; 4) steam generator; 5) main Du-500 piping; 6) annular water tanks; 7) active zone of reactor.

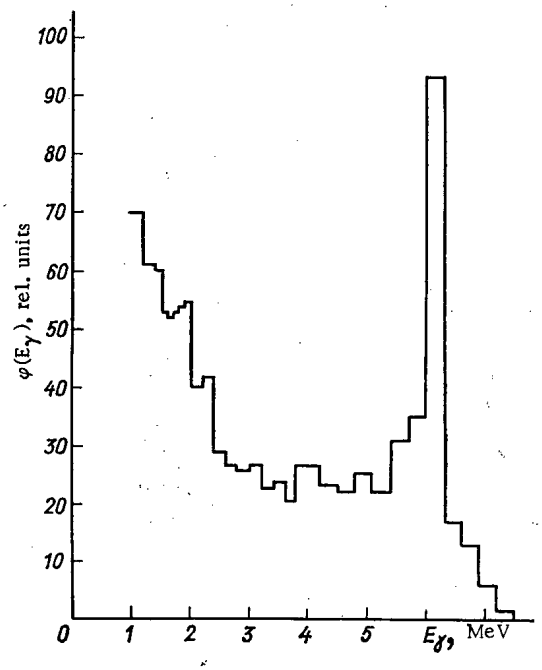

Fig. 2

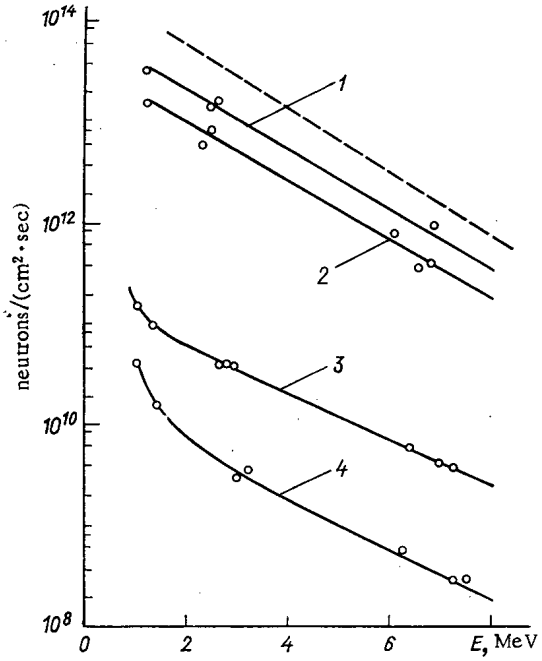

Fig. 3

Fig. 2. Spectral composition of γ radiation.

Fig. 3. Energy distribution of fast neutrons in the reactors at the Nonovoronezh nuclear power station [4] at the center of the radioactive zone of the reactors belonging to the first (1) and second (2) units, at the heat shield (3), and at the reactor body (4) in the second unit; ----) fission spectrum.

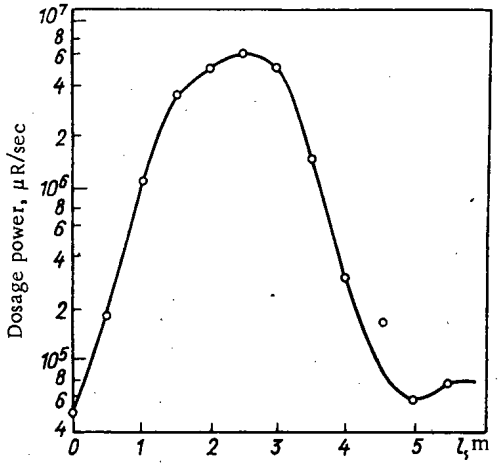

Fig. 4

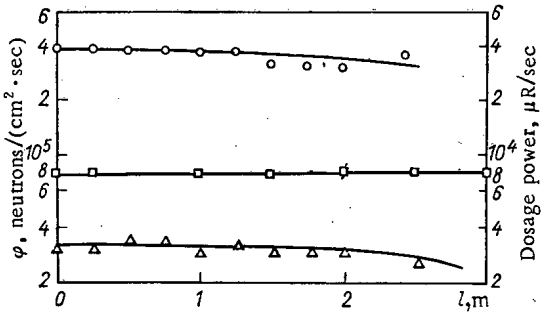

Fig. 5

Fig. 4. Power of γ radiation dosage in the channels of the ionization chamber.

Fig. 5. Distribution of neutrons and γ radiation beneath the reactor body: ○, △) thermal and fast neutrons; □) γ quanta.

power station, a special coolant-radioactivity monitor was used, based on the reaction ^{16}O (n, p)^{16}N. This monitor, installed in the main Du-500 circulating lines, allowed a range of power variations of 4-5 orders of magnitude to be covered, enabling measurements to be taken all the way up to full power.

The measurements were mainly made by the use of standard dosimeters, but in a number of cases specially developed instruments were employed. The measurements showed that the main contribution to the dosage near to the technical equipment of the primary coolant circuit was γ radiation with energies greater than 3 MeV, while at the same time none of the standard instruments had been calibrated for this energy interval. Figure 2 shows the energy distribution of γ radiation in the main circulating pump drives of the operational third unit at the Novovoronezh nuclear power station. Due to the absence of the appropriate calibration for dosimeters in the energy region 3-10 MeV, the errors in measuring the power of dosages can be as high as 50-100% [3]. To calibrate the dosimeters, a special device employing a through channel in the concrete shielding above one of the main circulating loops of the primary coolant circuit in the third unit at Novovoronezh was used. The device comprised a high-energy source of γ radiation of basic energy 6.13 MeV (^{16}N).

During experimental work concerned with the efficiency of biological protection, similar data were obtained for the main source of ionizing radiation on a nuclear power station: the reactor itself (Figs. 3-5). In units based on water-moderated water-cooled power reactors, the reactor itself is relatively small in size, so that due to the small dimensions of the body and the presence of water in it few protective materials are used in its construction, the basic material being concrete (see Fig. 1). The main capital expenditure on the construction of the biological protection is concerned with the erection of a concrete wall around the primary coolant circuit equipment, viz., the steam generator, pumps, and piping.

The dominant radiation from the coolant for which protection must be provided is γ radiation ^{16}N with an energy of 6.13 MeV. Consequently, the circulating pipes, steam generator, and the other equipment of the primary coolant circuit, which are located in the space within the reactor, will be powerful radiation sources. Therefore, we are concerned with three-dimensional sources of γ radiation, frequently tending to screen each other, having complex shapes, and greatly differing powers.

Historically, the situation was such that during the design of the first unit with a water-moderated water-cooled power reactor, main attention was devoted to constructing the biological shield of the basic source of ionizing radiation, the reactor itself. At the same time, the method of designing the biological protection for the primary coolant circuit of the reactor was somewhat simplified. Usually, the design of the primary circuit biological shielding during the planning of a nuclear-power station is directed toward one or two "dominant" sources which are not screening each other. Such a method of design can lead to errors in certain cases. To improve the method of calculating the powers of γ radiation for shielding a set of three-dimensional sources, a program of field investigations was conducted in the vicinity of the primary circuit plant of a reactor type VVÉR-440 (before and after the protection was installed).

The investigation included radiation yield and the distribution of radiation dosage power with distance from these sources, when only one, two, and more than two sources can be "seen" in practice from the points

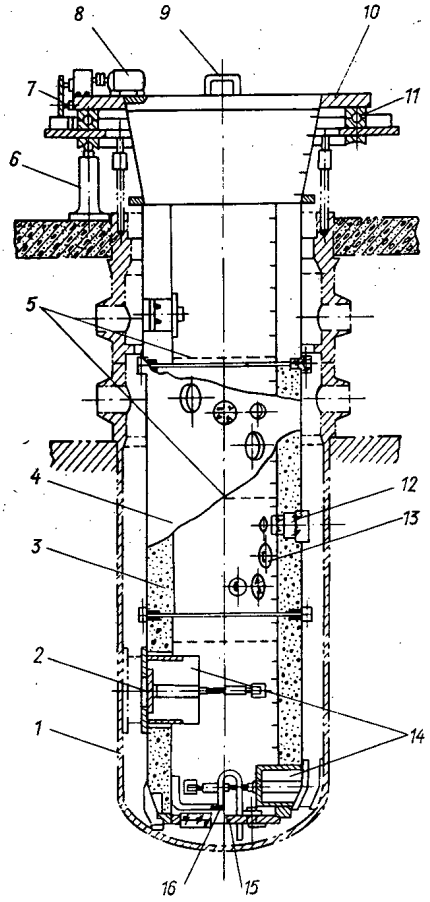

Fig. 6. Protective container for inspecting the walls of the reactor vessel. 1) Vessel of reactor; 2) retractable shutters of biological shielding; 3) body of container; 4) outer cover and biological shielding; 5) inspection area; 6) hydraulic jack for raising and lowering the container; 7,8) rotating gear and motor; 9) lug for transporting the container on the reactor hall crane; 10) upper support flange; 11) turning gear for axial rotation of container; 12) inspection window of shielding (lead glass); 13) manhole with detachable biological shielding; 14) retractable protective shell; 15) lower flange; 16) ejector for expelling liquid from the base of the reactor.

concerned. In this manner, the relationship of the γ radiation dosage power to the distance between the Du-500 primary circuit piping and the point of detection was investigated by means of thermoluminescent dosimeters for an operational VVÉR-440 reactor. While the experimental and calculation data were being compiled, it was shown that this experiment defined only the radiation from the Du-500 piping. Other experimental data characterizing the radiation field due to the primary coolant circuit plant was also analyzed.

As the value of the "nitrogen" activity of the coolant has an important bearing on the design of the biological protection of power station units incorporating reactors type VVÉR-440 (in fact, it determines the main mass of the concrete shielding), it was felt best to determine it from experimental data and compare the result

with calculated values obtained directly by the use of standard formulas and accepted constants [5]. The power of the γ radiation dosage at the surface of Du-500 at full reactor power, measured at a distance of 7 m from the body of the reactor, was used as a reference experimental value. The inverse transition formulas from this dosage power to the coolant radioactivity [6] and special calculations by the Monte Carlo method, carried out by A. N. Kozhevnikov, produced a "nitrogen" activity for the coolant at that particular point in the Du-500 piping, which was in close accord with the accurate design data. We should note that the Monte Carlo method takes more accurate account of the proportion of the dosage of scattered γ radiation arising from the Du-500 tubing than does the formula given in [6]. The studies showed that a normal radiation situation exists on nuclear power station units equipped with the type VVÉR-440 reactor. In locations that are permanently attended, the summated dosage power does not exceed the design level (1-4 mrem/h). In attended and unattended locations, the dosage powers of γ radiation corresponds on the average to the design values of 2.8 and 28 mrem/h, respectively.

The experimental data have defined the further improvements needed in the biological protection of nuclear power station units equipped with water-modulated water-cooled reactors. For example, a method of computer design of primary coolant circuit biological shielding for new nuclear power stations with water-moderated water-cooled reactors has been developed on the basis of data obtained during the investigation. A computer program has been compiled for calculating the radiation fields from complex arrangements of three-dimensional sources in the primary coolant circuit beyond barrier and shaped shielding. The program is suitable for choosing the profile of shielding from the point of view of minimizing its volume and its cost of erection. A design for rebuilding the equipment within the vessel of the first unit at Novovoronezh nuclear power station was developed on the basis of neutron flux densities in the region of the vessel. Experiments enabled the magnitude and distribution of induced radioactivity within the walls of the reactor vessel to be plotted more accurately. These data were used in the design of a protective container (Fig. 6) by the use of which we are able to save 600,000 rubles during each inspection of the reactor.

LITERATURE CITED

1. V. V. Badyaev et al., Radiation Safety and Protection on Nuclear Power Stations [in Russian], No. 1, Atomizdat, Moscow (1975), p. 182.
2. A. I. Glushchenko, Yu. V. Orlov, and V. D. Tsygankov, Radiation Safety and Protection on Nuclear Power Stations [in Russian], No. 1, Atomizdat, Moscow (1975), p. 222.
3. A. S. Kuzhil' et al., Radiation Safety and Protection on Nuclear Power Stations [in Russian], No. 1, Atomizdat, Moscow (1975), p. 85.
4. S. S. Lomakin et al., At. Energ., 31, No. 1, 54 (1971).
5. T. Rockwell, Protection (Screening) of Nuclear Reactors [Russian translation], Izd-vo Inostr. Lit. Moscow (1958).
6. B. R. Bergel'son and G. A. Zorikoev, Handbook on Protection From Extensive Sources [in Russian], Atomizdat, Moscow (1965).

AN EXPERIMENTAL STUDY OF THE WAY IN WHICH THE INTERNAL MODERATORS OF ANNULAR FUEL ELEMENTS AFFECT RESONANCE ABSORPTION IN THE URANIUM

I. M. Kisil', V. F. Lyubchenko,
I. P. Markelov, V. V. Orlov,
V. V. Frolov, and V. N. Sharapov.

UDC 539.125.5.173.162.3

According to theory, we employ the so-called equivalent scattering cross section [1, 2] for intermediate range IR resonances when calculating the effective integral J_{eff} of a uranium block with a moderator:

$$\Sigma_s^* = \overline{k}\Sigma_s, \tag{1}$$

where Σ_S is the macroscopic scattering cross section of the moderator. Coefficient $\overline{k}$ is derived from the averaged value $k(\lambda_i)$ for the individual resonances of the ^{238}U

$$\overline{k} = \frac{\sum_i k(\lambda_i) J_{\text{eff}\,.\,i}}{\sum_i J_{\text{eff}\,.\,i}}, \tag{2}$$

where subscript i refers to a resonance with energy E_{ri}

$$k(\lambda_i) = 1 - \frac{\eta_i}{\lambda_i}\operatorname{arctg}\frac{\lambda_i}{\eta_i}; \tag{3}$$

η_i is a function that takes account of the temperature relationship of resonance absorption;

$$\lambda_i = \alpha E_{ri}/\Delta_{\text{eff}}; \quad \alpha = 4A/(A+1)^2; \tag{4}$$

$$\Delta_{\text{eff}} = \Gamma_i \sqrt{\frac{\Sigma_0}{\Sigma_m + \Sigma_s^*}}, \tag{5}$$

where Γ_i is the resonance range; Σ_0 is the macroscopic cross section at resonance

$$\Sigma_m = 1/0.83d; \tag{6}$$

d is the external diameter of the block. The summation in formula (2) is carried out for a "powerful" (i.e., blocked) resonance. Consequently, $\overline{k}(\lambda)$ depends upon the atomic weight and scattering cross section of the moderator, the concentration of the nuclear absorber, the dimensions of the block, and the energy and parameters of resonance, and has the value $0 < \overline{k}(\lambda) < 1$. For heavy nuclei, $\overline{k}(\lambda) \approx 0.15$–$0.20$.* The relationship of $\overline{k}$ to the atomic weight A of the moderator and the equivalent scattering cross section $\sigma_m = (\Sigma_m + \Sigma_S^*)/\rho$ can be approximately represented as the relationship $\lambda_0 = (a\sqrt{\sigma_m})/A$, where a is an arbitrary dimensional coefficient.

The results of an experimental investigation into the J_{eff} of an annular uranium block with respect to the atomic weight of the scattering material has been published in [4–7]. The semiempirical Hellstrand formula was used during the investigation, together with the correction factors due to Carlwick and Pershagen [8]:

$$J_{\text{eff}} = 2.95 + 25.8\sqrt{(S + \gamma_k S_{\text{in}})/M}, \tag{7}$$

*This suggests that the Gurevich–Pomeranchuk formula [3] for the J_{eff} of a uranium block and for large-diameter blocks is valid, provided their initial supposition that $d\Sigma_S \ll 1$ is not satisfied. By employing Σ_S^* in place of Σ_S, we find that the condition $d\Sigma_S^* \ll 1$ is also satisfied for blocks of large diameter.

Translated from Atomnaya Énergiya, Vol. 41, No. 6, pp. 399-402, December, 1976. Original article submitted January 16, 1976; revision submitted May 20, 1976.

where S and S_{in} are the external and internal surface areas of the block, cm^2; M is the weight of uranium, g;

$$\gamma_k = P(L\Sigma_{sk}); \tag{8}$$

subscript k signifies the type of moderator in the internal cavity of the annular block; P is the probability of a neutron, which isotropically falls on to the surface of the moderator, passing through it without collision; L is the mean free path of a neutron in the internal cavity;

$$L = (4V/S)(d_k^2/d_0^2).$$

In this case, V and S are the volume and surface area of the moderator; d_0 is the diameter of the cavity, and d_k is the diameter of the moderator in the annular block.

We should note, however, that the variation in J_{eff} of the annular block under the influence of the moderator occupying the cavity is very small. This follows from formula (7): a variation in γ_k and Σ_{sk} of 10-20% leads to a variation of 1-3% in J_{eff}, which is generally the size of the experimental error.

The present article studies the relationship between the resonance absorption by the moderator of neutrons and the atomic weight of the moderator, by measuring the variation in the activity of a uranium foil placed on the inner surface of the annular uranium block when various moderators are introduced into the cavity. The variation in the activity of the foil is 10-20 times the variation in J_{eff}, which increases the accuracy of the effect being studied.

If N_k is the activity of the uranium indicator when the k-th moderator is introduced into the cavity, and N_0 is the activity when the moderator is absent, then simple calculation based on "sharp" resonance theory gives us the relationship

$$(N_k - N_0)/N_0 = \frac{1}{2} P(d\Sigma_{sk})(J_{eff}^{(2)} - J_{eff}^{(1)})/J_{eff}^{(1)}, \tag{9}$$

where $J_{eff}^{(1)}$ is the effective resonance integral for the indicator in an empty cavity; $J_{eff}^{(2)}$ is the integral when the indicator is enclosed by an infinite moderator (for a very thin indicator $J_{eff}^{(2)} = J_R$, where J_R is the unblocked resonance integral). By comparing the results of two analogous measurements with moderators k_1 and k_2, we find that

$$(N_{k1} - N_0)/(N_{k2} - N_0) = P(d\Sigma_{sk1})/P(d\Sigma_{sk2}).$$

Consequently, by measuring the activity of the indicators in the cavity it is possible for us to find $P(d\Sigma_{ski})$ or γ_k. On the other hand, γ_k can be found by means of an approximate formula [9]:

$$\gamma_k = 1 - \exp(-L\Sigma_{sk}^*), \tag{10}$$

from which we can determine Σ_{sk}^* (or $k = \Sigma_{sk}^*/\Sigma_{sk}$), depending upon the atomic weight of the moderator.

The relationship Σ_{sk}^* found in this way can be compared to theoretical calculations that take the finite width of ^{238}U resonance into consideration. Similar calculations were not performed for the conditions of the experiment; the authors attempted to compare the results with calculations [Eq. (2)] for a moderator arranged uniformly with respect to the block. Due to the different conditions to which they relate, it is only possible to consider a qualitative relationship between theory and experiment by this means, the adsorption being measured in a thin layer on the surface of the block, whereas the calculation refers to the mean absorption throughout a block of fairly large dimensions; furthermore, formula (2) supposes a low probability of scattering in a nucleus of mass A (approximating to the single-scattering case), while the experiment does not extrapolate to a small size of moderator, and the role played by multiple scattering can be considerable.

Results of Measurements.

The measurements were carried out in the central cell of a uranium–graphite reactor [10]. Annular uranium blocks of dimensions 34 × 3 mm and 34 × 9 mm were investigated with moderators in their internal cavities. For the purposes of the investigation, moderators were chosen which do not have resonance in the energy gap for the permitted resonances of ^{238}U. The diagram of the experimental channel is given in Fig. 1. The upper and lower parts of the continuous uranium have a height of up to 380 mm and a diameter of 35 mm, the height of the central part is 240 mm, and the inner and outer diameters of the annular block are 34 and 28 or 16 mm, respectively.

Disks of natural or enriched uranium, 19.6 mm in diameter and 0.1 mm thick, serve as indicators. The indicator on the upper surface is used to determine the way in which the moderator within the block influences the neutron flux over the external surfaces. The measurements showed that the effect of this attenuation did

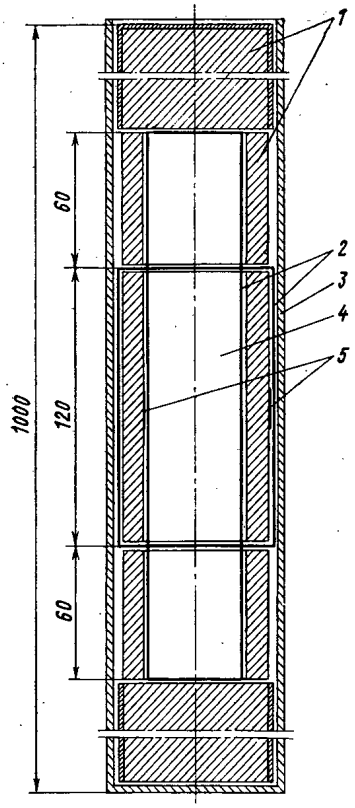

Fig. 1. Channel for measuring increments in the neutron flux at the inner surface of an annular uranium block. 1) Metallic uranium; 2) cadmium coatings; 3) Avialite tube 43 × 1 mm; 4) internal cavity to accommodate moderator; 5) indicator.

TABLE 1. Values of $\bar{k}(\lambda)$ Calculated from the Increments of Indicator Activity at the Inner Surfaces of Annular Uranium Blocks

Dimen. of block (mm)	Moderator	L, cm	$(N_k - N_0)/N_0$	$\bar{k}_e$	$\bar{k}_p$	Dimen. of block (mm)	Moderator	L, cm	$(N_k - N_0)/N_0$	$\bar{k}_e$	$\bar{k}_p$
34×3	Plexiglas	2,42	1,95±0,02	0,24±0,02	—		^{207}Pb	2,42	0,43±0,01	0,15±0,02	0,27
	^{12}C	2,42	1,45±0,02	0,54±0,03	0,76		^{207}Pb	0,74	0,14±0,01	0,16±0,02	0,26
	^{24}Mg	2,42	0,64±0,02	0,53±0,04	0,61		^{209}Bi	2,42	0,31±0,01	0,15±0,02	0,27
	^{27}Al	2,42	0,40±0,02	0,59±0,05	0,58	34×9	Plexiglas	1,33	2,66±0,04	0,40±0,03	—
	^{40}Ca	2,42	0,41±0,02	0,72±0,07	0,49		^{12}C	1,33	1,25±0,02	0,54±0,03	0,69
	^{56}Fe	2,42	1,60±0,02	0,26±0,02	0,43		^{24}Mg	1,33	0,50±0,02	0,50±0,04	0,59
	^{56}Ni	2,42	1,79±0,03	0,18±0,02	0,44		^{27}Al	1,33	0,29±0,01	0,52±0,04	0,50
	^{59}Ni	1,94	1,60±0,02	0,19±0,02	0,43		^{40}Ca	1,33	0,23±0,01	0,50±0,05	0,42
	^{59}Ni	1,35	1,29±0,02	0,21±0,02	0,43		^{56}Fe	1,33	1,28±0,02	0,24±0,02	0,35
	^{59}Ni	0,86	0,99±0,02	0,23±0,02	0,42		^{59}Ni	1,33	1,80±0,04	0,20±0,02	0,34
	^{59}Ni	0,74	0,89±0,02	0,25±0,02	0,42		^{96}Mo	1,33	0,52±0,02	0,18±0,02	0,27
	^{91}Zr	2,42	0,43±0,01	0,21±0,02	0,35		^{119}Sn	1,33	0,22±0,01	0,22±0,02	0,26
	^{96}Mo	2,42	0,58±0,02	0,16±0,02	0,34		^{207}Pb	1,33	0,28±0,02	0,12±0,02	0,21
	^{119}Sn	2,42	0,28±0,01	0,23±0,02	0,31						

not exceed 2%. For the purpose of these measurements, the monitor was coated with a 0.3-mm thickness of cadmium and placed in the reactor at a distance of 30 cm from the experimental channel, where the effects of the moderators under test would not be felt. The activities of the indicators and monitor following irradiation were determined by means of a gamma spectrometer having a NaI(Tl) crystal 40 mm in diameter and 20 mm thick. From these data we found the ratio N_k/N_m for the activation of the indicator on the inner surface of the annular block (N_k) to the activity of the monitor N_M.

For absolute calibration of coefficients γ_k, we measured $J_{eff.c}$ for an annular uranium block of dimensions 34 × 3 mm with a graphite moderator in its inner cavity. To find $J_{eff.c}$, we used the ratio

$$\frac{N_{ac}}{N_{ao}} = \frac{J_{eff.\,c} + \sigma^U_{a\,1/v}}{J_{eff.o} + \sigma^U_{a\,1/v}}, \qquad (11)$$

where N_{ac} and N_{ao} are the β activities of ^{239}U per unit mass of uranium in the annular block when irradiated with a graphite moderator in its inner cavity and with the inner cavity empty, respectively; $\sigma^U_{a1/v}$ is that part of the superthermal capture cross section of uranium which varies according to the law 1/v and equals 1.35b; $J_{eff.o}$ is the resonant integral of the annular block without the moderator, calculated by means of formula (7) for $\gamma_k = 0$ and equal to 14.35b. The isotope ^{239}U was isolated chemically by the method described in [11]. The value of N_{ac}/N_{ao} was found to be equal to 1.11 ± 0.01. These results enabled us to determine that $J_{eff} = 16.08$b for an annular block 34 × 3 mm in size, from which we find by means of formula (9) that $\gamma_c = 0.40 \pm 0.03$, $\Sigma^*_{sc} = 0.20 \pm 0.02$ cm^{-1}. When calibrating coefficients γ_k for an annular block of dimensions 34 × 9 mm, the value of γ_c was found by means of formula (9), on the basis of $\Sigma^*_{sc} = 0.20 \pm 0.02$ cm^{-1}. Table 1 gives ratio $[(N_k/N_M) - (N_o/N_M)]/(N_o/N_M)$ obtained from experimental values of N_k/N_M for annular blocks of dimensions 34 × 3 mm and 34 × 9 mm. The error in determining N_k/N_M was 0.5-1.0%. The value of N_o/N_M for the first annular uranium block was 0.634 ± 0.003, while that for the second was 0.454 ± 0.002. Table 1 also gives the value of k_e calculated from experimental data, and k_p calculated according to IR theory for uranium rods 3.4 mm in diameter containing a homogeneous mixture of uranium and moderator in the same quantities as in the annular block used in the experiments.

Conclusions. The effect that an internal moderator in a uranium block has on the resonant absorption of the ^{238}U has been established for a wide range of atomic weights in the scattering material. The results tend to confirm the conclusions drawn from theory regarding the relationship of this effect to the atomic weight of the moderator and other factors (the dimensions of the block, etc.).

The experimental results can be used to test the theory of resonant absorption with levels of intermediate range, for which it is necessary to absorb under conditions similar to those in which the measurements were conducted.

The authors would like to express their gratitude to V. G. Dubovskii for his assistance in organizing the experiments and discussing the results achieved, and to A. A. Luk'yanov and V. I. Naumov for their useful discussions of the work and valuable advice.

LITERATURE CITED

1. V. V. Orlov, in: Trudy FÉI [in Russian], Atomizdat, Moscow (1974), p. 157.
2. A. A. Luk'yanov, Moderation and Absorption of Resonant Neutrons [in Russian], Atomizdat, Moscow (1974).
3. I. I. Gurevich and I. Ya. Pomeranchuk, in: Reactor Design and the Theory of Reactors [in Russian], Akad. Nauk SSSR, Moscow (1955).
4. M. B. Egiazarov, in: Session of the Academy of Sciences of the SSSR on the Peaceful Use of Atomic Energy, July 1-5, 1955. Conference of the Department of Physical and Mathematical Sciences [in Russian], Akad. Nauk SSSR, Moscow (1955).
5. F. Hellstrand, J. Appl. Phys., 28, 1493 (1957).
6. O. V. Shvedov, V. F. Belkin, and V. A. Popkov, in: Information Bulletin of Nuclear Data Center [in Russian], No. 2, Atomizdat, Moscow (1965), p. 238.
7. O. V. Shvedov, V. F. Belkin, and V. N. Popkov, in: Information Bulletin of Nuclear Information Center [in Russian], No. 5, Atomizdat, Moscow (1968), p. 176.
8. L. Dresner, Resonance Abosrption in Nuclear Reactors [Russian translation], Gosatomizdat, Moscow (1962).
9. G. I. Marchuk, Method of Designing Nuclear Reactors [in Russian], Gosatomizdat, Moscow (1961).
10. T. V. Golashvili and I. M. Kisil', At. Energ., 13, No. 5, 435 (1962).
11. Yu. Yu. Glazkov, At. Energ., 11, No. 1, 5 (1961).

FORMATION OF VACANCY MICROPORES DURING BOMBARDING OF NICKEL BY SIMILAR IONS WITH ENERGY UP TO 300 keV

N. P. Agapova, I. N. Afrikanov,
V. G. Vladimirov, V. M. Gusev,
V. D. Onufriev, and V. S. Tsyplenkov

UDC 621.039.548.34

One of the most important engineering problems in the development of thermonuclear reactors is the choice of the material for the so-called first wall of the vacuum chamber, which must be able to withstand the action of hot plasma for a prolonged period.

In this connection considerable attention has been recently devoted to the investigation of the surface and volume radiation effects, in particular, to the behavior of the wall material during irradiation by a flux of fast (14 MeV) neutrons.

It is well known that bombarding of certain materials by fast neutrons at certain temperatures produces vacancy-type micropores in the irradiated samples; as a result a volume expansion (swelling) of the samples occurs. Thus in stainless steel, copper, nickel, and vanadium vacancy pores have been observed to form at a temperature of $(0.3\text{-}0.5)T_{pl}$ [1-5].

Up till now the radiation damages caused by fast neutrons were studied by irradiating the materials in fission reactors. However, there is the inevitable known hazard in using the results of these investigations in the development of thermonuclear reactors due the significant differences in the energies and the integral doses of neutrons. In view of this, at present bombarding of the materials by ions of elements occurring in the composition of the material is increasingly used for simulating the effect of neutron irradiation [6-10].

The advantage of the method of ion beams lies in the possibility of using it at different temperatures of the sample and the wide range of ion flux intensity and dose with exact compliance of the irradiation regime. Since the effective scattering cross section of ions is several orders of magnitude larger than that of neutrons, a few hours of ion bombardment in the accelerator is equivalent to about a year of irradiation in a fast reactor. The ion energy that is optimum for simulation is determined usually by striving to ensure the greatest possible similarity in the energy spectra of primary yield atoms produced by neutrons and ions. Thus the mean energy of primary yield atoms appearing during the passage of 14 MeV neutrons through nickel is ~465 keV. The irradiation by ions must be carried out in the temperature range in which the vacancies and internode atoms have high mobility, so that the unequal rate of formation of the defects by ions and neutrons would not cause different ratios between the concentrations of different defects in the irradiated samples. For nickel a qualitative similarity between the effects of ion and neutron irradiation is observed at a temperature of 400-600°C [11].

In the present work the formation of vacancy-type micropores in nickel irradiated by like ions with 300 keV energy was investigated by the method of electron microscopy.

Experimental Procedure. The investigated samples were irradiated by triply charged ions of nickel with an energy up to 300 keV in a ILU-2 ion accelerator [12] constructed at the I. V. Kurchatov Institute of Atomic Energy. An accelerator of this type is characterized by a large intensity of the ion beam and permits one to obtain multiply charged ions of different elements. In the present experiments Ni^{3+} ion current density was ~1.5 $\mu A/cm^2$.

Translated from Atomnaya Énergiya, Vol. 41, No. 6, pp. 402-405, December, 1976. Original article submitted August 17, 1975.

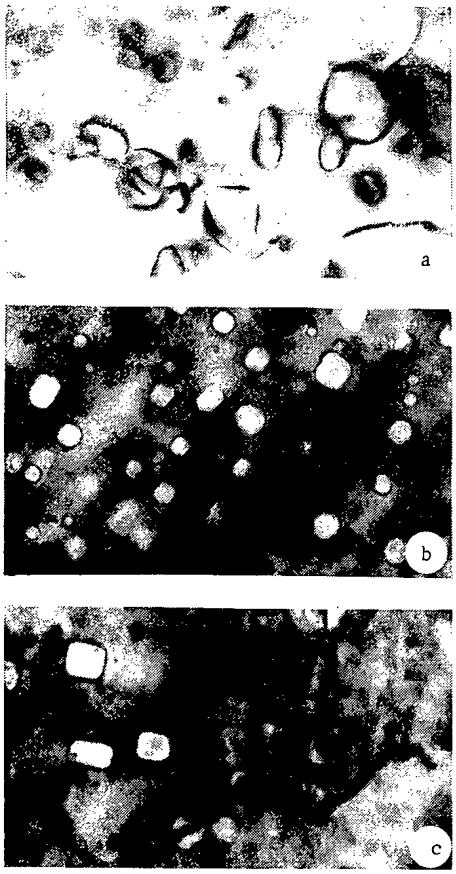

Fig. 1

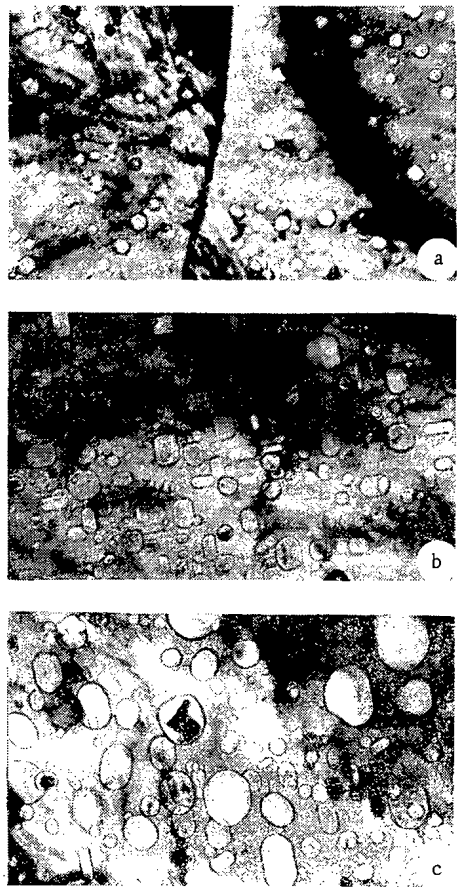

Fig. 2

Fig. 1. Structure of nickel after irradiation by nickel ions with 300 keV energy at a dose of $5 \cdot 10^{16}$ ions/cm^2 (a, b) at 400 and 450°C, respectively, and at a dose of $3 \cdot 10^{16}$ ions/cm^2 (c) at 500°C (×135,000).

Fig. 2. Structure of nickel after irradiation by nickel ions at a temperature of 550°C with a dose of 10^{17} ions/cm^2 with the energy of the ions equal to 100 (a), 200 (b), and 300 (c) keV (×135,000).

The targets to be irradiated were prepared from 99.99% pure NO type nickel. Samples of 3 mm diameter were cut out from 50-μ-thick foil obtained by multiple rolling with intermediate annealing at 850°C for 30 min. After the final rolling the foil was annealed for 1 h at 850°C.

Targets of two types were used in the experiments: electrically polished nickel disks of ~10 μ thickness (type A) and nickel disks electrolytically pretapered until the appearance of holes in them, whose edges were transparent to the electron beam (type B). The procedure of preparing the samples was described earlier in [13] in greater detail.

The samples were secured in a special cassette placed in the heating chamber of the receiving equipment of the accelerator. The temperature of the samples was regulated by a thermocouple. The vacuum in the target chamber was ~10^{-6} mm Hg. The energy of the nickel ions varied from 100 to 300 keV; the irradiation doses were $3 \cdot 10^{16}$, $5 \cdot 10^{16}$, and 10^{17} ions/cm^2. The irradiation was done at temperatures of 400, 450, 500, and 550°C.

After irradiation the samples of type A were thinned by pickling of the back side in chloroacetic electrolyte until holes appeared with edges that were transparent for the use of translucence electron microscope. The structure of the samples after irradiation was investigated with EM-300 and V9-613 electron microscopes.

Results of the Experiments. In order to determine the number of displacements after irradiation by nickel ions with 100, 200, and 300 keV energy we made some computations and used some published results [14]. The average number of displaced atoms is $\bar{\nu} = K(\bar{E}_{ec})/(2E_d)$, where E_{ec} is the fraction of ion energy spent in elastic collisions; E_d is the energy of displacement of a lattice atom (for nickel $E_d = 40$ eV); $K = 0.8$.

According to computations by the Lindhard model [15], in nickel the mean free path of nickel ions of 100, 200, and 300 keV energy is ~340, 630, and ~880 Å respectively. The energy E_{ec} is 63, 118, and 160 keV. Thus the average number of displaced atoms $\overline{\nu}$ is 630, 1180, and 1600 atoms per ion for 100, 200, and 300 keV, respectively.

Taking the mean free path into consideration it is easy to calculate the average number of displaced atoms appearing in the damaged layer of nickel for different doses and energies of the bombarding nickel ions. For a dose of 10^{17} ions/cm^2 the total number of displaced atoms per lattice atom in the damaged layer of nickel is ~230 atoms/ion for 100, 200, and 300 keV, i.e., in this case it is practically independent of the variation of the ion energy in the range 100-300 keV.

In irradiation by 14-MeV neutrons a flux of $\sim 1.5 \cdot 10^{23}$ neutrons/cm^2 in a thermonuclear and $\sim 3 \cdot 10^{23}$ neutrons/cm^2 in a fast reactor is required to produce this number of displacements.

Figure 1a, b, and c shows the microphotographs of type-A samples obtained with the electron microscope; the samples were irradiated by Ni^{3+} ions with 300-keV energy at a dose of $(3\text{-}5) \cdot 10^{16}$ cm^{-2}. It is evident from Fig. 1a that after irradiation at 400°C vacancy pores are not formed but dislocation loops with diameter up to 1500 Å appear. It is interesting to note that the dislocation loops do not contain packing defect. With the increase of the irradiation temperature to 450°C vacancy pores develop (see Fig. 1b). The concentration of the pores is $\sim 2.5 \cdot 10^{15}$ cm^{-3}; their average diameter is ~230 Å. The swelling $\Delta V/V$ computed from the microphotograph is ~2.5%. A further increase of the irradiation temperature to 500°C results in an increase of the average diameter of the pores to 300 Å (see Fig. 1c). The irradiation dose is $\sim 3 \cdot 10^{16}$ ions/cm^2. The concentration of the pores reaches $\sim 1.5 \cdot 10^{15}$ cm^{-3} and the swelling is ~3%. Therefore, the irradiation temperature has a significant effect on the form of the defects that appear in the sample: at 400°C large dislocation loops are observed; at 450°C vacancy pores are formed whose size increases with the temperature. As seen from Fig. 1b and c, the pores have clear crystallographic faceting and most of them are related to dislocations that are apparently the centers of pore generation.

Another series of experiments were conducted on targets of type B for investigating the effect of the energy of ions on the pore formation. The microphotograph of a sample irradiated by 100-keV nickel ions is shown in Fig. 2a. In this case the average diameter of the pores is ~100 Å; their concentration is $\sim 1.2 \cdot 10^{16}$ cm^{-3} and the swelling comprises ~1%. A zone depleted by the ions is clearly seen along the boundary of the grains and has a width of ~500 Å. This means that the boundary of the grains are sinks for the vacancies. An increase of the ion energy to 200 keV (see Fig 2b) for the same irradiation temperature leads to an increase of the average diameter of the pores up to ~125 Å, to an increase of their concentration to $1.9 \cdot 10^{16}$ cm^{-3}, and to an increase in swelling up to ~7.5%. The microphotograph of the structure of nickel irradiated by 300-keV nickel ions is shown in Fig. 2c. The average size of the pores is ~125 Å, their concentration is $\sim 3 \cdot 10^{16}$ cm^{-3}, and the swelling reaches ~9%. Thus, the swelling increases as the ion energy increases in the range 100-300 keV.

The results obtained here indicate the feasibility of using heavy-ion accelerators of moderate energy for conducting simulated experiments modeling the formation of vacancy micropores during irradiation by fast neutrons. Until recently, high-energy (from a few mega electron volts to tens of mega electron volts [6-8]) accelerators have been largely used for such experiments. The possibility of using ILU-2-type equipment for this purpose cuts down the cost considerably and methodologically simplifies the work of preparing and conducting the simulation experiments. In particular, due to the high intensity of the ion beam in this equipment, the fast passage of the accelerator into a given regime, and the simplicity of operation it is possible to irradiate a large number of samples in a relatively short time and the search for the damaged layer of the target in electron microscope analysis of the samples after irradiation is facilitated.

At the same time during the bombardment by ions of moderate energy, the role of the surface of the target as the place of sink of vacancies increases and as a result the possible effect of this surface on the size and concentration of the micropores also increases. Hence, a problem arises about the correct determination of the equivalent doses of ion and neutron irradiation.

LITERATURE CITED

1. C. Cawthorne and E. Fulton, Nature, 216, 575 (1967).
2. J. Nolmes and H. Brager, Trans. Amer. Nucl. Soc., 11, 479 (1968).
3. J. Brimhall and B. Mastel, J.Nucl. Mater., 29, 123 (1969).
4. B. Mastel and J. Brimhall, J. Nucl. Mater., 28, 115 (1968).
5. F. Wiffen and J. Stiegler, BNWL-870 (1968).

6. C. Chen, A. Mastenbrock, and J. Elen, Rad. Effects, 6, 127 (1972).
7. D. Mazey and F. Menzinger, J. Nucl. Mater., 48, 15 (1973).
8. W. Johnston, J. Nucl. Mater., 54, 24 (1974).
9. V. N. Bykov, V. I. Krotov, and S. Ya. Lebedev, in: Problems of Atomic Science and Engineering [in Russian], Ser. Fuel and Structural Materials, No. 1, TsNIIatominform (1974), p. 28.
10. V. N. Bykov, S. Ya. Lebedev, and S. D. Panin, ibid, p. 34.
11. G. Kulcinski, J. Laider, and D. Doren, Rad. Effects, 7, 195 (1971).
12. V. M. Gusev et al., Prib. Tekh. Eksp., 4, 19 (1967).
13. N. P. Agapova et al., Izv. Akad. Nauk SSSR, Ser. Fiz., 38, No. 11, 2337 (1974).
14. H. Norgett, B. Robinson, and J. Torrens, Rep. CEAR-4389 (1972).
15. J. Lindhard, M. Scharff, and H. Schiftt, Kgl. Danske vid Selskab, Mat. Fys. Medd., 33, No. 14 (1963).

EFFECT OF REACTOR RADIATION ON THE SUSCEPTIBILITY OF AUSTENITE STEEL TO INTERCRYSTALLITE CORROSION

S. N. Votinov, Yu. I. Kazennov,
V. L. Bogoyavlenskii, V. S. Belokopytov,
E. A. Krylov, L. M. Klestova,
and L. I. Reviznikov

UDC 621.039.531:620.193

Cases of premature degradation of some crucial constructions of nuclear reactors (casings of fuel elements, steam generators, etc.) indicate the pressing problem of intercrystallite corrosion disintegration of austenite steels [1, 2]. Therefore, the question of the role of reactor radiation in developing susceptibility to intercrystallite corrosion (ICC) of austenite steels 08Kh18N10, 09Kh16N15M3B, and 06KhN40B and their welded joints is of large theoretical and practical interest.

The chemical compositions of these steels are given in Table 1.

Procedure. The tests were conducted on 50 × 25 × 1-mm samples with transverse welded seam in the middle. The samples were cut from 1-mm-thick austenized (1050°C, 30 min) sheets. The welded joint was obtained by melting the sheets by argon arc with nonmelting electrode. The properties of the base metal were determined at a distance of at least 15 mm from the seam.

The samples were irradiated in the channel of SM-2 reactor at a temperature of 70°C and a flux of $3 \cdot 10^{20}$ neutrons/cm^2($E \geq 1$ MeV). Irradiated and unirradiated samples were subjected to intense isothermal heating for 0.5 to 1000 h in the temperature range 300-800°C.

The tests for the susceptibility to intercrystallite corrosion by the AM method (GOST 6032-58) were carried out by boiling the samples in standard sulfuric acid solution of copper sulfate in the presence of copper shaving for 24 h; by D method (GOST 6032-58) they were done by boiling in 65% solution of nitric acid for 48 and 96 h. The susceptibility to ICC after boiling was determined by the metallographic or the weight method. In the later case the corrosion rates were calculated in g/m$^2 \cdot$ h.

Results and Discussion. The rates of the test by AM method, presented in Fig. 1, show that the irradiated samples of 08N18N10 steel have a wider time-temperature range for the development of susceptibility to ICC than the unirradiated material. The susceptibility to corrosion along the grain boundaries after irradiation appeared for shorter holding periods at low temperatures and remained unchanged during relatively long holding times at high temperatures. Even though the C-shaped curves have been constructed from relatively limited experimental data, the effect of irradiation is clear (see Fig. 1). In the irradiated samples the intercrystallite corrosion is detected even after 1.5 h holding at 350°C, whereas in the unirradiated sample disintegration along

Translated from Atomnaya Énergiya, Vol. 41, No. 6, pp. 405-408, December, 1976. Original article submitted October 28, 1975.

TABLE 1. Chemical Compositions of the Investigated Materials

Type	Content of elements, mass %								
	C	Si	Mn	S	P	Cr	Ni	Mo	Nb
08Kh18N10	0,08	0,39	1,28	0,009	0,016	17,7	9,36	—	—
09Kh16N15M3B	0,06	0,44	0,48	0,006	0,014	16,49	14,79	3,38	0,48
06KhN40B	0,055	0,60	1,99	0,013	0,022	17,01	39,04	—	0,50

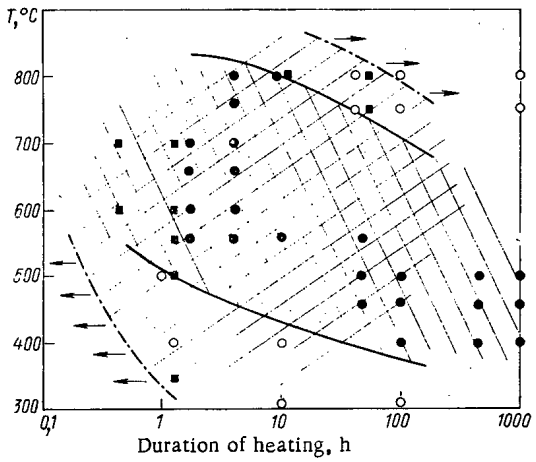

Fig. 1

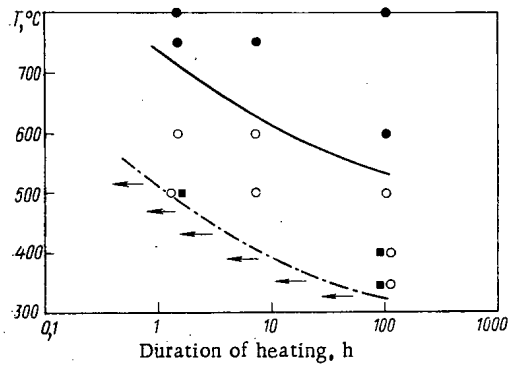

Fig. 2

Fig. 1. Time–temperature range of susceptibility of irradiated (-.-) and unirradiated (——) samples of 08Kh18N10 steel to ICC for tests by AM method (GOST 6032-58): ●, ○) unirradiated samples in the presence and absence of ICC; ■) irradiated samples in the presence of ICC.

Fig. 2. Time–temperature range of susceptibility of irradiated and unirradiated samples of 09Kh16N15M3B steel to ICC (basic metal) in tests by the D method (GOST 6032-58) (notations are same as in Fig. 1).

the boundaries of the grains developed only after 100 h at 400°C. The susceptibility to ICC as a result of irradiation increased also in the range of high temperatures. For example, unirradiated steel emerged out of the region of susceptibility to ICC after 50 h of heating at 800°C, whereas the irradiated steel continued to be subject to corrosion along the grain boundaries. Since among the irradiated samples none were found to be immune to ICC, the C-shaped curves for them are plotted conditionally. But the range of susceptibility to ICC for the irradiated metal can not be narrower than in Fig. 1, which is denoted by the arrows. A similar pattern of the effect of irradiation was observed in the investigation of the metal in the welded seam of 08Kh18N10 steel.

The effect of irradiation was found also by the tests on 06KhN40B alloy. For example, intense heating at 700°C (5 h) did not lead to intercrystallite corrosion of unirradiated samples, while in the irradiated material susceptibility to ICC was noted after holding the metal at this temperature for 1.5 h.

Steel 09Kh16N15M3B and its welded joints were found to be more immune to ICC in the tests by AM method than 08Kh18N10 and 06KhN40B steel. In the unirradiated state intercrystallite corrosion did not appear after intense heating in the entire investigated time–temperature range. The irradiation resulted in the development of susceptibility to corrosion along the grain boundaries after intense heating at 400 and 750°C (50 h).

The tests by the D method, which is more sensitive, revealed susceptibility of both unirradiated and irradiated samples of 09Kh16N15M3B to ICC. As seen from Fig. 2, the limit of the range of susceptibility to corrosion along the grain boundaries in the irradiated material has appreciably shifted to the lower temperatures and times compared to the unirradiated sample.

The irradiation did not change the nature and morphology of corrosion of steels. In the base metal and in the zone around the seam ICC appeared in the form of smearing of the grain boundaries, which was accompanied by falling out of whole grains in tests by the D method. In the metal of the seam not only the boundaries of the crystallites but also the boundaries of the crystallization cells and dendrites, and also the segregated zones between the axes of second order dendrites were smeared.

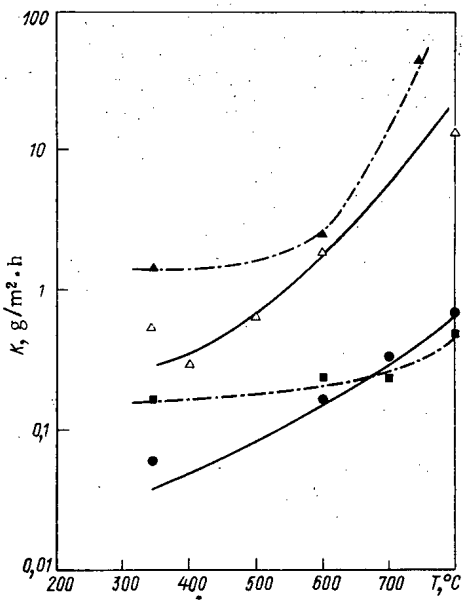

Fig. 3. Dependence of the rate of corrosion of irradiated and unirradiated 09Kh16N15M3B steel on the temperature of intense heating (holding time 50 h) in tests by AM (●, ■) and D (△, ▲) methods (GOST 6032-58): ▲, ■) irradiated metal; △, ●) unirradiated.

The results of weight measurements in the tests of 09Kh16N15M3B steel by AM and D methods are shown in Fig. 3; it is seen from this figure that the mass decrease was greater in the irradiated samples and this difference increases with the decrease of the heating temperature.

The analysis of the experimental data leads to the conclusion that the reactor irradiation enhances the susceptibility of austenite stainless steels and their welded joints to intercrystallite corrosion; a consequence of this is the extension of the time–temperature range of development of ICC especially into the side of lower temperatures. In the irradiated materials the susceptibility to ICC appears for shorter time of intense tempering in a wider range of temperatures.

The detected radiation effect should obviously be associated with the known phenomena of increased defectiveness of the crystal lattice and increase in the rate of diffusion processes in the metal due to irradiation [3, 4], which lead to a more rapid formation of segments with lower resistance to corrosion along the grain boundaries. The close values of the rate of corrosion of irradiated and unirradiated steel at heating temperatures over 600°C is apparently related to annealing of the radiation defects.

The extension of the range of susceptibility to ICC must be taken into consideration in evaluating the efficiency of austenite steel constructions under irradiation. It may be assumed that under the effect of irradiation the development of intercrystallite corrosion is also accelerated due to increase in the electrochemical reaction capability of unstable zones along the grain boundaries and the increase of stress in these segments in the presence of blocking of intragrain paths of slippage of the radiation defects. The presence of mechanical stresses and deformations must also affect the reduction of the incubation period before the development of susceptibility to intercrystallite corrosion.

A comparison of the results of tests of steels of different composition by the AM method shows that 09Kh16N15M3B (having higher resistance to ICC in the unirradiated state than 08Kh18N10 steel and 06KhN40B alloy) retained better stability even after irradiation. This indicates the possibility of a preliminary selection of materials for operation under irradiation from their resistance to ICC in unirradiated state. The effect of irradiation on the corrosion behavior of welded seams of the investigated austenite steels is essentially the same as the effect of irradiation on the behavior of the base metal.

LITERATURE CITED

1. V. P. Pogodin, V. L. Bogoyavlenskii, and V. P. Sentyurev, Intercrystallite Corrosion Cracking of Stainless Steel in Watery Media [in Russian], Atomizdat, Moscow (1970).
2. C. Cheng, J. Nucl. Mater., 56, 11 (1975).
3. M. S. Wexler, in: Diffusion in Metals with Voluminocentric Lattice [Russian translation], Metallurgiya, Moscow (1969).
4. S. N. Votinov et al., in: Radiation Physics of Solids and Reactor Material Handling [in Russian], Atomizdat, Moscow (1970).

COHERENT BEAM INSTABILITY IN THE IFVÉ ACCELERATOR*

V. I. Balbekov and K. F. Gertsev

UDC 621.384.612

The transverse coherent beam instability in the IFVÉ accelerator has an instability threshold of $\sim 4 \cdot 10^{11}$ protons/cycle and at an intensity of more than 10^{12} protons/cycle this leads to losses during the first 50-100 msec of acceleration. In the majority of cases, the losses are associated with vertical oscillations. The radial instability is less dangerous, as it develops more slowly and has a higher threshold.

Usually, the 10th amplitude harmonic of the instability is excited (betatron frequency about 9.8). A marked addition of other harmonics has been observed in the case of intensity scattering of the bunches, exceeding 10-20%. In this case, only a part of the bunches usually oscillates. For example, with gradual filling of the cycle, bunches with identical intensity are excited to an amount containing the greater portion of the beam (Fig. 1). The increment is approximately proportional to the number of particles contained in the oscillating bunches, and therefore an increase in the number of "inferior" bunches can lead to its increase, despite the reduction of the overall intensity (in this case the "high" bunches are stationary). In the case of equal intensity distribution with respect to both groups, independent oscillations of parts of the beam originate with different frequencies and increments.

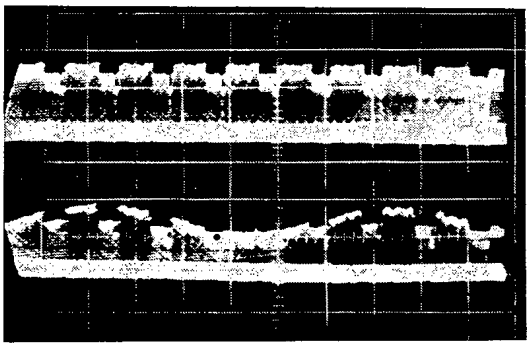

Fig. 1

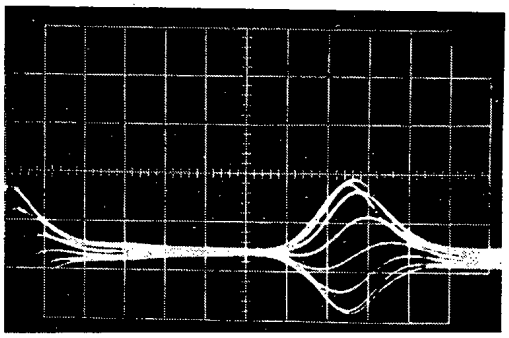

Fig. 2

Fig. 1. Sum and difference signals from a vertically positioned sensor of the beam during gradual filling of the cycle.

Fig. 2. Vertical oscillations of a bunch when $p(dQ/dp) = -6$.

*High-Energy Physics Research Accelerator.

Translated from Atomnaya Énergiya, Vol. 41, No. 6, pp. 408-412, December, 1976. Original article submitted December 23, 1975.

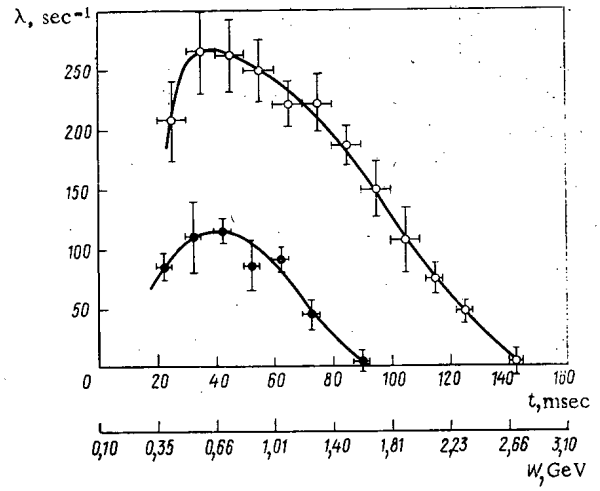

Fig. 3. Dependence of increments on the time and energy in a standard acceleration mode: ○) λ_z; ●) λ_r.

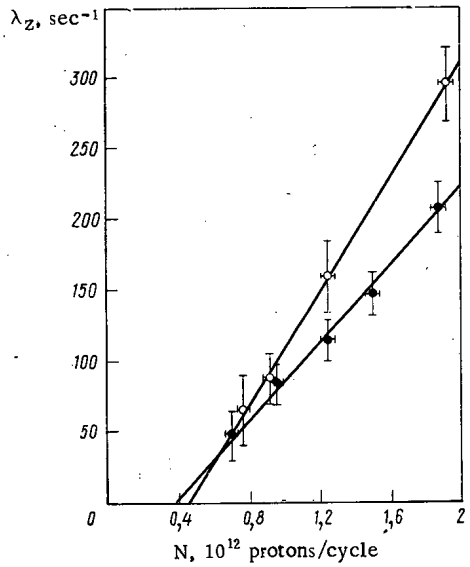

Fig. 4

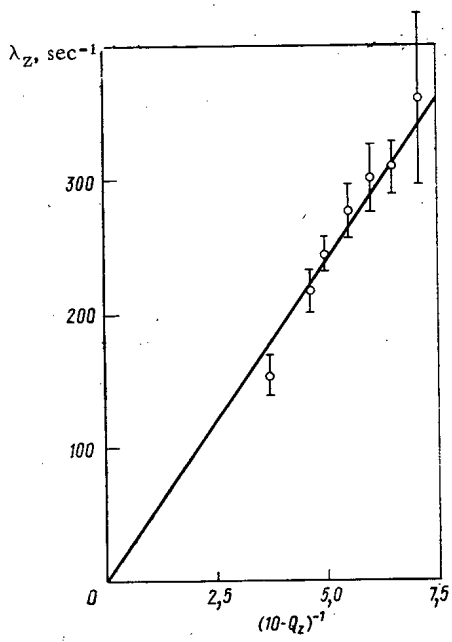

Fig. 5

Fig. 4. Dependence of the vertical oscillation increment on the beam intensity at energies of 0.66 (○) and 0.97 GeV (●).

Fig. 5. Dependence of the vertical oscillation increment on the betratron frequency at an energy of 0.66 GeV.

With vertical oscillations of an individual bunch (Fig. 2), the signal is proportional to the dipole moment, i.e., the product of the displacement and the linear charge density. The interval between successive scans is equal to five revolutions. The shape of the signal corresponds to theoretical concepts, according to which the transverse displacement of the beam within the limits of the bunch has the form

$$z = z_0 \cos\left[\Omega Q t - \frac{(\Omega Q)'\varphi}{q\Omega'}\right] = z_0 \cos\left[\frac{\Omega^2 Q'}{\Omega'} t - \frac{(\Omega Q')\vartheta}{\Omega'}\right], \quad (1)$$

where Ω is the angular velocity; Q is the betatron frequency; φ is the phase of the observed part of the bunch relative to the phase of the accelerating voltage; q is the multiplicity; the primes denote differentiation with respect to momentum and the frequencies and their derivatives refer to a synchronous particle [1].

In order to suppress the instability, a narrow-band system of feedback [2] is used, which contains two identical channels – for vertical and radial directions. During the investigation of instability, one of the channels switched off at 20-30 msec. The exponential increase of amplitude of the coherent oscillations was recorded with a storage oscillograph, and several measurements were carried out of the amplitude. The increment was calculated by the formula

$$\lambda = \frac{1}{t_2 - t_1}\left(\ln\frac{A_2}{A_1} + \frac{H_2 - H_1}{H_2 + H_1}\right), \qquad (2)$$

where $t_{1,2}$ are the instants of measurement; $A_{1,2}$ are the amplitudes; $H_{1,2}$ is the magnetic field strength. The second term is introduced to take account of adiabatic damping. The interval t_2-t_1 usually was equal to 2.5 msec and was chosen statistically during 15-20 acceleration cycles.

The curve shown in Fig. 3 was obtained with an intensity of $2 \cdot 10^{12}$. For every point, the time intervals are shown over which averaging was carried out, and the mean-square spread of the measured increments. At an energy of ≤ 0.4 GeV, the increase of the amplitudes deviates from the exponent in view of the effect of the initial oscillations and also because of the coupling resonance $Q_r = Q_z$.

Measurements of the dependence of the increment on the intensity were carried out for a different energy (Fig. 4). The intensity was controlled by the installation in the inlet channel of scattering screens of different transparency. The curves obtained are close to linear and the threshold of instability in both cases is equal to $\sim 4 \cdot 10^{11}$.

In order to establish the causes of instability, the dependence of the increment on the betatron frequency was measured (Fig. 5). When the frequency is changed, the beam intensity was changed somewhat, $N = (1.9\text{-}2.2) \cdot 10^{12}$. The increment is reduced to the average intensity of $2 \cdot 10^{12}$ by the formula (see Fig. 4)

$$\lambda = 1.6\lambda_m / (N \cdot 10^{-12} - 0.4). \qquad (3)$$

The relation obtained, $\lambda_z \sim (10 - Q_z)^{-1}$, is characteristic for wall instability in a chamber with thin walls. Actually, in the given case, the wall thickness (0.4 mm) is considerably less than the thickness of the skin layer (2-2.5 mm).

Further investigations showed that the increments depend on the pressure of the residual gas (Fig. 6). The pressure in the experiment was increased by the switching-off part of the pumps. In this case, the increment of the 10th harmonic decreased, which can be explained by the interaction of the beam with positive ions

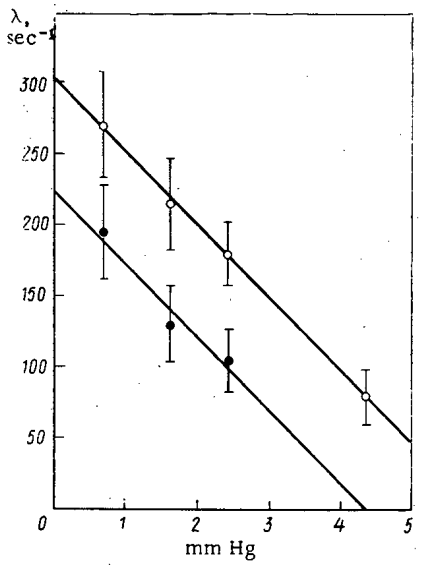

Fig. 6

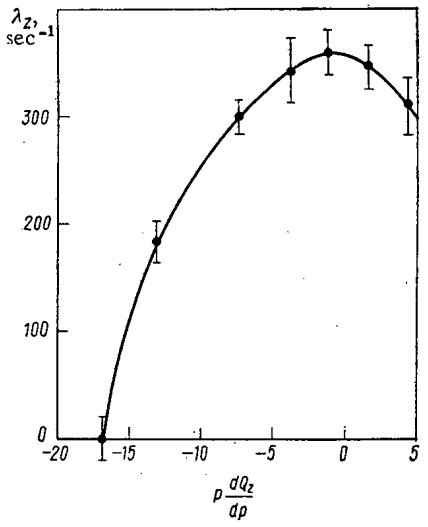

Fig. 7

Fig. 6. Dependence of the increments on the pressure of the residual gas at an energy of 0.97 GeV: ○) λ_z; ●) λ_r.

Fig. 7. Dependence of the increment of the vertical oscillations on the chromaticity at an energy of 0.97 GeV.

that are formed by ionization of the residual gas. This interaction [3] leads to the excitation of a coherent instability of harmonics with the wave number $k < Q$ and their suppression when $k > Q$. We note in this connection, that with a maximum pressure of $4.3 \cdot 10^{-6}$ mm Hg an instability of the 9th harmonic of the radial oscillations was observed sometimes; however, the increment in view of its small value could not be measured. Electron instabilities seem to be of low probability, as the buildup of an appreciable number of electrons in the bunched beam with the stated parameters is impossible.

In determining the dependence of the increment on the chromaticity, the latter was adjusted by changing the correction current in the square pole faces (Fig. 7). The current in the windings which focus and defocus the units was chosen so that the chromaticity of the radial betatron oscillations remained constant. With a change of current, the betatron frequency and the beam intensity were changed somewhat. The increment is reduced to the average frequency $Q_z = 9.825$ by the formula (see Fig. 5)

$$\lambda_z = \lambda_m \ (10 - Q_z)/0.175. \tag{4}$$

Normalization with respect to intensity was carried out by formula (3). Figure 7 coincides completely with the previous results. Actually, the wall and ion instabilities are multireversible. For the oscillation mode of the bunch shown in Fig. 2 and formula (1), the dependence of the increment on the chromaticity should be determined by the factor

$$\Lambda \simeq 1 - \left(\frac{\Omega Q'}{q\Omega'}\right)^2 \overline{\varphi^2} \simeq 1 - \left(p \frac{dQ}{dp} \frac{\gamma^2}{q} \sqrt{\overline{\varphi^2}}\right)^2, \tag{5}$$

where $\sqrt{\overline{\varphi^2}}$ is the mean-square phase length of the bunch. The first two terms of the expansion in series are written here, so that this formula can be used when $\Lambda \gtrsim 0.5$. It follows from formula (5) and Fig. 7 that $\sqrt{\overline{\varphi^2}} \simeq 0.4$. Processing of the oscillogram in Fig. 2 gives $\sqrt{\overline{\varphi^2}} \simeq 0.5$.

Let us compare quantitatively the results obtained with the theoretical results. The increment of the vertical instability can be written in the form

$$\lambda_z = \frac{r_p R \Lambda_z (N - N_{th})}{\pi \gamma Q_z (k - Q_z)} \left[\frac{c^2 g \epsilon_z}{4\pi\sigma d b^3} - \frac{\eta \gamma^2 \omega_z^2 \tau^2 P}{(\gamma^2 - 1) a_z (a_r + a_z)(\omega_z^2 \tau^2 + 1)}\right]. \tag{6}$$

The numerical values of the variable parameters refer to an energy of 0.97 GeV: $r_p = e^2/mc^2 = 1.54 \cdot 10^{-16}$ cm is the classical radius of the proton; $R = 2.36 \cdot 10^4$ cm is the average radius of the accelerator; $N = 2 \cdot 10^{12}$ is the beam intensity; $N_{thr} = 0.4 \cdot 10^{12}$ is the threshold intensity; Λ_z is a factor which takes account of the dependence of the increments on the chromaticity and is determined by formula (5) or from Fig. 7; $\gamma = 2.03$ is the relativistic factor; $Q_z = 9.825$ is the betatron frequency; $k = 10$ is the number of the harmonic; $c = 3 \cdot 10^{10}$ cm/sec is the velocity of light; $g = 1.57$ is the coefficient of linear expansion of the vacuum chamber due to corrugation; $\epsilon_z = 0.85$ is a factor which takes account of the ellipticity of the chamber cross section; $\sigma = 1.3 \cdot 10^{16}$ sec^{-1} is the conductivity of the chamber wall; $d = 0.04$ cm is the thickness of the chamber wall; $b = 5.75$ cm is the half-height of the chamber; $\eta = 0.82 \cdot 10^9$ mm Hg$^{-1} \cdot$ sec^{-1} is the number of ions formed by a single proton per second at a pressure of 1 mm Hg; $P = 6.9 \cdot 10^{-7}$ mm Hg is the pressure; $a_z = 1$ cm is the half-height of the beam; $a_r = 2$ cm is the half-width of the beam; $\omega_z = 1.94 \cdot 10^5$ sec^{-1} is the coherent oscillation frequency and $\tau = 5 \cdot 10^{-6}$ sec is the effective time of interaction of the ions with the proton beam.

The first part of this formula, which takes into account the wall effect, differs from the well-known expression for the wall instability increment [4, 5] by the factors g, ϵ_z, and δ/d, where the latter is introduced because the thickness of the skin layer δ is considerably greater than the wall thickness d. The effect of the ions is taken into account in the second part of formula (6) in accordance with [3]. It should be noted that the parameter τ depends on the model used and the calculation is carried out with difficulty; the value taken is a quite rough estimate.

When $\Lambda_z = 1$, formula (6) gives $\lambda_z = 450$ sec^{-1}, and the wall contribution amounts to 510 sec^{-1}; the ion contribution is 60 sec^{-1}. The corresponding experimental values (see Figs. 6 and 7) are: $\lambda_z = 360 \pm 20$ sec^{-1}, wall contribution 400 sec^{-1} and the ion contribution is 40 sec^{-1}, which are $\approx 30\%$ less than the calculated values. It is possible that the discrepancy is explained by the scatter of intensity of the bunches. It was mentioned above that scatter weakens the coupling of the bunches and leads to a reduction of the increments. In the calculation, all the bunches were assumed to be identical.

The cause of the increase of the increments with increase of energy when $W < 0.65$ GeV (see Fig. 3) could not be established. Although with a low energy the damping effect of the ions increases, this is inadequate for explaining the observed relations. The chromaticity of the betatron oscillations in this region is small

$\left(-p\frac{dQ}{dp} \sim 4-5\right)$, so that its effect is almost absent. It is possible that here there is strong cubic nonlinearity of the magnetic field and a correspondingly higher threshold of instability, but the experimental verification of this hypothesis was not undertaken.

Radial instability has much in common with vertical instability. Mainly the 10th harmonic is excited; the form of the radial oscillations of the bunch is the same as in Fig. 2; the increments depend approximately identically on the energy (see Fig. 3). The radial increment increases with approach to complete resonance and decreases with increase of pressure of the residual gas (see Fig. 6). The experimental and calculated values of the increment differ by no more than a factor of two. However, the characteristics of the radial instability are considerably less stable than the vertical instability. This can be seen, for example, from Figs. 3 and 6. According to the first, the increment at 57 msec amounts to ~ 100 sec^{-1}, and according to the second, it is ~ 200 sec^{-1}, although the principal parameters of the accelerator were unchanged. Certain data confirm that the cause should be found first and foremost in the instability of the threshold.

Thus, the cause of coherent instability in the IFVÉ accelerator is the interaction of the beam with the chamber walls, and the interaction with positive ions makes a relatively small stabilizing contribution. For vertical instability, the calculated and experimental data coincide with an accuracy of up to 30%. In respect of radial instability, the conclusions should be considered as preliminary, because the experimental data are incomplete, although there are no factors which contradict the supposition of a single excitation mechanism for both types of oscillations.

The authors thank V. L. Ushkov for assistance given by him during the measurement of the dependence of the increment on the pressure.

LITERATURE CITED

1. C. Pellegrini, Nuovo Cimento, 64-A, 447 (1969).
2. K. F. Gertsev et al., IFVÉ Preprint, SKU 74-85 (1974).
3. G. Hereward, CERN MPS/Int., DL-64-8 (1964).
4. V. I. Balbekov and A. A. Kolomenskii, At. Energ., 19, No. 2, 126 (1965).
5. L. Laslett, V. Neil, and A. Sessler, Rev. Scient. Instrum., 36, 436 (1965).

MULTIORBIT INDUCTION ACCELERATORS

A. A. Zvontsov, V. A. Kas'yanov, and V. L. Chakhlov

UDC 621.384.6

It is well known that the space charge of the beam limits the number of particles accelerated in a cycle. Their number can thus be increased by simultaneously accelerating several beams in the one emitter unit. Consequently, we must have several equilibrium orbits in the one emitter unit. We shall call accelerators of this type multiorbit accelerators. The equilibrium orbits in the form of concentric circles are situated in the one plane, while several such planes situated one above the other can be contained in a single unit. The field strength at orbits of radii $r_{01}, r_{02}, \ldots, r_{0i}$ must satisfy the conditions

$$\bar{H}_z(t) = 2H_{z0i}(t) \quad \text{for} \quad r = r_{0i};$$

$$\bar{H}_z(t) > 2H_z(t) \quad \text{for} \quad r < r_{0i};$$

$$\bar{H}_z(t) < 2H_z(t) \quad \text{for} \quad r > r_{0i}, \quad 0 < n(r_{0i}) < 1,$$

where n is the index giving the rate of decay of the field, $\overline{H_Z}(t)$ is the field strength averaged over the area enclosed by an orbit, and H_{Z0i} is the field strength at the i-th equilibrium orbit.

If the accelerated particles have equal energies the field strength at the radii $r_{02}, \ldots, r_{0i}$ is connected with the controlling field strength at the r_{01} orbit by the relation

$$H_{z0i} = H_{z01} r_{01}/r_{0i} = H_{z01}/\alpha_i.$$

The total limiting volume charge is determined by the approximate formula

$$Q = \frac{e}{m_0 c^2 (1-\beta^2)^{3/2}} r_{01} H_{z01} \sum_{i=1}^{k} \frac{s_i \nu_{xi}}{\alpha_i},$$

where s_i and ν_{xi} are the transverse cross-sectional area of the region where the focussing forces act around the i-th equilibrium orbit, and the frequency of radial betatron oscillations respectively. In this type of accelerator it is possible to obtain a powerful pulse of radiation at a given time, or several less dense pulses displaced in time with respect to each other.

Controlling fields with this behavior are produced by pole pieces of comb-type construction, for example, or by current-carrying coils. Calculations show that the ratio of the mass of the electromagnet of a multiorbit accelerator to the total mass of k electromagnets with a single equilibrium orbit decreases asymptotically to some number which indicates the relative contribution of the "additional" devices to the overall mass of the electromagnet. Such an accelerator can produce spatially composite radiation fields, e.g., ribbon-type fields, while the radiation dose strength can be regulated along the length of the ribbon by varying the focussing forces and the volume of the region in which they act. In this case the specific characteristics of the accelerator are enhanced by a factor of three or four.

(No. 880/8419. Original article submitted July 14, 1975; abstract submitted July 20, 1976. Complete text 0.5 author's folios, 2 Figs., 3 Refs.)

Translated from Atomnaya Énergiya, Vol. 41, No. 6, pp. 413-416, December, 1976.

PRESSURE CHANGE IN A VESSEL WITH SATURATED WATER ON BEING UNSEALED

A. V. Alferov, V. V. Fisenko, and A. D. Shcherban'

UDC 621.039.58

The present article considers the change in pressure in an adiabatically isolated vessel filled with saturated water and having an aperture through which the water can leak out. The result of such measurements can be used to evaluate the consequences of an emergency in the primary circuit of a nuclear reactor connected with a breakdown in its pressure sealing. On decompression of the reactor circuit the water pressure rapidly falls to a value corresponding to the saturation pressure at the given temperature. The change in pressure of the water after it has boiled is investigated on the following assumptions: the circuit parameters are regarded as being concentrated, the vessel filled with saturated water is regarded as an adiabatically isolated system, and the state of the medium in the vessel is regarded as an equilibrium state during the leakage process.

Two extreme models for the behavior of the medium in the vessel are described. There is the heterogeneous model which assumes that during the leakage process the free level of saturated water is maintained in the vessel, and that all the steam which is formed remains above this level. There is also the homogeneous model which treats the medium in the vessel as a uniform two-phase mixture.

The analysis shows that on the decompression of a vessel containing a homogeneous two-phase mixture the rate of pressure change in the vessel is proportional to the square of the velocity of sound in the mixture

$$\frac{dp}{d\tau} = -a_m^2 \frac{G}{V_0}, \qquad (1)$$

where a_m is the velocity of sound for thermodynamic equilibrium in a homogeneous two-phase medium [1], G is the quantity of steam–water mixture leaking out of the vessel per unit time, and V_0 is the geometric volume of the vessel.

Equation (1) for determining the rate of pressure change in the vessel can be used not only for the model in which the state of the medium in the vessel is homogeneous but also for the model in which it is heterogeneous. In the latter case the velocity of sound is calculated from values of the thermophysical parameters of the coolant determined for the vessel as a whole.

Calculated, Eq. (1), and experimental data, obtained under conditions close to those of normal operation in a "Humboldt Bay" atomic electric power plant [2] are compared in Fig. 1. In this case the flow rate through the breakdown cross section was determined in accordance with the recommendations of [3].

We have thus considered two limiting models for the process of parameter change in an adiabatically isolated vessel with a two-phase medium when there is a leakage of coolant from the vessel. In one model the phases are in a separate state in the vessel, and in the other model the medium is a two-phase homogeneous mixture.

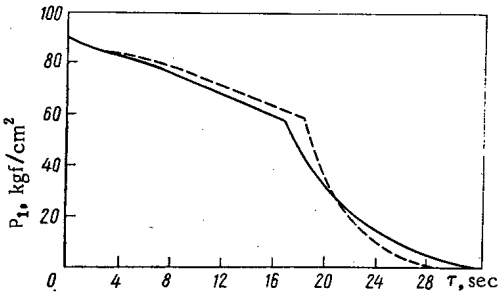

Fig. 1. Pressure change in a vessel with a leak. – – – –) Calculations from the author's model, ——) experiment.

It is shown that in both cases the rate of pressure change in the vessel is proportional to the square of the velocity of sound in the two-phase mixture at thermodynamic equilibrium.

(No. 881/8432. Original article submitted July 18, 1975;
abstract submitted February 5, 1976. Complete text
0.45 author's folios, 1 Fig.; 7 Refs.)

LITERATURE CITED

1. L. D. Landau and E. M. Lifshitz, Mechanics of Continuous Media [in Russian], Gostekhizdat, Moscow (1954).
2. E. A. E. Barton, ASME , Rep. 61-WA-222 (1962).
3. V. V. Fisenko, Text from Proceedings of the Fifth All-Union Conference on Heat-Exchange and Hydraulic Resistance of Two-Phase Flow in Sections of Power Machines and Apparatus [in Russian], Izd. Polzunov TsKTI, Leningrad (1974), p. 230.

QUANTITATIVE ESTIMATES OF THE ENERGY OF X-RAY FIELD BACKSCATTERED FROM AIR

F. L. Gerchikov

UDC 539.171:539.12

The increasing engineering application of x-ray radiation in instruments, control systems, and analysis requires detailed estimates of the background of x-rays backscattered from air for optimum equipment synthesis.

Let an x-ray radiator generating energy E_0, MeV, with the average energy of the quanta equal to E_γ be located in air at a distance H from the surface of the earth (Fig. 1). Assuming that the radiation in a collimation angle $2\psi_0$ is isotropic and a total absorption detector with unit cross section is located at the same height as the radiator at a distance d (base) from it, we obtain the energy of x-radiation backscattered from air at the input of the detector $E_a = E_0 L_a$. The transmission coefficient of the energy of radiation backscattered from air is $L_a = f(E_\gamma, d, \psi_0, H)$.

Choosing the numerical values of this equation in the ranges $E_\gamma = 0.06$–0.2 MeV, $d = 0.1$–3m, $\psi_0 = 7.5$–$75°$, the values of L_a and their dependence on the right-hand side of the equation can be determined on a BÉSM-4 computer.

The results of the computation showed that the background energy of x-rays from the air is determined by the energy of the quanta of the primary radiation, the geometry of the receiving–tramsitting channel, and the collimation angle of the radiation (Fig. 2). Choosing these parameters, one can obtain the optimum signal-to-noise ratio at the input of the detector for minimum mass-size and energy characteristics of the equipment.

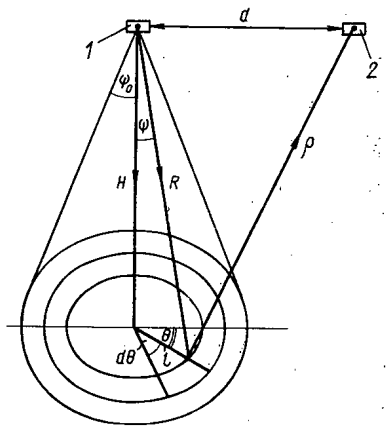

Fig. 1. Geometry of the experiment: 1) radiator; 2) detector.

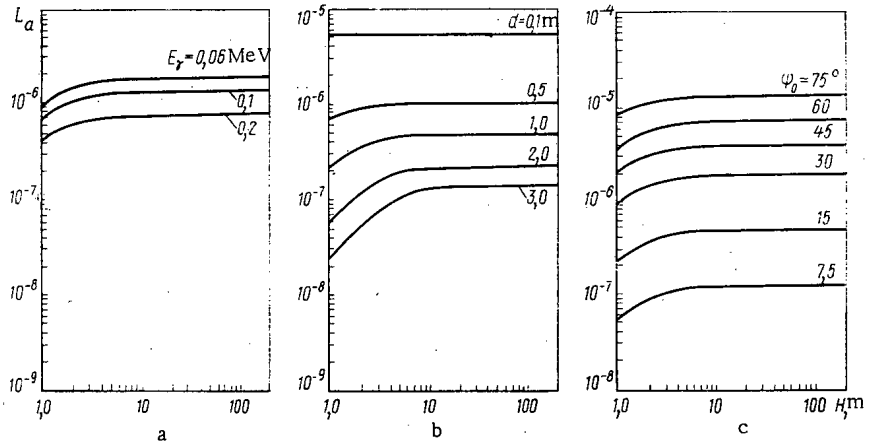

Fig. 2. The dependence of the energy of backscattered x-ray radiation in air on the energy of the quanta of primary radiation for d = 1 m, $2\Psi_0 = 60°$ (a); on the base for $E_\gamma = 0.06$ MeV, $2\Psi_0 = 30°$ (b); on the angle of collimation of the radiator for $E_\gamma = 0.06$ MeV, d = 1 m (c).

(No. 882/8573. Original article submitted December 12, 1975; abstract submitted August 10, 1976. Complete text 0.35 author's folios, 3 Figs., 9 Refs.)

COMPUTATION OF THE RADIATION FIELD OF A UNIDIRECTIONAL POINT SOURCE OF FAST ELECTRONS BY THE MONTE CARLO METHOD

A. V. Plyasheshnikov and A. M. Kol'chuzhkin

UDC 539.121.72

The radiation field of a unidirectional point source of fast electrons is computed in this work by the Monte Carlo method in the model of grouping of the small energy transfers [1, 2]. These computations showed that the maximum half-width of the radial distribution of the transmitted electrons expressed in units of the initial range R_0 has a weak dependence on the initial energy E_0 of the beam and the atomic number of the absorber Z and comprises $\sim 0.3\ R_0$.

The half-width of the radial distribution of the reflected electrons increases monotonically with the thickness of the barrier z and for $z \sim 0.3\ R_0$ it reaches saturation corresponding to reflection from semi-infinite absorber. The half-width of the radial distribution of electrons reflected from a semi-infinite absorber, which equals $\sim 0.3\ R_0$, increases with the increase of E_0 and decrease of Z.

The radial distribution of the absorbed energy of electrons in an absorber consisting of plane layers of different substances gets sharply reduced in width during the transit of the beam from the lighter substance to the heavy substance. For a reverse combination of the layers, a strong widening of the radial distribution in the light absorber is observed.

It is shown that the form of the energy distribution of electrons from a unidirectional point source has a weak dependence on the distance of the point of observation from the axis of the beam.

LITERATURE CITED

1. A. V. Plyasheshnikov and A. M. Kol'chuzhkin, Izv. Vyssh. Uchebn. Zaved., Fizika, 1, 81 (1975).
2. A. V. Plyasheshnikov and A. M. Kol'chuzhkin, At. Energ., 39, No. 1, 53 (1975).

(No. 883/8686. Original article submitted March 9, 1976.
Complete text 0.45 author's folios, 6 Figs., 9 Refs.)

FLOATING CONTROL OF A POWER REACTOR WITH RESPECT TO A PARAMETER WITH TIME LAG

B. G. Ogloblin and K. N. Prikot

UDC 621.039.562:621.039.514

The paper considers the possibility in principle of regulating, with respect to a parameter with time lag, a power reactor which has no self-regulating effect. The root hodograph method can be used to obtain an analytic form for the condition which determines the permissible time lag of the parameter to be regulated. This can be done without having to have recourse to the simplifications of nuclear reactor kinetics which are usual in an analytic investigation, by replacing the six groups of retarded neutrons by one or two equivalent groups, and confining the number of internal inverse couplings in the reactor to one or two. This condition has the following form

$$T_L < T_{L\max} = \left[\sum_{i=1}^{6} \lambda_i + \sum_{j=1}^{5} S_j + \sum_{\nu=1}^{r} \frac{K_\nu}{T_\nu}\right]^{-1},$$

where T_L is a time constant characterizing the time lag of the parameter to be regulated, $T_{L\max}$ is a time constant of the parameter to be regulated for which the system under consideration becomes structurally unstable, λ_i are the decay constants of the nuclear-precursors of the i-th group of retarded neutrons, S_j are the roots of the characteristic equation of the transfer function of a zero power nuclear reactor (j = 1.5), and K_ν and T_ν are the transfer coefficient and time constant in the transfer function of an aperiodic link describing the ν-th internal inverse coupling in the reactor. The sign of the transfer coefficient K_ν is determined by the sign of the internal inverse coupling.

On the basis of operating stability conditions it is shown that in the general case the amplification coefficient of the regulator is bounded above and below. The results obtained can be used to determine the allowable time lag for the neutron power regulator.

(No. 884/8692. Original article submitted March 9, 1976. Complete text 0.4 author's folios, 1 Fig. 5 (Refs.)

DETERMINATION OF NEUTRON SPECTRUM FROM MEASUREMENTS WITH A SMALL NUMBER OF DETECTORS

G. M. Obaturov and A. A. Tumanov

UDC 539.125.164

The present paper considers the processing of data from a small set of spectrometer detectors intended for emergency dosimetry. This set consists of solid-state tracking detectors with fissionable layers of ^{239}Pu in cadmium, ^{239}Pu, ^{237}Np, and ^{238}U behind a boron filter of thickness 1 $g \cdot cm^{-2}$ of ^{10}B, and of an activation detector of ^{31}P (n, p) in cadmium. Preliminary information about the fluence, kerma and spectrum of the neutrons is extracted by the method of effective threshold cross sections using the mean values of the specific kerma for the separate energy intervals determined by the threshold value of the energy. Values of the possible errors of some of the effective cross sections and specific values of the kerma for the neutron spectrum under consideration are appreciably reduced on being refined with the help of spectral indices.

More detailed spectral information is obtained on establishing the neutron spectrum φ (E). Here it is assumed that the simple parametric representation of the neutron spectrum is possible

$$\varphi(E) = x_1 \frac{1}{\beta\sqrt{2\pi}} \exp[-(u-\alpha)^2/2\beta^2] + x_2 E^{\gamma}, \quad (1)$$

$$u = \ln E_0/E; \quad E_0 = 10 \text{ MeV}.$$

The parameters α, β, γ, x_1, and x_2 are determined by adjusting the representation (1) to give the best fit to the data of the detectors. The searching process is repeated several times, and in subsequent cases parameters are considered from some regions determined in the preceding case. The parameters α and β are initially estimated with the help of specified spectral indices.

Theoretical and experimental tests have shown that the spectrum, fluence and kerma of the neutrons are reproduced well over the whole range of energies. The errors in the fluence and kerma of the neutrons are < 4 and 9%, respectively. A mean-square error of ± 10% in the detector readings which is normally distributed increases the error in the fluence and kerma by roughly a factor of two.

The work carried out shows the usefulness of a small spectrometer set and simple methods of processing detector data for solving various problems in neutron dosimetry within a wide range of energies.

(No. 885/8742. Original article submitted April 9, 1976.
Complete text 0.5 author's folios, 2 Tables, 6 Figs. and
7 Refs.)

LETTERS

SPUTTERING OF METALLIC SURFACE BY FISSION FRAGMENTS

B. M. Aleksandrov, I. A. Baranov,
N. V. Babadzhanyants, A. S. Krivokhatskii,
and V. V. Obnoskii

UDC 546.799

The study of the sputtering of metals under the action of bombarding particles makes it possible to obtain data about radiation damage, pertaining to the instant when the particle interacts with the material. Taking into account the importance for the theory [1-4] of the presence or absence in metals of damage commensurate with that detected during sputtering of fine-grained nonconducting thin layers by fission fragments [5] or during observation of tracks in thin films with the aid of an electron microscope [6], it is possible to measure the sputtering of a 20-μ nonoxidizing gold foil by fission fragments from an external source. For comparison, we also found the sputtering of thin layers of gold previously deposited on glass (nonconducting substrate) and on platinum (conducting substrate) by thermal evaporation in a vacuum of $3 \cdot 10^{-5}$ mm Hg. A thin layer of ^{252}Cf emitting $6 \cdot 10^6$ fission fragments per second served as the source of fragments. The energy of a heavy and a light fragment after passage through two protective nickel films was 70 and 90 MeV, respectively. The foil sputtering took place in a vacuum chamber with freezing-out of oil vapor. Sputtering of thin layers of gold on platinum and glass was carried out simultaneously in this chamber with fission fragments from two other ^{252}Cf sources. Electron-microscopic examination of control samples on thin carbon film present on glass during evaporation of the gold showed that only ~25% of the glass surface was covered with a gold layer having a grain size of 30-150 Å. During sputtering of the foil and thin layers on glass and platinum nickel films of a thickness of ~100 $\mu g/cm^2$ acted as collectors of the sputtered gold atoms. These collectors were located between the fission-fragment sources and the sputtered surface, at a distance of 1 mm from the latter. The integrated fission-fragment flux on the gold foil during the sputtering was $4.0 \cdot 10^{11}$, and that on gold on glass was $5 \cdot 10^{11}$ and on gold on platinum, $4.8 \cdot 10^{11}$ fission fragments per sec. After the sputtering, these three collectors were irradiated in a reactor with a thermal neutron flux of density $8 \cdot 10^{13}$ neutrons/($cm^2 \cdot$ sec) at a temperature of 60°C for 3 days to accumulate ^{198}Au. At the same time, a pure nickel collector and a standard collector on which 0.0033 μg of gold had been deposited from solution were also irradiated. The quantity of ^{197}Au striking the collectors as a result of sputtering by fission fragments was determined by comparing the area of the gamma peaks with the energy 411 keV (^{198}Au) obtained by analyzing the collectors and the standard collector after irradiation in the reactor. Measurements on a γ-ray spectrometer with NaI crystal and silicon-lithium detector (the resolution of the latter was better than 1 keV) showed that $5.4 \cdot 10^{12}$, $1.2 \cdot 10^{14}$, and $1.4 \cdot 10^{15}$ atoms ^{197}Au, respectively, struck the collectors located above the gold foil, glass, and platinum. The following sputtering coefficients were found in this way to within ~25%: 13, 240, and 3000 atoms/fission fragment for the gold foil, for gold on glass, and for gold on platinum, respectively. It is clear that the sputtering coefficient of heavy gold foil proved to be smaller by a factor of $\sim 10^2$ than that of fine-grained gold layers on glass and platinum. The large coefficients for sputtering of thin layers by fission fragments are explained [7] by mechanisms of either ion fragmentation or a thermal electronic peak based on inelastic interactions of fission fragments with atoms of matter [2]. The low sputtering coefficient of the gold foil can probably be explained primarily by elastic interactions [8]. It should be noted that when gold foil was sputtered by fragments by the fission of ^{235}U by thermal neutrons the value obtained for the sputtering coefficient was 720 ± 240 atoms/fission fragment [9], i.e., a value differing from the results of the present paper by a factor of 10^2. It should also be noted that in actual fact a thin film and not bulk metal was sputtered in [9] since the foil thickness was less than the fission-fragment path. Since the sputtering was carried out in a reactor, along with fission fragments recoil nuclei also sputtered the foil surface, and this must have made a significant contribution to the sputtering [10].

Translated from Atomnaya Énergiya, Vol. 41, No. 6, pp. 417-418, December, 1976. Original article submitted June 23, 1975.

A number of papers have studied the sputtering of uranium and plutonium metal plates by fission fragments which were produced inside the material and upon leaving it had a continuous energy spectrum. The sputtering coefficients varied from 30 to $1 \cdot 10^3$ atoms/fission fragment. The results are discussed in [4]. In all cases the surface of the uranium and plutonium metal was covered with an oxide film of uncontrolled thickness; this affected the sputtering of the layer surfaces [11]. Moreover, neutrons participated along with fission fragments in the sputtering of the uranium and plutonium.

Experiments show that when a fission fragment penetrates into bulk metal it does not produce extensive damage as in the case in thin fine-grained layers. The results confirm the conclusions from electron-microscopic examination and eliminates the discrepancy noted in [5] a propos of the data of [9]. The cause of intensive sputtering of a thin fine-grained layer of gold on platinum remains unexplained.

The authors thank L. M. Krizhanskii and V. V. Smirnov for discussing the results, V. P. Éismont for giving us the opportunity to make measurements on a gamma spectrometer with a silicon-lithium detector, and E. S. Rozhkov and G. A. Firsanov for their assistance in the work.

LITERATURE CITED

1. Proc. Inter. Topical Conf. on Nuclear Track Registration, V. I. Clermont-Ferrand (1969).
2. D. Morgan and V. Vliet, Contemp. Phys., 11, 173 (1970).
3. Ya. E. Geguzin, in: Proceedings of School on Radiation and Other Defects in Solids [in Russian], Vol. 1, Tbilisi (1974), p. 258.
4. V. A. Bessonov, At. Energ., 37, No. 1, 52 (1974).
5. B. M. Aleksandrov et al., At. Energ., 38, No. 1, 47 (1975).
6. J. Kelsch, O. Kammerer, and P. Buhl, J. Appl. Phys., 33, 1475 (1962).
7. B. M. Aleksandrov et al., At. Energ., 33, No. 4, 821 (1972).
8. G. Brinkman, Effect of Nuclear Radiation on the Structure and Properties of Metals and Alloys [Russian translation], Metallurgizdat, Moscow (1957).
9. N. Riehl, Kerntechnik, 3, No. 12, 518 (1961).
10. R. I. Garber et al., Pis'ma Zh. Eksp. Teor. Fiz., 7, 296 (1968).
11. B. M. Aleksandrov et al., At. Energ., 36, No. 2, 139 (1974).

THE COMPOSITION OF THE RADIOLYSIS PRODUCTS OF THE SYSTEM $CO_2 - H_2O(D_2O) -$ OIL, FORMED IN A KS-150 REACTOR

M. I. Ermolaev, A. K. Nesterova, and V. F. Kapitanov

UDC 621.039.524:543.3:547.29

Radiolysis of H_2O, D_2O, CO_2, and mineral oils gives rise to a number of organic products including mono-, di-, tri-, and hydroxycarboxylic acids [1-3]. In a heavy-water moderator in contact with CO_2 and the impurities H_2O and oil which are present in it at a pressure of 65 atm, organic acids accumulate, sharply reducing the pD of D_2O.

In industrial conditions, the only analysis is determination of the permanganate and bichromate oxidizability of D_2O, but this is not enough to control the accumulation of the acids formed which can corrode the structural materials.

Translated from Atomnaya Énergiya, Vol. 41, No. 6, pp. 418-419, December, 1976. Original article submitted November 4, 1975.

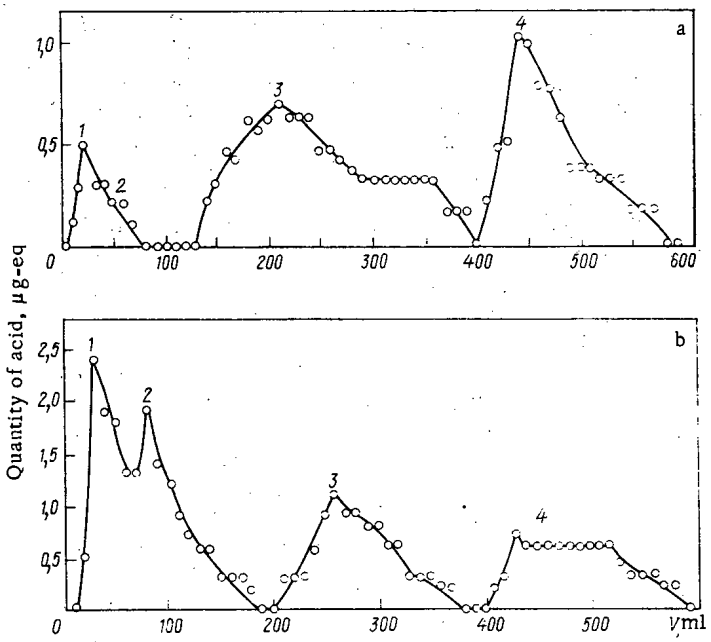

Fig. 1. Separation chromatograms of volatile acids from irradiated water (a) and standard mixture (b). 1) n-Butyric acid; 2) propionic acid; 3) acetic acid; 4) formic acid.

In this article we give a method of separating and determining volatile monocarboxylic acids, formed in microquantities, by means of liquid chromatography and infrared spectroscopy without previous concentration.

The investigation involved chromatographic separation of the monocarboxylic acids, determination of their amount, and subsequent identification of the evolved oxygen by means of the infrared absorption spectra.

For separation of n-butyric, propionic, acetic, and formic acids, the chosen carrier was silicon (IV) oxide (GOST 9428-60) with particle sizes of 16-60 mesh. It was dried at 110-120°C for 2 days (unlike the silica gel used by Stradomskaya and Goncharova [4] and by the authors of [5]). The nonmobile phase was H_2O which is necessary for effective separation. The maximum quantity of H_2O was 37% of the mass of carrier. The optimum ratio between the carrier and the volume of the sample was 7:1. n-Butyric and propionic acids were eluted with benzene. Acetic acid was washed out with 1%, and formic acid with 2% solutions of butanol in benzene; we selected fractions of 10 ml and determined their oxygen contents by alkalimetry.

In the irradiated water, the concentrations of n-butyric acid and propionic acid was $1.7 \cdot 10^{-6}$, of acetic acid $10.8 \cdot 10^{-6}$, and of formic acid $6.6 \cdot 10^{-6}$ g-eq/ml with a relative error of less than 10%. Figure 1 shows chromatograms of the water under test and of a standard mixture of acids.

The separation of the volatile monocarboxylic acids was determined with two standard mixtures. The first mixture contained 12.5 μg-eq of n-butyric, propionic, acetic, and formic acids in 1 ml; the second contained these acids and also 9.1 μg-eq of oxalic, succinic, aconitic, glycolic, tartaric, malic, and citric acids (in the same volume).

N-butyric, propionic, acetic, and formic acids in the irradiated water were identified by IR spectroscopy as follows. The total acids were separated from the other radiolysis products by elution with a 2% solution of butanol in benzene. With the aid of a 0.01N aqueous solution of NaOH the total acids were reextracted from the solvent layer, which was separated; the alkaline extract was evaporated to a dry residue at 60-70°C and mixed with potassium bromide, and the absorption spectrum of the separated acids was recorded between 3900 and 400 cm^{-1} in a UR-20 infrared spectrometer.

Identification was effected by comparing the spectrum (Fig. 2) with the spectra of standard sodium salts, since the absorption spectra of the salts are more specific than those of the acids [6]. As the characteristic absorption bands we used those at frequencies of 770 cm^{-1} for sodium formate, 462 cm^{-1} and the doublet with maximum absorptions at 625 and 650 cm^{-1} for sodium acetate, 510 and 817 cm^{-1} for sodium propionate, and 485, 700, and 750 cm^{-1} for sodium butyrate.

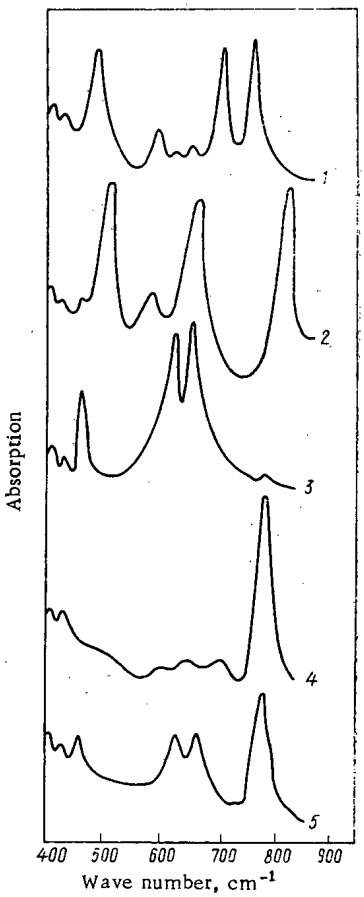

Fig. 2. Infrared absorption spectra of mixture of sodium salts of volatile acids separated chromatographically from irradiated water and from the standard salts of n-butyric, pripionic, acetic, and formic acids. 1) Sodium butyrate; 2) propionate; 3) acetate; 4) formate; 5) irradiated water.

Analysis of the absorption spectra revealed that the radiolysis products of the system $CO_2-H_2O(D_2O)$ –oil contain acetic and propionic acids (see Fig. 2). The presence of n-butyric and propionic acids was not confirmed by IR spectroscopy, because their contents in the sample, as determined chromatographically, were an order of magnitude smaller.

LITERATURE CITED

1. A. O. Allen, Radiation Chemistry of Water and Aqueous Solutions [Russian translation], Gosatomizdat, Moscow (1963).
2. S. Lind, Radiation-Chemical Processes in Gases [Russian translation], Atomizdat, Moscow (1965).
3. M. N. Gaisinskii, Nuclear Chemistry and Its Applications [Russian translation], IL, Moscow (1961).
4. A. G. Stradomskaya and I. A. Goncharova, Hydrochemical Materials [in Russian], Vol. 39, Gidrometeoizdat, Leningrad (1965), p. 169.
5. Unified Method of Water Analysis [in Russian], Khimiya, Moscow (1971).
6. E. Childers and G. Strathers, Anal. Chem., 27, 737 (1955).

DETERMINING THE THERMAL POWER OUTPUTS OF SMALL HIGH-TEMPERATURE NUCLEAR POWER PLANTS

A. I. El'tsov, A. K. Zabavin,
Yu. A. Kotel'nikov, A. A. Labut,
E. P. Larin, I. P. Sviridenko,
and Yu. L. Shirokovskii

UDC 621.039.577:621.039.566

In the operation of nuclear reactors, their thermal power outputs are usually determined by means of the results of measurements of the mean neutron flux density in the core together with data from measurements of the thermal balance. In this case, when the reactor is first taken to 1-5% of its rated power output, control is effected by means of readings of the neutron flux meters, normalized to unit thermal power output during the process of physical start-up. After stabilization, the thermal power is determined from the equation of heat balance and is compared with the value obtained by the first method. In this comparison (and also during further operation), the power calculated from the heat balance serves as a basis for correcting the results of the neutron physics measurements. Since the neutron flux meters are an important element of the reactor moderator control system, stringent requirements are imposed on the methods and precision of determination of the thermal power.

These methods have now been fairly well worked out. However, in tests on small high-temperature nuclear power plants, e.g., thermoelectric and thermoemissive reactor-converters, determination of the thermal power from measurements of the heat balance involves special features. To improve the accuracy of determination, it is here not sufficient to reduce the error of measurement of the temperature and heat-transfer-agent flow rate in the equation of thermal balance. It is also necessary to take account of the heat lost to the surrounding medium from the outer surface of the reactor. These losses may constitute 10% or more of the total power. The amount of heat removed from the reactor in the form of electrical energy is also rather large.

Let us consider the determination of the thermal power of a small high-temperature nuclear power plant, taking as an example the method used in tests on the Topaz-3 thermoemissive reactor–converter (Fig. 1). In steady conditions of electrical power generation, this reactor can be regarded as a closed thermal system with the boundary conditions that the heat-transfer-agent temperature is t_1 at the input and t_2 at the output. For such a system the thermal power N_T can be found from the equation of heat balance,

$$N_T = G(c_{p_2} t_2 - c_{p_1} t_1) + N_e + N_{loss}, \quad (1)$$

where G is the mass flow rate of the heat-transfer agent, c_{p_1} and c_{p_2} are the specific heats of the heat-transfer agent at temperatures t_1 and t_2 respectively, N_e is the electrical power delivered to the external load, and N_{loss} is the power lost to the surrounding medium.

In Eq. (1), all the quantities except N_{loss} can be determined from measurements and the known relation $c_p = f(t)$. To increase the accuracy of the measurements it is necessary to increase the number of measurements of all quantities in Eq. (1) at every level of reactor power output. This will enable us to use mathematical statistics to calculate the errors. Then in the equation we must put the arithmetic means of the quantities.

The relation between the power losses and the temperature of the external surface of the reactor-converter can be found experimentally during the process of raising the reactor to its working temperature with an external heat source. As a rule, such warming-up is possible for high-temperature research reactors. In par-

Translated from Atomnaya Énergiya, Vol. 41, No. 6, pp. 420-421, December, 1976. Original article submitted December 9, 1975.

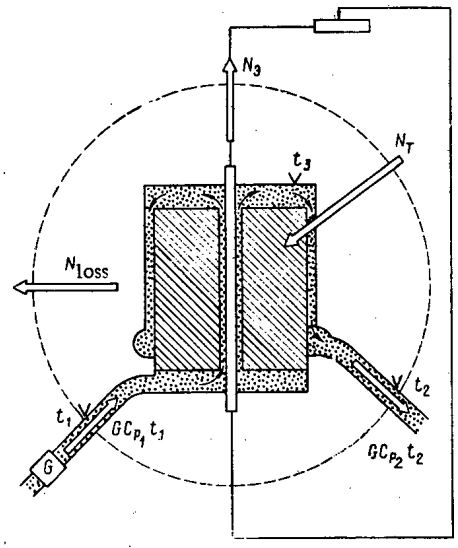

Fig. 1

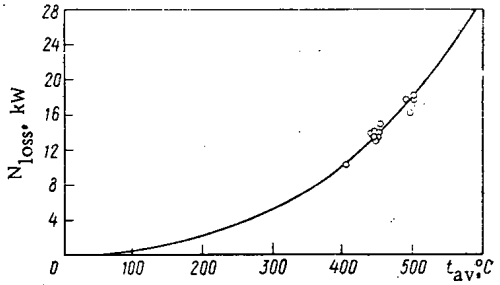

Fig. 2

Fig. 1. Diagram of Topaz-3 reactor-converter.

Fig. 2. Power losses from exterior surface of reactor vs temperature.

ticular, before testing, experimental thermoemissive reactor-converters are warmed up in order to degas the interior cavities and interelectrode gaps and to study the temperature effects and reactivity coefficients. In this case $N_T = 0$, $N_e = 0$, and Eq. (1) becomes

$$N_{loss} = G\,(c_{p_1} t_1 - c_{p_2} t_2). \tag{2}$$

After stabilization, by measuring G, t_1 and t_2 in Eq. (2) at each temperature we determine the power losses corresponding to each value of the weighted mean temperature t_{av} of the exterior surface of the reactor-converter. From the results we can plot N_{loss} vs t_{av}. As t_{av} we can take the temperature of any point on the external surface of the reactor. It is important that it must be accurately measurable both during heating-up and during later operation of the reactor at its nominal power. In tests of the Topaz-3 plant, for example, as the weighted-mean temperature we took the arithmetic mean temperature $t_{av} = 0.5(t_2 + t_3)$ of the outer casing through which the heat-transfer agent, after passing through the core, arrives at the outlet pipe (Fig. 1). The advantage of this choice is as follows.

For safety reasons, tests on experimental small nuclear power plants are often made in special test chambers with water-cooled walls [1]. Heat from the exterior surface of the reactor is transmitted to the walls of the chamber in the form of radiant energy, by conduction along the output cables, pipes, and structural supports, and by conduction and convection through the surrounding gas. If in the chamber we maintain a vacuum of 10^{-2}-10^{-3} mm, the fraction of the heat lost by conduction and convection will be very small in comparison with the heat transmitted by radiant heat exchange. This enables us to use, with sufficient accuracy for practical purposes in approximation of the experimental data with the relation $N_{loss} = f(t_{av})$, the equation of radiative heat exchange,

$$N_{loss} = \sigma F \varepsilon_{cb} (T_{av}^4 - T_c^4),$$

where σ is the Stefan–Boltzmann constant, F is the area of the exterior surface of the reactor–converter between the cross-sections in which temperatures t_1 and t_2 are measured, ε_{cb} is the corrected degree of blackness of the system (exterior surface of reactor – wall of test chamber), and T_{av} and T_c are the temperatures of the exterior surface of the reactor and the wall of the test chamber respectively.

If we take $\varepsilon_{cb} = \text{const}$ and $T_c = \text{const}$, then the equation of radiative heat exchange becomes

$$N_{loss} = aT_{av}^4 - b, \tag{3}$$

where $a = \sigma F \varepsilon_{cb}$ and $b = \sigma F \varepsilon_{cb} T_c^4$ are constant coefficients.

Using Eq. (3) we approximated the experimental data obtained during warming-up of the Topaz-3 reactor–converter (Fig. 2). This graph was used to determine the power loss and to calculate the thermal power output of the Topaz-3 during power tests by means of Eq. (1).

There is no difficulty in satisfying the adopted condition T_c = const either during warming-up or in operation, because the wall temperature of the test chamber can be controlled by varying the coolant-liquid flow rate. Though the condition ε_{cb} = const is approximate, it can be assumed with sufficient accuracy for practical purposes over a limited range of working temperatures of the exterior surface. The data in [2] show that ε_{cb} depends weakly on temperature for stainless steels and other structural materials in the system.

A comparison of the measured temperature of the wall of the test chamber with that calculated from Eq. (3) with $N_{loss} = 0$ by means of the equation

$$T_{av} = (b/a)^{0.25}$$

for the Topaz-3 plant gave a deviation not exceeding a few degrees. This confirms our choice of parameters for the approximation equation.

In repeated measurements of the heat balance at a constant level, the thermal power found from Eq. (1) did not deviate from the arithmetic mean value by more than ± 1.7 kW. At level of 150 kW or more, this reproducibility of the results is perfectly acceptable.

Note that the power loss can be determined in other ways, e.g., from the flow rate and heat gain of the liquid which cools the walls of the test chamber. However, as a rule this method is more laborious and less accurate.

The above method of determining the thermal power output can be applied to a wide class of nuclear energy plants. Its advantage is the possibility of determining the influence of structural improvements in later experimental models on the power loss to the surrounding medium, of finding the efficiency of the plant more precisely, of increasing the accuracy of the results of thermophysical investigations, etc.

LITERATURE CITED

1. V. A. Kuznetsov et al., At. Energ., 36, No. 6, 450 (1974).
2. Handbook on Radiative Properties of Solids [in Russian], Énergiya, Moscow (1974).

INFLUENCE OF IRRADIATION ON THE OXIDATION KINETICS OF THE ALLOY Zr + 2.5% Nb

M. G. Golovachev, V. V. Klyushin, and V. I. Perekhozhev

UDC 621.039.531:669.296.293

We have investigated the oxidation of the alloy of zirconium with 2.5 mass % niobium inside or outside a reactor at temperatures of 255-425°C in liquid nitrogen (~20 ml H_2O/m^3). The gas flow rate was 0.5 m/sec or 5-10 liters/h. The density of the neutron flux was about $3.5 \cdot 10^{13}$ neutrons/($cm^2 \cdot$ sec) ($E \geq 1.1$ MeV). The specimens were screened from fission fragments and were weighed on a VLAO-100 analytical balance.

During the tests (maximum duration 590 h) all the specimens became covered in a black film which adhered to the metal. The dependence of the oxidation kinetics of the alloy on the test conditions is shown in Fig. 1. The results of a mathematical analysis of the data are listed in Table 1.

Translated from Atomnaya Énergiya, Vol. 41, No. 6, p. 422, December, 1976. Original article submitted December 19, 1975; revision submitted May 7, 1976.

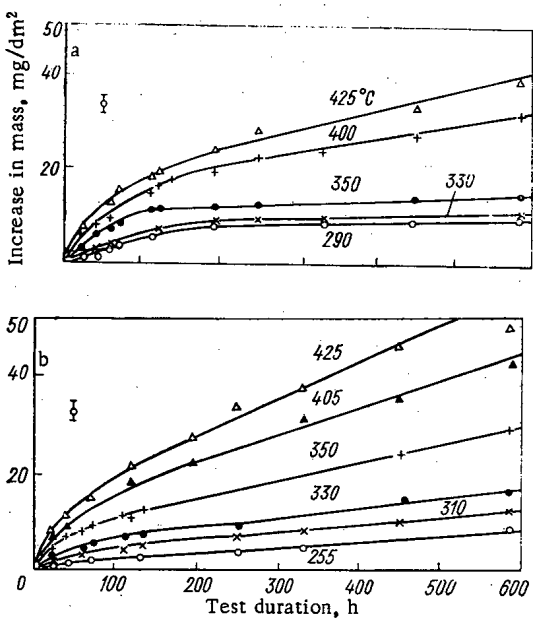

Fig. 1. Oxidation kinetics of alloy Zr + 2.5% Nb in moist nitrogen, at various temperatures. a) No irradiation; b) under irradiation.

TABLE 1. Oxidation Kinetics Constants

Oxidation conditions	Temp., °C	$\Delta m = k_1 \lg \tau$; k_1	$(\Delta m)^n = k_2\tau$	
			k_2	n
Under irradiation	255	0,3	—	—
	310	—	0,1	1,70
	330	—	0,2	1,72
	350	—	0,8	1,89
	405	—	1,8	1,91
	425	—	3,5	1,96
No irradiation	290	0,7	—	—
	330	0,7	—	—
	350	1,0	—	—
	400	—	1,3	1,92
	425	—	2,2	1,96

Analysis of the data after the tests shows that irradiation of the alloy Zr +2.5 mass % Nb by a flux of neutrons in moist nitrogen increases the mass of the specimens by 20-50%. This effect may be due to the influence of neutron irradiation on the structure of the oxide film and on the composition of the medium.

INFLUENCE OF BORON ON RADIATION EMBRITTLEMENT OF LOW-ALLOY STEEL

V. A. Nikolaev and V. I. Badanin

UDC 621.039.531

Interest in the influence of boron on the properties of ferrite-pearlitic steel for the casings of water-moderated water-cooled power reactors has been stimulated by the following factors. In the first place, alloying with 0.002-0.005% of boron increases the hardenability, and hence the strength, of the steel, without appreciably impairing its weldability [1]. Furthermore, information on the marked radiation embrittlement of steel containing boron [2] reveals the necessity of assessing the possible role of this element as an impurity in steel ($\sim 10^{-3}$% or less).

In this connection we attempted to study the radiation embrittlement of steel 15Kh2MFA with about 0.004% of added boron; to elucidate the causes of the observed effects, we used boron of various isotopic compositions.

Method. The investigations were performed on metal from a 100-kg batch induction-melted in the laboratory. When casting this into 16-kg ingots, a master alloy of Fe +10% B with a natural mixture of the isotopes ^{10}B and ^{11}B (18.4 and 18.6%), or with 95% enrichment in ^{10}B or ^{11}B, was added to the ladle.

To prepare the master alloy with enriched boron, we mixed elementary boron with powdered iron carbonyl; from the mixture we pressed tablets which were then sintered in vacuum. The melt was made with Armco iron as charge. The chemical composition of the steel is shown in Table 1.

The ingots were drop forged and rolled to 10-mm sheet. The sheets were hardened from 960°C in oil and tempered at 690°C. After heat treatment the material had the structure of finely dispersed sorbite with a primary austenitic grain size of 4-5.

The mechanical properties were determined on impact specimens $5 \times 5 \times 27.5$ mm in size with a V-shaped notch 1 mm deep and 0.25 mm in radius, and also on fivefold tensile specimens 3 mm in diameter. The liability to radiation embrittlement was estimated [3] from the difference between the critical brittleness temperatures T_c of the steel in its initial state and after neutron irradiation.

The materials were irradiated in the core and reflector of a VVR-M reactor with flux density ratios of 1:1 for fast neutrons ($E > 0.5$ MeV) and 1:10 for thermal neutrons. The method was described in detail in [3].

Experimental Results. Figure 1 shows the dependence of the rise in T_c for the steel on the isotopic composition of the boron and the fluence during irradiation in the core. After irradiation at about 50°C by a fluence of $5 \cdot 10^{19}$ neutrons/cm^2, the change in T_c for the steel was the greater, the greater the enrichment with ^{10}B. For the two extreme contents of ^{10}B (about 5 and 95%), the shift in T_c differed twofold. A comparison with data on the influence of irradiation on the yield point (Table 2) reveals that for radiation hardening of steel with the same fluence there is no dependence on the isotopic composition of the boron.

When the fluence is increased to $5 \cdot 10^{20}$ neutrons/cm^2 T_c increases by 190-200°C in materials of all compositions. From the results it follows that for steel with added ^{11}B the graph of T_c vs fluence has the usual ratio $\Delta T_c \simeq AF^{1/3}$ (where F is the fluence in units of 10^{18} neutrons/cm^2) for the value $A \sim 24$. For the remaining materials this relation does not obtain, showing that the saturation effect is attained earlier if ^{10}B is present in the steel.

When the irradiation temperature is raised to 300-350°C, the shift in T_c is much less, but in this case also the embrittlement increases with the ^{10}B content (Fig. 1, curve 3). The influence of irradiation temperature was investigated in more detail for steel with added natural boron. The results (Fig. 2) were compared with the data for steel of similar chemical composition (Table 1) but containing not more than 0.0005% B. The

Translated from Atomnaya Énergiya, Vol. 41, No. 6, pp. 422-425, December, 1976. Original article submitted January 6, 1976.

TABLE 1. Chemical Compositions of Materials

Boron content, mass %	Other elements, %
0,004 ^{11}B	—
0,003 B	0,14 C; 1,72 Cr
0,005 ^{10}B	0,2 Ni; 0,81 Mo; 0,32 V; 0,2 Cu
0,0005 B	0,009 P

TABLE 2. Influence of Irradiation by a Fluence of $5 \cdot 10^{19}$ neutrons/cm^2 at 50°C on Yield Point of Steel*

Boron content, mass %	$\sigma_{0.2}$, kgf/mm^2	
	before irradiation	after irradiation
0,004 ^{11}B	75	96
0,003	75	95
0,005 ^{10}B	76	97

*Tested at 20°C

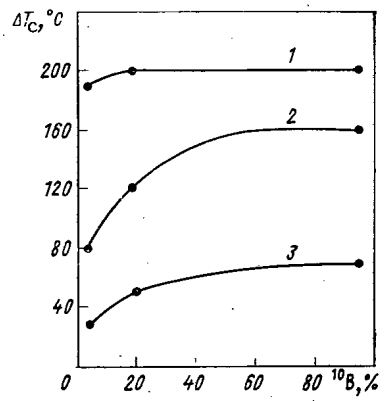

Fig. 1

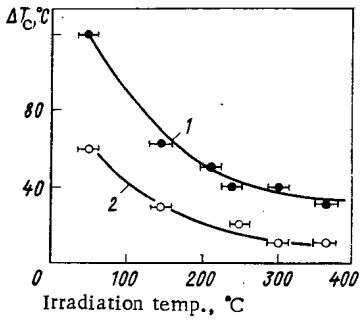

Fig. 2

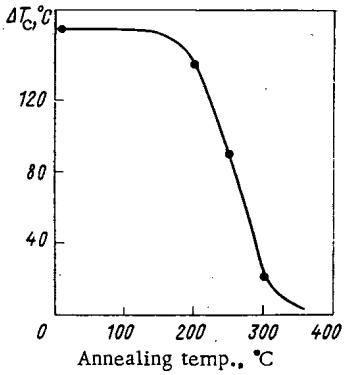

Fig. 3

Fig. 1. Dependence of rise in T_c of steel on isotope composition of boron after irradiation. 1) $5 \cdot 10^{20}$ neutrons/cm^2, 50°C; 2) $5 \cdot 10^{19}$ neutrons/cm^2, 50°C; 3) $\sim 1 \cdot 10^{20}$ neutrons/cm^2, 300-350°C.

Fig. 2. Rise in T_c for steel with 0.003% boron (1) or no boron (2) vs irradiation temperature in core [fluence $(0.5\text{-}1) \cdot 10^{20}$ neutrons/cm^2].

Fig. 3. Influence of annealing temperature on restoration of T_c for steel containing ^{10}B after irradiation with a fluence of thermal neutrons of $6.8 \cdot 10^{20}$ neutrons/cm^2 at 50°C.

extra embrittlement due to the boron falls rather rapidly as the irradiation temperature rises, especially between 150 and 250°C. This relation does not differ appreciably from that observed in steels with no boron added [3, 5].

To elucidate the influence of boron on the embrittlement we studied the possibility of restoring T_c of irradiated steel by postirradiation annealing. Experiments were performed on steel with added ^{10}B; to increase the contribution of this isotope to the embrittlement we irradiated the specimens mainly with thermal neutrons (in the reflector).

Fig. 3 shows that after annealing for 1 h T_c is partially restored even at 200°C, while at 300°C it reaches 85-90%. The temperature range of restoration of T_c for steel with boron is typical of most steels of the ferritic–pearlitic class [4, 5].

The data show that the influence of boron merely intensifies the normal embrittlement, the external manifestations of which are well known.

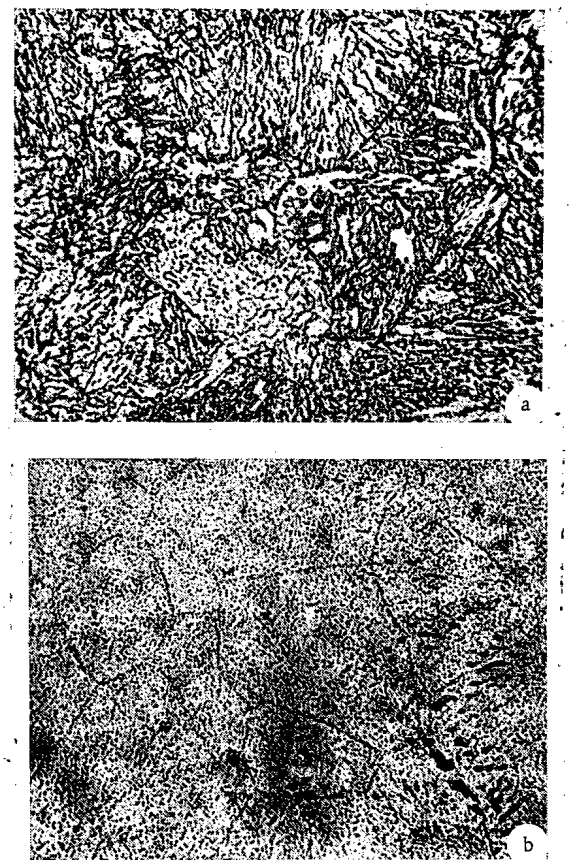

Fig. 4. Microstructure (a) and autoradiogram of boron distribution (b) of steel 15Kh2MFA.

Increase of embrittlement under the influence of boron probably occurs as a result of formation of fragment nuclei with high kinetic energies (about 1.8 or 0.6 MeV) by the reaction $^{10}B(n, \alpha)^{7}Li$. Their retardation in the matrix forms additional defects in the lattice. Owing to the large reaction cross section, the ^{10}B is rapidly burnt up (for a fluence of thermal neutrons of $5 \cdot 10^{20}$ neutrons/cm^2 the burn-up is about 90%). Therefore, its influence is manifested at comparatively low doses and is hardly appreciable in the conditions for the saturation effect.

Radiation strengthening of steel does not depend on the ^{10}B content. This is evidently because of the nature of the distribution of boron, which can be seen by track autoradiography [6].

To study the distribution of boron* we used steel specimens with added ^{10}B. To obtain a coarse grain the specimens were heat treated by heating under hardening to 1200°C, followed by tempering, as in the other cases at 690°C. The resulting autoradiograms when compared with the microstructure (Fig. 4) showed that the density of tracks is very nonuniform and is maximal at the boundaries of the former austenitic grains, which are thus also sites of preferential concentration of boron. The distribution of tracks left by alpha particles in the autoradiograms simultaneously reflects the distribution of zones in which retardation of alpha particles and lithium ions leads to an increase in the number of atomic displacements. Naturally, a macroscopic characteristic such as the yield point, which is determined by the deformation resistance of the whole bulk of the metal, cannot be influenced by such a local increase in defect concentration. Therefore the yield point depends almost entirely on the uniformly distributed defects due to fast neutrons. At the same time, the most damaged zones in the crystal lattice, adjoining grain boundaries, can apparently serve as sites of preferential formation of crack nuclei, and consequently the appearance of such sites may influence the breaking strength of the steel.

Thus the role of boron in embrittlement of steel is essentially equivalent to an increase in fluence. It is known that T_c increases practically linearly with the fluence as the Ni, Cu, or P content of the steel increases [3]. Therefore we can expect that the presence of boron should be more markedly manifested, the higher the

*The track autoradiography experiments were performed by N. V. Mishina and N. B. Odintsov.

content of these elements in the steel. This means that when steel is alloyed, for example, with nickel, it may be necessary to limit and control the boron impurity content in order to ensure high radiation stability.

LITERATURE CITED

1. C. Cottrell, J. Brit. Weld., 1, 315 (1954).
2. H. Myers and M. Grounes, in: Proc. of Third Intern. Conf., Geneva, 1964, A/conf. 28/P/420.
3. V. A. Nikolaev and V. I. Badanin, At. Energ., 37, No. 6, 491 (1974).
4. A. D. Amaev et al., Fourth Geneva Conference, Report No. 705 [in Russian], (1971).
5. C. Serpan and J. Hawthorne, Trans. ASME. J. Basic Engng., 89, No. 4, 877 (1967).
6. R. Fleischer, P. Price, and R. Walker, Science, 149, No. 3682, 383 (1965).

MEASUREMENT OF THE RATIO $\sigma_f(^{239}Pu)/\sigma_f(^{235}U)$ FOR NEUTRON ENERGIES OF 0.27-9.85 MeV

É. F. Fomushkin, G. F. Novoselov, Yu. I. Vinogradov, and V. V. Gavrilov

UDC 539.173.4:621.039.9

The energy dependence of the ratio of the fission cross sections of ^{239}Pu and ^{235}U for neutrons has been studied by many investigators by various methods. However, at present there is a rather large disagreement between the results. Even in the appraised data in the compilations of Davey [1], Byer [2], Greene et al. [3], Sowerby et al. [4], and Kon'shin et al. [5], it reaches 7-8%. The curves characterizing the ratio differ in shape, especially at neutron energies of about 1-10 MeV. To refine our ideas of the structure of the graph of $\sigma_f(^{239}Pu)/\sigma_f(^{235}U)$, it is advisable to carry out investigations by the same method over a wide range of neutron energies.

The preliminary results of measurements of the ratio of the fission cross sections of ^{239}Pu and ^{235}U, given here, were obtained by the time-of-flight method with an underground nuclear explosion as the pulsed neutron source. Similar measurements of comparatively well-studied characteristics also enable us to assess the feasibility of using the method in other nuclear physics investigations.

The method of measurement was described in [6]; we shall merely mention its essential features. As the fission-fragment detector we used a film of polycarbonate with a molecular mass of 90,000. Time-of-flight scanning was effected by an electromechanical apparatus: One of its units was a drum with the polycarbonate film cemented on, rotating at about 10^4 rpm at the moment of the neutron pulse. Layers of fissile isotopes were arranged near the film in the neutron flux; between each layer and the film there was a slit-type fission-fragment collimator.

With this method of measurement, the time resolution is governed by the rate of rotation of the drum, the flight distance, and the width of the fragment collimator slit,

$$\Delta t/L = \Delta\varkappa/vL,$$

where L is the flight distance, v is the linear velocity of the film relative to the collimator, and $\Delta\varkappa$ is the collimator slit width.

In our measurements, the time resolution was 7.5 nsec/m (total width by half height). The influence of scattered neutrons outside the direct flux was accounted for by additional collimators with layers of ^{235}U and ^{239}Pu.

Calibration of the layers, i.e., measurement of the ratio of the effective numbers of fissile nuclei in the layers (with allowance for the probability of passage of fragments through the collimator) was effected by

Translated from Atomnaya Énergiya, Vol. 41, No. 6, pp. 425-426, December, 1976. Original article submitted January 21, 1976.

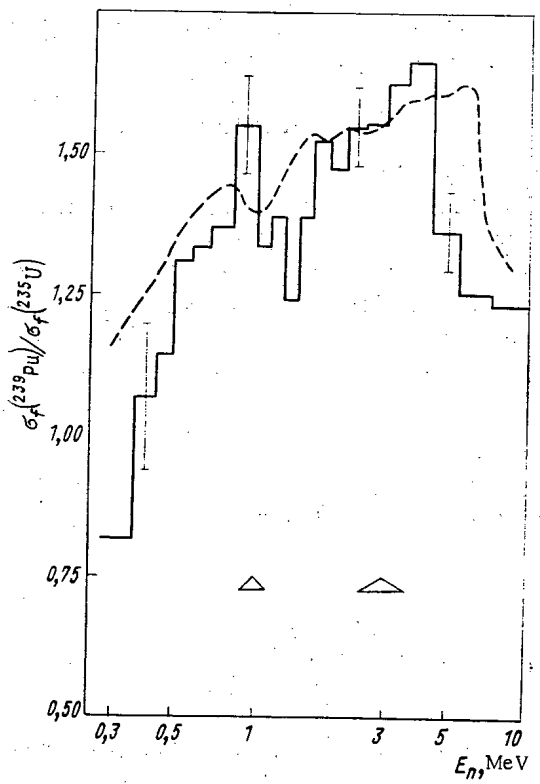

Fig. 1. Energy dependence of ratio of fission cross sections of ^{239}Pu and ^{235}U. ——) Present authors' data; – – – –) estimate of Sowerby et al. [4].

TABLE 1. Ratio $\sigma_f(^{239}Pu)/\sigma_f(^{235}U)$ vs Neutron Energy

$E_{n.min}$, MeV	$E_{n.max}$, MeV	$\sigma_f(^{239}Pu)/\sigma_f(^{235}U)$	Error, %	$E_{n.min}$, MeV	$E_{n.max}$, MeV	$\sigma_f(^{239}Pu)/\sigma_f(^{235}U)$	Error, %
0,27	0,36	0,81	14,4	1,42	1,62	1,39	5,1
0,36	0,44	1,07	12,1	1,62	1,85	1,53	4,9
0,44	0,50	1,15	10,9	1,85	2,15	1,47	4,6
0,50	0,59	1,31	8,4	2,15	2,50	1,56	4,4
0,59	0,69	1,34	7,3	2,50	3,00	1,57	4,6
0,69	0,83	1,37	6,3	3,00	3,60	1,62	4,7
0,83	1,01	1,55	5,5	3,60	4,45	1,67	4,9
1,01	1,13	1,33	6,6	4,45	5,60	1,37	5,1
1,13	1,26	1,39	6,1	5,60	7,28	1,25	4,8
1,26	1,42	1,24	5,4	7,28	9,85	1,23	6,2

means of fission by thermal neutrons. The experimental unit, including the layers of ^{239}Pu and ^{235}U, the collimator, and a small piece of detector film, was installed in a graphite prism 100 × 100 × 100 cm in size. This prism was irradiated by fast neutrons from a ^{235}U critical assembly [7]. At the site of the test specimen, the temperature of the thermal neutrons was 309 ± 18°K.

The fission cross sections for 0.0253 eV neutrons were 742.5 ± 3.0 b for ^{239}Pu and 582.2 ± 1.3 b for ^{235}U [8]. The g factors were, respectively, 1.066 ± 0.014 [9] and 0.973 ± 0.003 [10].

The polycarbonate detector films were processed in identical conditions with 6.25 N NaOH solution. The films were examined and the tracks counted in classes with an optical microscope. The results showed that the total background of scattered neutrons in the range of times of flight under examination did not exceed 1.5%. We made a correction for the contents of ^{239}Pu, ^{235}U, and other fissile isotopes in the specimens. Since the probability of passage of fragments through the collimator depends on the angular distribution, we also made a cor-

rection (about 1%) for the difference between the energy dependences of the angular anisotropy of fission of the nuclei under investigation. The results of the measurement of the ratio $\sigma_f(^{239}Pu)/\sigma_f(^{235}U)$ for 20 neutron energy ranges ($E_{n.min}$ and $E_{n.max}$) are shown in Fig. 1 and listed in Table 1. The quoted statistical errors correspond to a confidence probability of 68% and were determined from the number of tracks due to fission fragments in the corresponding intervals and the corrections. The calibration error (± 1.8%) was due to the error of measurement for thermal neutrons and the error in the values used for the g factors and the fission cross section for 0.0253 eV neutrons.

For comparison, Fig. 1 shows the curve recommended by Sowerby et al. [4]. We see that the results obtained by the authors in the neutron energy range $0.5 \leq E_n \leq 4.5$ MeV agree with the curve of the cross-section ratio. The marked deviation from the recommended curve at higher energies may be due to the inadequate energy resolution. However, there are certain results, e.g., those of Savin et al. [11], which agree with this curve at high neutron energies ($E_n > 4.5$ MeV) as well. The discrepancy at low energies is apparently due to background sources which were not taken into account.

Improvements to the method and further research will improve the accuracy and reliability of measurements of the fission characteristics of heavy nuclei.

LITERATURE CITED

1. W. Davey, Nucl. Sci. Engng., 32, 35 (1968).
2. J. Byer, Atom. Energy Rev., 10, No. 4, 529 (1972).
3. N. Greene, J. Lucins, and C. Craven, Rep. ORNL-TM-2797 (1970).
4. M. Sowerby, B. Patric, and D. Mather, Ann. Nucl. Sci. Eng., 1, 409 (1974).
5. V. A. Kon'shin et al., in: Nuclear Constants, [in Russian], No. 16, Atomizdat, Moscow (1974), p. 329.
6. É. F. Fomushkin et al., At. Energ., 39, No. 4, 295 (1975).
7. Yu. M. Odintsov, A. S. Koshelev, and A. A. Malinkin, At. Energ., 38, No. 4, 209 (1975).
8. S. Mughabhab and D. Garber, Neutron Cross Sections, Vol. 1, Resonance Parameters, BNL-325 (1973).
9. C. Wagemans and A. Deruytter, Ann. Nucl. Sci. Eng., 2, 25 (1975).
10. G. Hanna et al., Atom. Energy Rev., 7, No. 4, 3 (1969).
11. M. V. Savin et al., At. Energ., 29, No. 3, 218 (1970).

NUCLEAR γ RESONANCE METHOD FOR INVESTIGATING ÉI-69 AUSTENITE STEEL IRRADIATED WITH γ QUANTA OR FAST NEUTRONS

I. M. V'yunnik, P. O. Voznyuk, and V. N. Dubinin

UDC 548-162:539.16.04

As is known, radiation damage produced by γ and neutron irradiation affects the decomposition of austenite in the annealing of ÉI-69 steel [1, 2]. It was of interest to investigate more thoroughly the state of austenite in hardened steel immediately after irradiation. For this purpose, irradiated specimens were investigated by using the nuclear γ resonance (NGR) method (Mössbauer effect), which provides additional information on radiation defects.

Hardened polycrystalline specimens of ÉI-69 steel (0.42% C, 13.35% Cr, 13.68% Ni, 2.08% W, 0.33% Mo and 70.14% Fe) with a uniform composition (carbon-supersaturated austenite) were irradiated at room temperature with 1.2 MeV γ quanta from radioactive cobalt ^{60}Co (irradiation dose, $8.8 \cdot 10^{18}$ quanta/cm^2) and fast neutrons from the VVR-M reactor at 60°C (mean fluence, $3.5 \cdot 10^{18}$ neutrons/cm^2).

Translated from Atomnaya Énergiya, Vol. 41, No. 6, pp. 427-428, December, 1976. Original article submitted January 21, 1976.

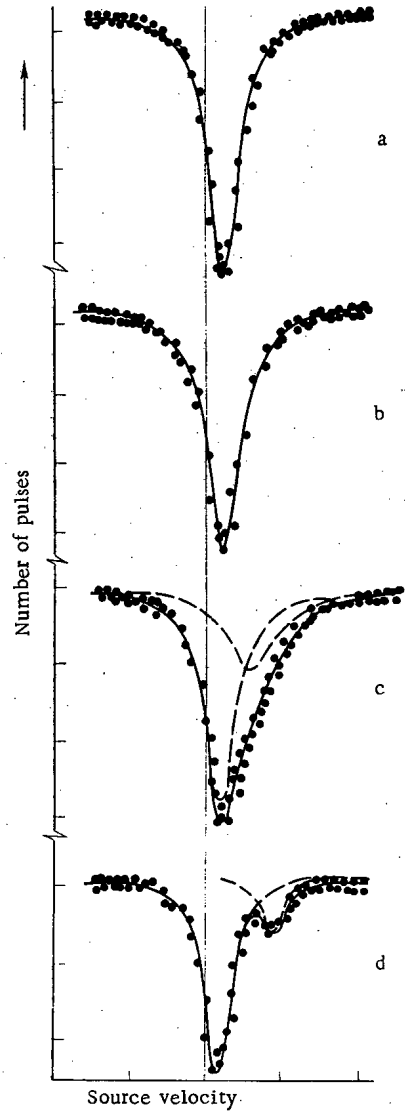

Fig. 1. Absorption spectra of iron atoms. a) In a steel matrix; b, c) in steel irradiated with γ quanta and fast neutrons, respectively: d) in steel irradiated with fast neutrons and annealed at 500°C over a period of 30 min.

The specimens for investigations based on the NGR method were prepared by electrolytic dissolution of sheets of irradiated and nonirradiated steel. We obtained deposits with high concentrations of the carbide phase and other nonmetallic high-dispersion phases, which cannot be observed by means of an x-ray diffractometer. The thickness of the specimens (absorbers) was equal to $2 \cdot 10^{-4}$ g/cm^2 with respect to ^{57}Fe. The prepared specimens were investigated in an electrodynamic Mössbauer spectrometer operating under constant-acceleration conditions. The gamma radiation source was ^{57}Co in a chromium matrix. The source and the absorber were kept at room temperature.

The results of investigations based on the NGR method are shown in Fig. 1. The velocity of the radiation source relative to the absorber is laid off on the axis of abscissas, while the number of pulses per analyzer channel is laid off on the axis of ordinates. The spectra were processed by means of a computer, using the method of least squares. It was assumed that the lines had the Lorentz form.

The spectrum of hardened steel contains the usual austenite line with the width $\Gamma = 0.53 \pm 0.03$ mm/sec, shifted by $\delta = 0.21 \pm 0.03$ mm/sec with respect to the line of sodium nitroprusside in Fig. 1a. Only negligible line broadening, $\Gamma = 0.48 \pm 0.03$ mm/sec, occurs apparently as a result of γ irradiation, which is seen in Fig.

1b. In steel irradiated with fast neutrons, the NGR spectrum consists of the asymmetric line (Fig. 1c) resulting from the superposition of two lines (dashed curves): the singlet of the steel matrix with the width $\Gamma = 0.52 \pm 0.03$ mm/sec and $\delta = 0.21 \pm 0.03$ mm/sec and a line with the width $\Gamma = 0.76 \pm 0.05$ mm/sec, the center of which is shifted by $\delta = 0.62 \pm 0.05$ mm/sec with respect to the line of sodium nitroprusside.

Radiation defects develop in hardened ÉI-69 steel as a result of irradiation; most iron atoms are located in normal regions of the crystal lattice that are not distorted by defects, so that the singlet of the steel matrix is observed in experiments (Fig. 1 b and c). The broadening of this singlet may be connected with the concentration nonuniformity caused by radiation defects in irradiated austenite. The appearance of the second, greatly broadened line (c) indicates that some iron atoms enter the new phase formed under the action of neutron radiation.

A much larger number of defects appears in hardened ÉI-69 steel irradiated with fast neutrons than in steel irradiated with γ quanta (in our case, $5 \cdot 10^{20}$ and $1.2 \cdot 10^{17}$, respectively). For instance, such defects may consist of vacancy clusters [3], which promote the development of precipitation particles in hardened steel. At the initial stage of irradiation, an iron atom, bound to two carbon atoms, constitutes the basic precipitation nucleus [4]. It can be assumed that this precipitation also takes place in hardened ÉI-69 steel under the action of neutron radiation. Then, the line with the isomeric shift $\delta = 0.62 \pm 0.05$ mm/sec may be caused by the metastable carbide phase Me_mC_n, the isomeric shift of which is close to Fe_5C_2 [5].

As a result of annealing at 500°C over a period of 30 min, the metastable carbide phase in ÉI-69 steel irradiated with fast neutrons passes into the stable phase $Me_{23}C_6$, which is indicated by the appearance of lines with the isomeric shift $\delta = 0.96 \pm 0.03$ mm/sec (Fig. 1d) in the spectra [6]. Precipitations of the carbide phase $Me_{23}C$ were not observed in unirradiated specimens at this annealing temperature.

LITERATURE CITED

1. I. M. V'yunnik, I. D. Konozenko, and M. P. Krulikovskaya, At. Energ., 37, No. 3, 245 (1974).
2. I. M. V'yunnik and M. P. Krulikovskaya, KIYaI-74-18 Preprint, Kiev (1974).
3. V. M. Raetskii and S. N. Votinov, Fiz. Met. Metalloved., 29, 284 (1970).
4. A. Damask et al., Philos. Mag., 22, 549 (1970).
5. Chemical Applications of Mössbauer Spectroscopy [Russian translation], Mir, Moscow (1970), p. 164.
6. P. O. Voznyuk, I. M. V'yunnik, and V. N. Dubinin, Fiz. Met. Metalloved., 36, 1310 (1973).

EFFECT OF TEMPERATURE ON THE POROSITY OF NICKEL IRRADIATED WITH NICKEL IONS

S. Ya. Lebedev and S. D. Panin

UDC 621.039.51

The effect of helium on the formation of pores in nickel and the dependence of the radiation porosity on the dose in irradiation with nickel ions at a constant temperature of the specimen (500°C) were investigated in [1, 2].

We consider here the development of porosity at different temperatures of the target. The method used for preparing the specimens and the irradiation method were similar to those used earlier. Specimens of commercially pure nickel, which had a thickness of 0.15 mm, were first annealed in a vacuum at 800°C over a period of 1 h. Irradiation with 46-keV nickel ions was effected with a current density of 3 $\mu A/cm^2$ to a dose of $1.6 \cdot 10^{17}$ ions/cm^2, which corresponded to approximately 40 displacements per atom [3]. The mean duration of irradiation was equal to 2.3 h. The specimen temperature varied in the 350-700°C range.

Electron-microscope investigations of irradiated specimens have shown that vacancy porosity occurs at specimen temperatures ≥ 400°C. The results obtained in processing the photomicrographs are given in Table 1.

Translated from Atomnaya Énergiya, Vol. 41, No. 6, pp. 428-429, December, 1976. Original article submitted March 9, 1976.

TABLE 1. Investigation Results for Irradiated Specimens

Temp., °C	Pore density, cm^{-3}	Pore size, Å	Swelling %
400	$4,5 \cdot 10^{17}$	20	0,22
450	$1,85 \cdot 10^{16}$	70	1,25
500	$1,46 \cdot 10^{16}$	100	2,45
550	$1,05 \cdot 10^{16}$	165	8,2
600	$3 \cdot 10^{15}$	340	12,1
650	$7 \cdot 10^{13}$	550	5,6
700	$5,75 \cdot 10^{12}$	1600	1,25

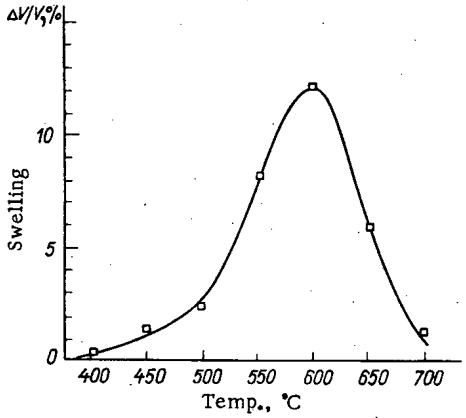

Fig. 1

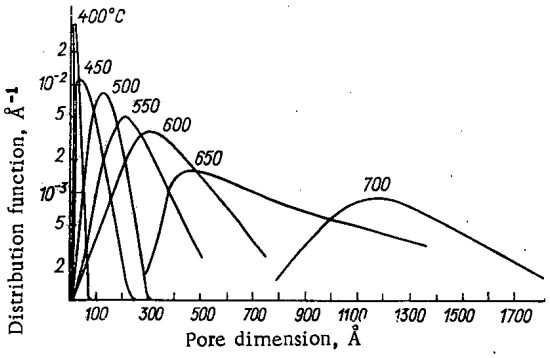

Fig. 2

Fig. 1. Temperature dependence of the swelling of nickel irradiated with Ni^+ ions to a dose of $1.6 \cdot 10^{17}$ ions/cm^2.

Fig. 2. Distribution function of pore dimensions in nickel irradiated with Ni^+ ions at different temperatures to a dose of $1.6 \cdot 10^{17}$ ions/cm^2.

A large number of small pores with the mean dimension $< d_v > 20$ Å is observed at temperatures above 400°C. Moreover, there is a large number of small dark spots, which, like the pores, are uniformly distributed over the specimen's area under observation. The pores increase with temperature, and we find $< d_v > 1600$ Å at 700°C. At the same time, the density of pores $< N_v >$ drops sharply with an increase in temperature. This indicates that, at the low-temperature limit of pore formation, the incipient vacancy clusters are probably thermally stable in irradiation with a constant flux of bombarding particles. The low mobility of vacancies is the cause of the high density of small pores in the matrix. As the temperature rises, the vacancy mobility increases, which results in more intensive pore development. Our experimental data agree with the theory of uniform generation and development of vacancy porosity in irradiated metals [4].

Figure 1 shows the temperature dependence of swelling ($\Delta V/V$) for nickel. The rather narrow swelling peak has a maximum at 600°C. The maximum volume change corresponds to $0.5T_{me}$°K. The swelling maximum observed at 600°C is in good agreement with data on nickel irradiation with 500-keV nickel ions [3]. The noticeable swelling at temperatures below 500°C can be explained by the high density of small pores.

Figure 2 shows the distribution functions of pore sizes, obtained by processing histograms for different temperatures. It is evident that the function broadens with an increase in temperature, and its maximum shifts toward larger sizes. We observe a certain asymmetry of the curves, which indicates that the pores grow as a result of fusion of small pores. This behavior agrees with the dependence observed for cold-rolled M-316 stainless steel, irradiated in the DFR reactor [5].

The distribution function indicates that, with an increase in the irradiation temperature, the pore size increases, while the pore density diminishes. This confirms the assumption that generation of new pores does not occur; rather, there is a continuous growth of the pores formed at the initial stage of irradiation.

LITERATURE CITED

1. S. Ya. Lebedev, S. D. Panin, and S. I. Rudnev, At. Energ., 38, No. 6, 426 (1975).
2. S. Ya. Lebedev, S. D. Panin, and S. I. Rudnev, At. Energ., 39, No. 5, 362 (1975).
3. J. Delaplace, N. Aram, L. Le Naour, J. Nucl. Mater., 47, No. 3, 278 (1973).
4. Yu. V. Konobeev and V. A. Pechenkin, in: Problems of Atomic Science and Technology, Radiation Damage Physics and Radiation Science of Materials Series [in Russian], Vol. 1, Atomizdat (1974), p. 41.
5. C. Cawthorne et al., in: Proc. Reading Conf. on Voids Formed by Irradiation of Reactor Materials, Harwell, BNES (1971), p. 35.

NUMERICAL γ-RAY ALBEDO FROM LIMITED SECTIONS OF THE SURFACE OF REFLECTING BARRIERS

D. B. Pozdneev and M. A. Faddeev

UDC 539.122:539.121.72

Data about the distribution of reflected γ quanta of a point isotropic source on the surface of a semi-infinite scatterer are given in [1-4]. However, no such information is available about barriers of finite thickness, although it is of considerable interest for radioisotope instrument manufacture, radiometry, and other areas of applications.

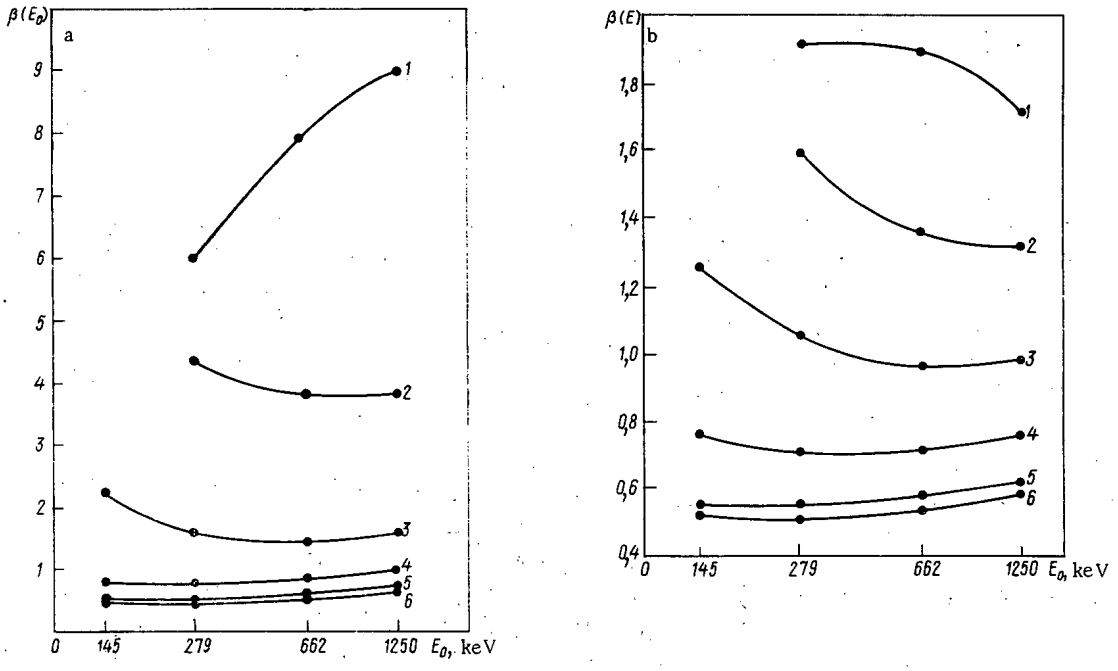

Fig. 1. Values of β: monodirectional (a) and isotropic (b) sources: 1) Pb; 2) Sn; 3) Fe; 4) concrete; 5) C; 6) Be.

Translated from Atomnaya Énergiya, Vol. 41, No. 6, pp. 430-431, December, 1976. Original article submitted March 3, 1976.

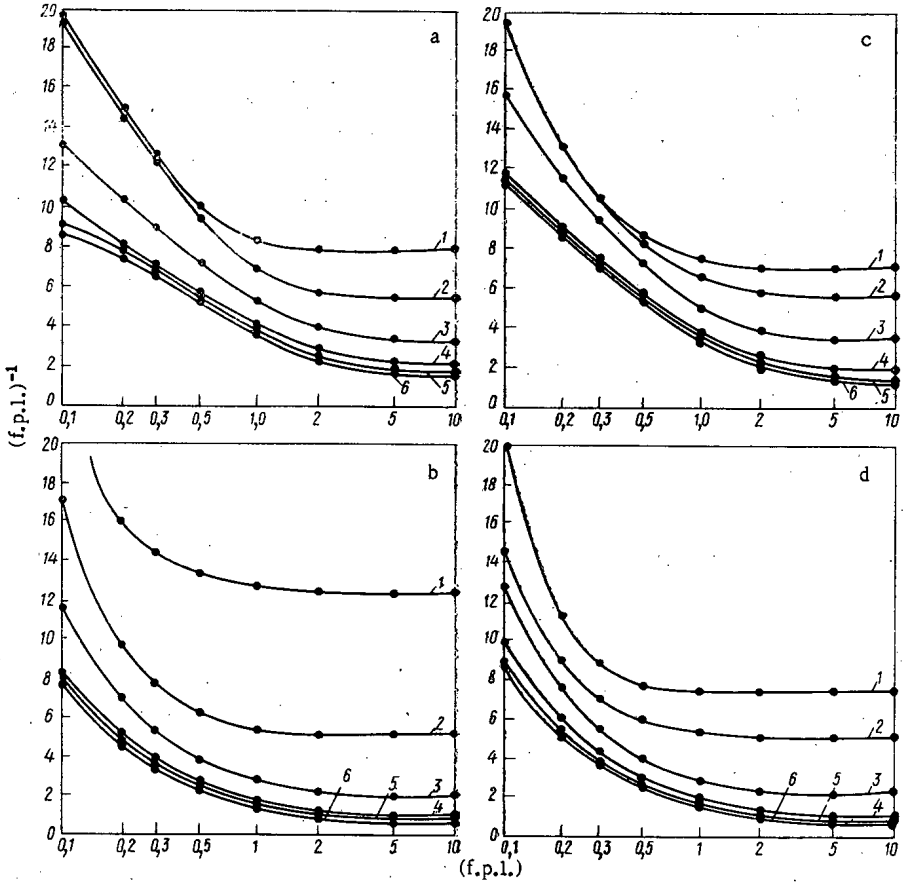

Fig. 2. Values of α at E = 1.25 (a, b) and 0.279 MeV (c, d): a, c) isotropic source; c, d) monodirectional source; 1) Pb; 2) Sn; 3) Fe; 4) concrete; 5) C; 6) Be.

From analysis of data on the γ-ray albedo, obtained from Monte Carlo calculations according to a program described in [3], it follows that the numerical γ-ray albedo $a(r, d)$ from a circular region of radius r on the surface of a barrier of thickness d can be described to within ± 10% by the empirical formula

$$a(r, d) = a(\infty, \infty)[1-\exp(-\beta r)]\{1-\exp[-\alpha(r)(d-c)]\}, \quad (1)$$

where $a(\infty, \infty)$ is the asymptotic value of the albedo from a semi-infinite scatterer made of the same material when the primary-quanta source has a fixed energy of E_0, and β, $\alpha(r)$, and c are empirical quantities (Figs. 1 and 2).

Formula (1) was obtained from the results of calculations for point isotropic sources and monodirectional beams normally incident upon the surface of a barrier at the point r = 0 for E_0 = 0.145, 0.279, 0.662, and 1250 MeV and for barriers made of Be, C, concrete, Fe, Sn, and Pb of varying thickness ranging from 0.1 to 5 free-path lengths (f.p.l.). The value of c for an isotropic source is 0.5 free-path lengths of primary quanta of energy E_0, and c = 0 for a monodirectional source. Using this formula, it is not difficult to find the number of reflected γ-ray quanta emitted from a surface portion of unit area, bounded by radii r_1 and r_2 of concentric circles with center at the point r = 0.

LITERATURE CITED

1. B. P. Bulatov et al., Gamma-Ray Albedo [in Russian], Atomizdat, Moscow (1968).
2. O. S. Marenkov, At. Energ., 21, No. 4, 297 (1966).
3. D. B. Pozdneev and M. A. Faddeev, Kernenergie, 16, No. 4, 105 (1973).
4. T. Nakamura and T. Hyodo, J. Nucl. Sci. Technol., 6, No. 3, 143 (1969).

YIELDS OF ^{200}Tl, ^{201}Tl, ^{202}Tl, AND ^{204}Tl DURING PROTON AND DEUTERON IRRADIATION OF MERCURY

P. P. Dmitriev, G. A. Molin,
Z. P. Dmitrieva, and M. V. Panarin

UDC 539.172.12

Irradiation of mercury with protons and deuterons produces ^{200}Tl ($T_{1/2}$=26.1 h), ^{201}Tl ($T_{1/2}$=73 h), ^{202}Tl ($T_{1/2}$=12 days), and ^{204}Tl(3.78 yr), whose half-life makes them convenient for use in applied and research problems.

In this paper, the $^{200-202}$Tl yield is measured as a function of the proton and deuteron energy during irradiation of thick mercury targets and theoretical yield curves are calculated for ^{204}Tl.

The irradiated samples were prepared from mercuric oxide, the conversion factor for the yield for HgO to the yield in metallic mercury is 1.17. The proton and deuteron energy was varied with copper stopping foils. The methods employed to irradiate the samples and to measure the integrated irradiation current and the activity of the isotopes were the same as in [1, 6] which reported on work also done on the cyclotron of FÉI (Obninsk).

Isotopes $^{200-202}$Tl decay through electron capture (EC) and therefore their quantum radiation contains strong components of KX and LX rays produced by K and L capture as well as K and L conversion. Isotope ^{204}Tl experiences β decay (97.46%) and electron capture (2.54%) to the ground state of ^{204}Pb and ^{204}Hg, respectively, and hence does not emit γ quanta.

Table 1 gives the most intense components of quantum radiation accompanying the decay of $^{200-202}$Tl and ^{204}Tl. The gamma yield was obtained from the decay scheme given in [2, 3], taking the conversions into account. The yield of γ, LX, and KX quanta from $^{200-202}$Tl is calculated by the formulas

$$n(KX)=\varepsilon_k\omega_k+\omega_k\sum_i n_{\gamma_i}\alpha K_i;$$

$$n(LX)=\varepsilon_L\omega_L+n_{KL}\varepsilon_k\omega_L+\omega_L\sum_i\left(n_{\gamma_i}\alpha_{L_i}+n_{KL}n_{\gamma_i}\alpha_{K_i}\right).$$

Here ω_k, ω_L, and α_k, α_L are the fluorescence yield and the K- and L-conversion coefficients, respectively; n_{KL} is the number of L vacancies freed per K vacancy. The probabilities of K and L capture, ε_k and ε_L, were calculated by the formulas and data of [4]; ω_k, ω_L, and n_{KL} are also given there. The values of α_k and α_L were taken from [2, 3, 5], and the LX quanta were assigned the energy of the most intense transition $L\alpha_1$ = $L_3 - M_5$. The yield of KX and L quanta of ^{204}Tl were obtained in [4].

The experimental yield curves for $^{200-202}$Tl and the theoretical curves for ^{204}Tl are given in Figs. 1 and 2. The reactions producing $^{200-202}$Tl and ^{204}Tl are given in Table 2.

Table 3 presents measured yields for given proton and deuteron energy. The calculation of the theoretical yield curves for ^{204}Tl was similar to that in [6]. No data are available in the literature about the yield and cross section for nuclear reactions producing $^{200-202}$Tl and ^{204}Tl.

As is seen from Table 3, when the protons and deuterons are slowed down the absolute error of the energy value increases. It thus follows that the path and energy of the particles are related by $R \sim E^{7/4}$, whence $dE/E = K\,dR/R$ or $dE = KE\,dR/R$, i.e., the absolute error is proportional to the absorbed energy.

Let us consider the production of $^{200-202}$Tl and ^{204}Tl of high radioisotopic purity. Radioisotopically pure ^{204}Tl and ^{202}Tl, free of $^{200-202}$Tl, are obtained after appropriate cooling. Irradiation of mercury with protons and

Translated from Atomnaya Énergiya, Vol. 41, No. 6, pp. 431-434, December, 1976. Original article submitted April 16, 1976.

TABLE 1. Energy and Quantum Yield of γ, KX, and LX Quanta

Isotope	Energy of K_α, K_β, LX	Quantum yield, %	References
^{200}Tl	1205,7	30,7	[2]
	367,97	89,3 *	
	K_α 70,14	71,3	Present paper
	K_β 80,71	20,7	" "
	LX 9,99	34	" "
^{201}Tl	167,43	8,8 *	[3]
	K_α 70,14	69,8	Present paper
	K_β 80,71	20,2	" "
	LX 9,99	45	" "
^{202}Tl	439,4	92 *	[3]
	K_α 70,14	71,3	Present paper
	K_β 80,71	20,7	" "
	LX 9,99	32	" "
^{204}Tl	K_α 70,14	1,14	[4]
	K_β 80,71	0,33	[4]
	LX 9,99	0,76	[4]

*γ-ray peaks used to measure the activity.

TABLE 2. Energy Thresholds of Reactions of Production of $^{200-202}$Tl and ^{204}Tl, MeV

Reaction	Isotope			
	^{200}Tl	^{201}Tl	^{202}Tl	^{204}Tl
pn	3,26	1,20	1,91	1,16
$p2n$	9,53	9,02	*	*
$p3n$	17,31	—	15,45	*
dn	—	—	—	*
$d2n$	5,51	3,45	4,16	3,41
$d3n$	11,80	11,3	*	*
$d4n$	19,65	*	17,75	*

*The isotope is not produced in the given reaction.

reaction.

TABLE 3. Yield of $^{200-202}$Tl and ^{204}Tl

Origin and energy of particles, MeV	Yield, μCi/μA·h			
	^{200}Tl	^{201}Tl	^{202}Tl	^{204}Tl *
(Hg + p):				
22,4±0,43	1020±130	860±110	21,9±2,8	0,0077
20,3±0,47	765±98	685±87	16,4±2,1	0,0077
17,1±0,52	450±57	410±63	10,8±1,4	0,0071
14,3±0,56	195±25	160±20	7,2±1,0	0,0060
10,4±0,61	15±1,9	20,0±2,5	1,6±0,2	0,0020
(Hg + d):				
22,5±0,41	1065±135	595±76	61,0±7,8	0,10
21,1±0,43	790±100	460±59	51,0±6,5	0,098
20,2±0,46	725±93	400±51	46,4±5,9	0,092
18,8±0,49	530±68	245±31	43,8±5,6	0,085
17,4±0,50	380±49	165±21	36,5±4,7	0,075
14,3±0,55	135±17	55,0±7,0	19,5±2,5	0,043
10,1±0,62	10,0±1,3	5,0±0,7	1,5±0,2	0,008

*The values of the ^{204}Tl yield were calculated.

deuterons produces ^{198}Tl($T_{1/2}$ = 5.3 h) and ^{199}Tl($T_{1/2}$ = 7.4 h) whose activity becomes insignificant 3 days after the irradiation. The content of the admixture ^{204}Tl in the case of proton irradiation is smaller than in the case of deuteron irradiation by a factor of ~ 10-20 and upon completion of the irradiation is ~0.0008% for ^{200}Tl, ~0.001% for ^{201}Tl, and ~0.04% for ^{202}Tl. Radioisotopically pure ^{200}Tl can be obtained by the reaction ^{197}Au (α, n) ^{200}Tl. When gold was irradiated with 44-MeV alpha particles the ^{200}Tl yield was 32 μCi/μA·h, i.e., smaller by a factor of ~30 than when mercury was irradiated with protons and deuterons.

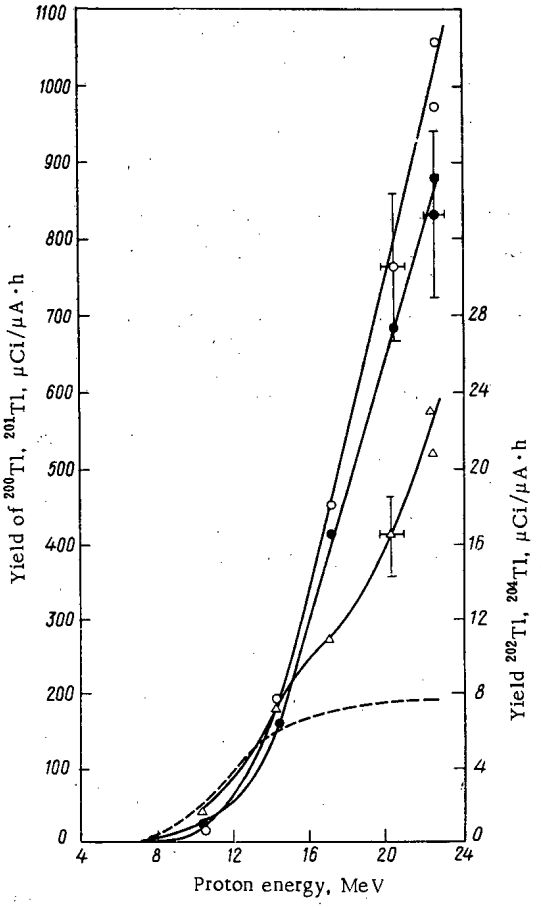

Fig. 1

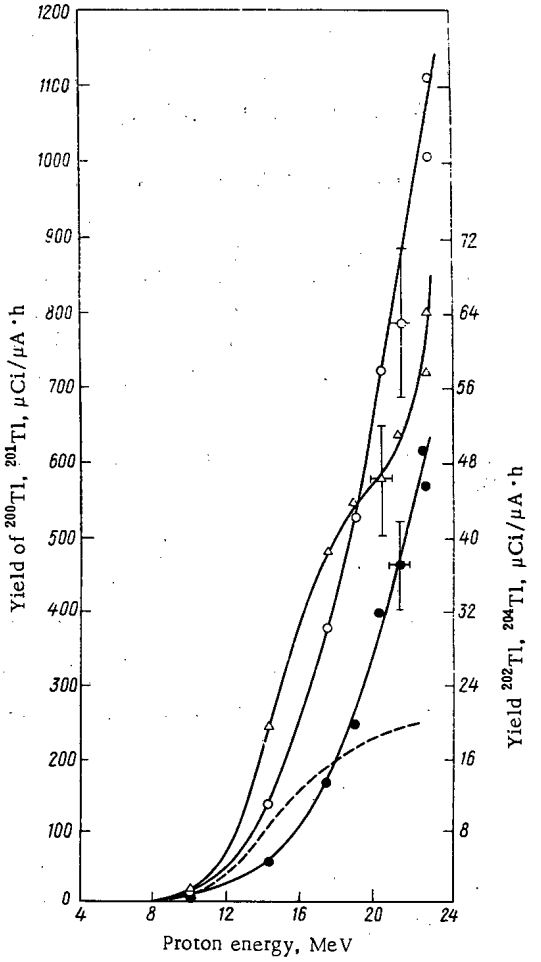

Fig. 2

Fig. 1. Yield of $^{200-202}$Tl and ^{204}Tl vs proton energy for thick mercury targets: ○) ^{200}Tl; ●) ^{201}Tl; △) ^{202}Tl; – – –) ^{204}Tl (×1000).

Fig. 2. Yield of $^{200-202}$Tl and ^{204}Tl vs deuteron energy for thick mercury targets: ○) ^{200}Tl; ●) ^{201}Tl; △) ^{202}Tl; – – –) ^{204}Tl (×200).

Isotopes $^{200-202}$Tl free from ^{204}Tl are obtained by irradiating mercury with alpha particles. Then, (αxn) reactions produce ^{200}Pb ($T_{1/2}$ = 21.5h), ^{201}Pb ($T_{1/2}$ = 9.4 h), ^{202m}Pb ($T_{1/2}$ = 3.62 h), ^{202}Pb ($T_{1/2} = 3 \cdot 10^5$ yr) which are parent isotopes of $^{200-202}$Tl. The isotope ^{202m}Pb decays as follows: ^{202m}Pb → ^{202}Tl (9.5%), ^{202m}Pb → ^{202}Pb (90.5%). After ~1.5 days only ^{200}Pb and ^{201}Pb remain in the lead fraction, and after ~4 days, only ^{200}Pb, which is in dynamic equilibrium with ^{200}Tl. Because of the long half-life, the ^{202}Pb activity is negligible. High-purity ^{201}Tl can be obtained by the reaction ^{203}Tl(p, 3n) ^{201}Pb, the reaction threshold being 16.5 MeV. The proton energy should not exceed the threshold of the reaction ^{203}Tl(p, 4n) ^{200}Pb, which is 25 MeV. Enriched mercury isotopes can be used to obtain $^{200-202}$Tl of extremely high radioisotopic purity.

The authors thank G. N. Grinenko for his assistance in the work.

LITERATURE CITED

1. P. P. Dmitriev et al., At. Energ., 31, No. 2, 157 (1971); 39, No. 2, 135 (1975).
2. T. Comppa et al, Nucl. Phys., A163, 513 (1971).
3. R. Auble, Nucl. Data Sheets, 5, 561 (1971).
4. M. Martin and P. Blichert-Toft, Nucl. Data Tables, A8, Nos. 1-2 (1970).
5. R. Hager and E. Selzer, Nucl. Data Tables, 4, Nos. 1-2 (1968).
6. P. P. Dmitriev et al., At. Energ., 32, No. 5, 426 (1972).

ALBEDO OF A CYLINDRICAL ROD

V. V. Orlov and V. S. Shulepin

UDC 539.125.52:621.039.51.12

A system of multigroup albedo equations was obtained in [1] for the probability of reflection of neutrons from a cylindrical rod or from an external spherical medium. As shown in [1, 2] in the two limiting cases (a cylinder of very small and very large radius) the equations of [1] lead to a solution that is close to the exact one. The objective of the present paper is to verify the exactness of the equations of [1] for a cylinder of intermediate radius.

An idea of the exactness of the system of equations in [1] can be obtained by solving the one-velocity albedo equation

$$d\beta/dR = \Sigma_s - 2\beta(\Sigma_s + 2\Sigma_c) + \Sigma_s\beta^2 + (1/R)(1-\beta), \quad (1)$$

where β is the albedo, Σ_S is the neutron scattering cross section, Σ_C is the absorption cross section, and R is the radius of the rod. The initial condition when $R=0$ is $\beta(0)=1$. In the case $\Sigma_S=0$ Eq. (1) is of the form

$$\beta = [1-\exp(-4R\Sigma_c)]/4R\Sigma_c. \quad (2)$$

When $\Sigma_S \neq 0$ the solution of Eq. (1) can be rewritten as

$$\beta = 1-[a_0R/(1+a_1R+a_2R^2+a_3R^3+\ldots)]. \quad (3)$$

Substitution of Eq. (3) into Eq. (1) makes it possible to determine the coefficients a_n. The radial relation (3) is analogous to the formula for the albedo of a cylindrical rod, obtained in [3]. Numerical calculations showed that the solution (3) displays good convergence right up to $R\Sigma = R(\Sigma_S+\Sigma_C) = 2$.

The exactness of Eq. (1) was verified by comparing the results of calculation by Eqs. (2) and (3) with the exact results given in [4]. The calculation was performed for $R\Sigma$ over the interval [0; 2] for different ratios $h=\Sigma_S/\Sigma$ (Table 1).

According to Table 1, the exactness of Eq. (1) is satisfactory for all h when $R\Sigma \leq 0.5$ or for $h > 0.7$ when $R\Sigma \leq 2$. As noted above, Eq. (1) also leads to correct results in the interval $R \to \infty$ for any h.

Equation (2) is inexact for large $R\Sigma$ and small h because under these conditions a large contribution to the albedo is made by neutrons which do not experience collision in the rod and whose angular distribution is highly anisotropic. Equation (1) can be made more exact by introducing the albedo of unscattered neutrons.

TABLE 1. Albedo of Rod for Different $R\Sigma$

h	Exact solution						Solution of Eq. (1)					
	2,0	1,5	1,0	0,5	0,25	0,17	2,0	1,5	1,0	0,5	0,25	0,17
0,0	0,053	0,095	0,186	0,404	0,623	0,726	0,125	0,166	0,245	0,432	0,632	0,730
0,2	0,115	0,165	0,263	0,482	0,683	0,773	0,179	0,233	0,317	0,504	0,689	0,775
0,4	0,199	0,256	0,363	0,574	0,749	0,823	0,270	0,319	0,407	0,590	0,753	0,825
0,6	0,324	0,389	0,499	0,686	0,823	0,877	0,386	0,437	0,529	0,695	0,825	0,878
0,8	0,542	0,604	0,694	0,824	0,906	0,936	0,568	0,623	0,705	0,827	0,907	0,936
1,0	1,0	1,0	1,0	1,0	1,0	1,0	1,0	1,0	1,0	1,0	1,0	1,0

LITERATURE CITED

1. V. V. Orlov, At. Energ., 38, No. 1, 39 (1975).
2. Yu. N. Kazachenkov and V. V. Orlov, At. Énerg., 18, No. 3, 226 (1965).

Translated from Atomnaya Énergiya, Vol. 41, No. 6, p. 434, December, 1976. Original article submitted March 9, 1976.

3. A. Amauyal, P. Benoist, and J. Horowitz, J. Nucl. Energy, 6, 79 (1957).
4. J. Stuart, in: Problems of Nuclear Energy [in Russian], No. 6, Izd. Inost. Lit., Moscow (1958), p. 71.

OPERATIVE MONITORING OF FISSION PRODUCTS IN SODIUM COOLANT OF FAST REACTOR

V. B. Ivanov, V. I. Polyakov,
Yu. V. Chechetkin, and V. I. Shipilov

UDC 621.373/374

To monitor the state of the active zone of fast reactors during operation and to predict the radiation situation when attending to the equipment it is necessary to know the level of the radioactivity of the fission products and the rate at which they are accumulated in the loop. Existing systems for monitoring the hermeticity of jackets with respect to delayed neutrons and radioactive gases do not directly yield such information.

The choice of radionuclides whose activity can be measured to solve the problem posed is determined by the half-life, the character of their leakage through defects in the fuel jackets, and the contribution of their radiation to the dosage rate from the equipment. The principal difficulty in measuring the activity of fission products is determined by the fact that during the reactor operation this activity is smaller by a factor of 10^3–10^6 than that of the short-lived activation isotope ^{24}Na.

To ensure operative monitoring of the variations in the activity of selected nuclides in the loop, it is necessary to carry out measurements right in the sodium channel, the duration of these measurements not exceeding several hours. Measurement by the usual one-detector and Compton suppression spectrometer systems with such ratios of the radioactivity monitored and interfering nuclides is possible only with very long measuring times. Compton (CS) and summing Compton (SCS) spectrometers yield a decrease in the Compton distribution by a factor of 100-1000 but in doing so they also have a significant loss in the efficiency of recording the total absorption peak. Because of their more compact geometry contiguous semiconductors (duodes) in the SCS mode make it possible to attain a lower efficiency loss than in the case of the SCS mode with dectors separated by a considerable distance. Studies of various types of detectors showed that thin composite planar detectors in the SCS mode are more sensitive than are detectors of the same total volume in the one-detector mode [1, 2].

The block diagram of an SCS, which was tested in measurements in a sodium loop bypass connected to the first loop of a BOR-60 reactor, is given in Fig. 1. The coolant flowed through a 16-mm tube. It took 100 sec for the sodium to arrive from the active zone. The detector was set up 2 m from the tube behind a 2-cm collimator. The detector used in the experiment was a Ge(Li) duode consisting of two planar detectors, D1 and D2, put together with a thin beryllium spacer. The total sensitive region was 12 cm^3. The overall energy resolution for an energy of 662 keV with input loads of 10^3 and $1 \cdot 10^5$ was 5 and 6 keV, respectively. Energy windows of 120-220 keV and 220-460 keV, respectively, were installed in the time channels of detectors D1 and D2 to record the spectra of the sum of coincident energy in the 340-680-keV range. The resolving time of the coincidence circuit was 75 nsec. The choice of the energy windows was determined by the desire to simultaneously monitor nuclides ^{137}Cs (662 keV) and ^{131}I (364 and 637 keV).

The γ-ray spectrogram obtained with the spectrometer operating in the SCS mode (Fig. 2) in 150 min exhibits total absorption peaks with an energy of 364.5, 511, 637, and 662 keV. The specific activities found from the results of this experiment for ^{131}I and ^{137}Cs, respectively, were $(3 \pm 0.6) \cdot 10^{-3}$ and $(2 \pm 0.4) \cdot 10^{-3}$ Ci/kg sodium with a ^{24}Na radioactivity of 48 ± 5 Ci/kg. In a one-detector mode with a detector of the same volume no sought γ-ray peaks were resolved.

Thus, the SCS technique with a composite semiconductor detector allowed the fission-fragment nuclides to be distinguished against the background of the ^{24}Na activity in the first loop with a useful-to-interfering ac-

Translated from Atomnaya Énergiya, Vol. 41, No. 6, pp. 435-436, December, 1976. Original article submitted April 20, 1976.

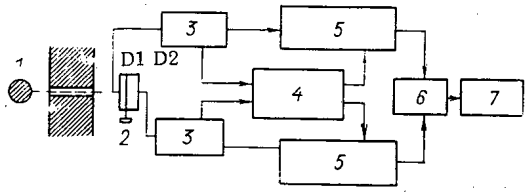

Fig. 1

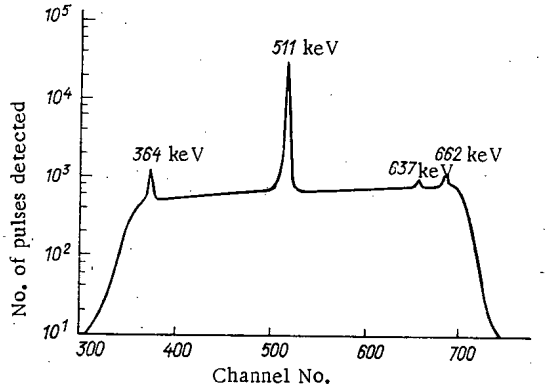

Fig. 2

Fig. 1. Block diagram of summing Compton spectrometer with Ge(Li) duode and measuring geometry: 1) piping with sodium coolant; 2) Ge(Li) duode; 3) fast charge-sensitive preamplifier; 4) logic circuit for selection and sampling of energy windows; 5) circuit for amplification and controlled shaping based on two delay lines ($1 \times 1\,\mu$sec); 6) summator-integrator; 7) pulse-height analyzer.

Fig. 2. γ-Ray spectrum of sodium coolant in the first loop of a BOR-60 reactor.

tivity ratio of the order of 10^4. Optimization of detector size and construction, improvement of the loading properties of the spectrometric channel with lower counting loss due to pulse pile-up, and the choice of energy windows in the spectrometric and measuring channels will make it possible to obtain a lower limit of measuremeant for the summing Compton spectrometer and to determine the activity of other fission products.

The development of the SCS technique, in the opinion of the authors, will make it possible to ensure reliable continuous monitoring of the behavior of fission products in a sodium coolant and the development of defects in fuel element jackets.

LITERATURE CITED

1. D. Walker and J. Palms, IEEE Trans. Nucl. Sci., NS-17, No. 3, 296 (1970).
2. V. Ivanov and V. Shipilov, Nucl. Instrum. and Methods, 119, 313 (1974).

REGENERATION OF FAST-REACTOR FUEL

A. F. Tsarenko

A meeting of IAEA experts on the regeneration of fast-reactor fuel was held in Leningrad from May 17 to 21, 1976, with the participation of representatives of the USSR, France, Great Britain, the USA, the Federal German Republic, Italy, Belgium and Japan. The agenda included a discussion of the state of the art in the regeneration of fuel from active zones: storage and shipping to a processing radiochemical plant; cleansing fuel assemblies from sodium; preparation for regeneration and the actual regeneration; waste handling.

The papers by the experts and the discussion showed that the level and scale of research on fuel regeneration in various countries are closely bound up with the level of development of the reactors themselves. The fullest reports of all on the topics under discussion were presented by specialists of the USSR and France.

The following reactors are at present in successful operation in the world: BR-10, BOR-60, BN-350 (USSR); from 1967-1970 "Rhapsodie-Fortissimo" (France, 24-37 MW), from 1963 DFR [60 MW(T)] and from 1974 PFR [600 MW(T), Gt. Britain]. At the present time the following reactors are under construction or in the planning stage: in the Soviet Union BN-600 and BN-1500; in the United States FFTF [440 MW(T)], 1979, Clinch River [350 MW(T)], 1983, PLBR [1000-2000 MW(E)]; in France, jointly with the Federal German Republic and Italy, "Super Phoenix" [1200 MW(E)]; and Italy PEC [130 MW(T)], 1979. The Federal German Republic planned to start construction in 1976 of reactor KNK-2 [58 MW(T)] and in the same year Japan was to start construction of JOYO [100 MW(E)], and in 1983, MONHU [300 MW(E)].

The development of reactor BN-1500 in the USSR, and the rate at which plutonium is accumulated during the regeneration of fuel from atomic power plants with thermal reactors (water moderated water cooled power reactor, VVÉR, RBMK) permit the conclusion that the widespread introduction of fast reactors will begin no earlier than 1990. The atomic power industry of the USSR will present atomic power plants with both thermal and fast reactors, with the relative proportion of the latter gradually increasing. It is advisable to centralize the regeneration of the fuel from such reactors in a radiochemical plant; according to calculations one plant should handle fuel from atomic power plants with a total rating of 6-12 million kW, i.e., e.g., from 4 to 8 BN-1500 reactors. This requires the plant site be chosen in keeping with the conditions of long-term storage of the radioactive waste as well as the safety of the population in the vicinity of the plant and protection of the environment from radioactive contamination. If one proceeds from the premise that the power input will be determined by the plutonium build-up, reducing the cooling time of the fuel after discharge from the reactor from 3 yr to only 1 yr makes it possible for the rating of atomic power plants with fast reactors to be increased from 20 to 55 million kW, or 2.5 times, by the year 2000.

United States experts discussed the principal parameters of scientific-research and experimental-design work on the regeneration of fuel from fast reactors with liquid metal coolants (LMFBR). These reactors are looked upon in the USA as one means of satisfying the national energy requirements starting from 1990. A "hot" experimental facility for regenerating fuel is to come into operation in 1988, and a pilot plant in 1995-2000.

France, which has been developing fast reactors for the past 18 years, is at present the only country with industrial experience in the regeneration of spent mixed uranium–plutonium fuel (department AT-1 of the plant in Cape Ag, and the experimental department of the plant at Marcoule). In Gt. Britain the research is concentrated at the experimental plant at Dounreay.

The research in Italy has been directed at adapting the JTREC experimental plant at Rotondella with a capacity of 10 kg oxide fuel for the regeneration of PEC reactor fuel. Similar work is being done in the Federal German Republic on the MJLLJ experimental facility with samples of DFR reactor fuel.

Translated from Atomnaya Énergiya, Vol. 41, No. 6, pp. 438-440, December, 1976.

The Belgian research program envisages the construction of an experimental plant in the nuclear research center in Mole by 1980; this plant is intended for experiments on cutting fuel elements on the thermal oxidation processing of fuel, and on dissolution and gas scrubbing.

In the late 1980s Japan plans to build an experimental plant for developing a technology for the regeneration of fuel from an experimental and a pilot reactor.

In all countries at the present time the aqueous extraction technology (extraction recovery of uranium and plutonium from aqueous nitrate media with a solution of tri-n-butyl phosphate in inert solvents) is recognized to be technically feasible, but it is necessary to solve problems associated, in the first place, with the storage and shipment of mixed fuel, prepared for the operation preceding regeneration. In this plan the principal effort should be to create effective methods for removing metallic sodium from fuel assemblies, decladding the fuel, dissolution, clarification, as well as for storing and shipping spent fuel elements.

Storing, Cleansing Spent Assemblies From Coolant Residue, and Shipment

Of all the possible methods of heat removal during storage of spent fuel from fast reactors (cooling with gas, sodium, bismuth-lead alloy, fused salts, organic materials) preference is given to sodium. Upon being discharged from the reactor, assemblies are held in a sodium medium in a storage vessel inside the reactor, and then for longer cooling are transferred to a sodium- and inert-gas filled (intermediate) storage vessel outside the reactor, and finally put into a water pond. The assemblies of the Rhapsodie and Phoenix reactors, for example, are held in the vessel inside the reactor for two months (the heat release drops to 0.4 and 6.0 kW, respectively, per assembly), and then in a medium of argon (first) or sodium (second) are put into a storage vessel outside the reactor with an inert gas or sodium, respectively.

Assemblies of the PFR reactor are cooled for 9 months in the internal storage vessel of the reactor, and are then shipped to the reprocessing plant. Assemblies of the BN-350 reactor remain in internal storage for two months until the residual release is reduced from 20-30 to 6-7 kW per assembly. In the external storage vessel, consisting of a rotating drum with sodium, the assembly moves in an inert-gas medium. During the transfer (~4 min) the temperature of the fuel element cladding reaches 480°C. The holding period does not exceed the time between rechargings. When the heat release has been reduced to 3-4 kW per assembly, the assembly is cleansed from sodium and then transferred to a water-filled cooling pond.

The most common method of cleansing assemblies from sodium is to treat them with water vapor with nitrogen, argon, or carbon dioxide gas as gas carrier. An experiment using a lead bath to remove sodium and to contain defective fuel elements (USSR) has demonstrated this method to be promising. However, some technical problems remain to be solved. To prevent radioactivity from entering the storage vessel from assemblies with defective fuel elements, it is deemed advisable to place the assemblies in hermetically sealed containers.

Problems due to the high level of heat release and radioactivity arise during shipment of spent fuel. The heat release of one assembly may reach 5-10 kW, depending on the assembly size, the irradiation conditions, and the cooling time. Present-day technology makes it possible to construct a shipping container designed for a heat removal of about 40 kW, which means one container can take 6 to 10 assemblies. The mass of such a container is 50-60 tons.

It was achnowledged at the meeting that the shipment of spent fuel in a sodium medium, as well as the use of other heat-transfer media such as lead, have not yet been investigated sufficiently.

Decladding the Spent Fuel

Alongside the mechanical method of cutting fuel elements (France, Gt. Britain, USA) other methods have been developed: laser cutting (USSR, Britain), melting the claddings of corrosion-resistant steel (USSR), etc. Work is under way along such lines as constructing equipment for cutting individual fuel elements after dismantling the assembly, as well as for cutting assemblies as a whole.

The decladding of spent fuel requires the solution of complex problems involved in the high heat release, cleansing from gaseous and fugacious fission products, and nuclear safety. Experts of some countries (France, USSR) voiced the opinion that the holding ("cooling") period for assemblies should be no less than 6-12 months.

Dissolution of Spent Fuel and Clarification of the Solution

Dissolution of uranium–plutonium oxide fuel in concentrated (8-12 M) nitric acid proceeds in two stages: rapid dissolution of the bulk of the fuel and the slow dissolution of the residual fraction, constituting highly dispersed particles (from > 1 to 10 μ) consisting of the fuel composition ($UO_2 - PuO_2$), as well as alloys containing fission products (Ru, Mo, Rh, Pd, Tc) and plutonium. The quantity of undissolved plutonium evidently depends on the conditions of the fuel fabrication, irradiation, and dissolution. Therefore, the fuel is dissolved into two stages, HF additives being used in the second stage (USSR, France). For this purpose apparatus of periodic and continuous operation is being developed.

Most of the experts emphasized the need for thorough clarification of solutions prior to extraction. Work is under way to develop reliable filters and filtering centrifuges; filtration and centrifuging can be employed as two stages in the clarification process in any order.

In Dounreay a high-speed centrifuge (20,000 rpm) is used for clarification, and in department AT-1, a pulsating filter is employed for that purpose. Soviet specialists propose flocculants in the solution clarification stage.

Technology of Fuel Regeneration

It was acknowledged at the meeting that in the near future fuel from the active zone will be regenerated by an aqueous-extraction technology of the "Purex process" type. The feasibility of highly efficient quantitative regeneration of fuel by such methods is regarded as having been demonstrated experimentally.

Experience has been gained in regenerating mixed uranium-plutonium fuel on the experimental and pilot scale. The most important experience has been accumulated in department AT-1 which has already regenerated about 1 ton of mixed oxide fuel from the Rhapsodie reactor with a burnup of up to 100,000 MW-days/ton. The experimental department at Marcoule has also started regenerating mixed fuel from the active zone. Several cycles have also been carried out at the MJLLJ plant in Karlsruhe (Federal German Republic) and at the Dounreay plant.

A serious problem with adapting aqueous-extraction technology to the regeneration of active-zone fuel is that of radiation decomposition of the organic extractant and nitric acid in the first extraction cycle. This problem is solved by using extraction apparatus with a short phase-contact time. Pulsating columns, and especially centrifugal extractors, are just such apparatuses.

A very high plutonium content (up to 200 kg/ton) presents problems of accomplishing the complete simultaneous extraction of plutonium and uranium, preventing the formation of a third phase, salt-free separation of plutonium from uranium, monitoring and computing the plutonium content in solutions in conformity with the safety requirements and the system of guarantees, and attaining discharge concentrations of plutonium in the technological waste.

An interesting method is that of electrochemical selective reduction and re-extraction of plutonium in the stage of separation from uranium. This method has been successfully tested in the regeneration of fuel samples at the MJLLJ plant in the Federal German Republic; there are plans to introduce the method in the WAK plant (Federal German Republic) and in Marcoule.

Work on the fluoride method of fuel regeneration is under way at present in the USSR, France, and Japan. The state of the development of this method is such that it cannot be introduced into industry. The basic problems which must be solved are connected with attaining a high degree of separation of uranium and plutonium, deeply purifying plutonium from fission products, and completely extracting uranium and plutonium from the final product. Putting the fluoride method into industrial use requires an extensive program of scientific research and testing and design work and technological investigations. Fuel from the BOR-60 and Rhapsodie reactors with a short holding time (3-6 months) has been regenerated in single operations in the Fregat (USSR) and Atilla (France) pilot plants, demonstrating the basic feasibility of the gaseous fluoride technology.

Method of Decontaminating Waste Gases

It is known that gaseous wastes of radiochemical reprocessing plants are the major source of radioactivity entering the environment. The need to reduce the radioactive discharges into the atmosphere requires the introduction of efficient gas scrubbing systems in the plant. The state of the technology for trapping iodine, krypton, xenon, tritium, and ^{14}C was discussion at the meeting in these terms. The iodine trapping methods are

in the pre-industrial stage at present but none of them has found universal application. These are the "wet" methods [alkaline scrubbing, scrubbing with mercury nitrate solution, "Iodox process" – scrubbing gasses with fuming (concentration of more than 20 M) nitric acid] and dry methods based on the use of filter media in which silver salts are the active reagents. In eliminating krypton, more attention is paid to methods of cryogenic distillation in comparison with methods of absorption with fluorocarbons.

As for the elimination of tritium, only attempts are being made to solve the problem. A method is being developed in the Federal German Republic and France for localizing (and building up) tritium in recirculating aqueous solutions of the main regeneration processes. Even if tritium is successfully concentrated in a small volume of waste, the problem of storing and eliminating waste will remain.

In plants regenerating fast-reactor fuel the content of radioactive isotopes and plutonium will be significantly higher than in thermal-reactor fuel. Therefore, the ratio of the radioactivity discharged into the environment to the activity in plants after the regeneration of fast-reactor fuel should be one-thousandth of that in plants regenerating thermal-reactor fuel. To attain this level it is necessary to make a substantial improvement in the methods of localizing radioactivity in all stages of regeneration, to prevent losses of plutonium, and to develop effective methods for trapping gaseous and fugacious fission products.

Waste Disposal

The general consensus is that the safe disposal of waste from the regeneration of fast-reactor fuel will be based on methods which have already been accepted or are being developed for the fuel cycle of thermal reactors. Most programs are based on vitrification, which is recommended for solutions with a heat release of less than $5 \cdot 10^4$ W/m^3. For fast reactors it is necessary either to increase the holding of fuel for regeneration to more than a year, to mix the waste from fast and thermal reactors, or to develop hard matrices allowing storage at higher temperatures.

MEETING OF FOUR NUCLEAR DATA CENTERS

V. N. Manokhin

Four nuclear data centers held their regular (12th) meeting in Vienna on April 26-27, 1976. It was attended by representatives of the National Neutron Cross Section Center (Brookhaven, USA), Neutron Data Compilation Center (Saclay, France), Nuclear Data Center (Obninsk, USSR), Nuclear Data Section (IAEA, Austria), as well as Rumania and Poland. Brief reports on the work of each center over the previous year were read at the meeting.

The National Neutron Cross Section Center is engaged in work on Series V of the evaluated nuclear data file ENDF/B. The second volume of the new BNL-35 atlas has been completed. In 1975 evaluated data on fission products and reactor dosimetry were turned over for general use in the IAEA in 1975.

The Neutron Data Compilation Center has done a great deal of work on creating a SINDA bibliographical catalog on collecting numerical data and on writing a program for data format conversion.

The Nuclear Data Section prepared the SINDA-76 catalog for publication, having previously eliminated redundant and erroneous information. The CINDU-11 catalog of nuclear data possessed by the NDS has been published. And WRENDA-76, a register of inquiries for nuclear data, is being prepared for publication.

Since April 1975 the Nuclear Data Center (NDC) has recorded 75 papers on magnetic tape. In all, to the present time it has recorded some 300 out of a total of 450 papers, containing numerical data, published in 1959-1975. The evaluated data (complete files) of a number of isotopes have been handed over to the IAEA. Four "Nuclear Constants" compilations were published and 110 inquiries were satisfied in 1975. The NDC has prepared for publication the proceedings of the Third All-Union Conference on Neutron Physics. The evaluation of all cross sections of nickel and chromium has been completed.

Translated from Atomnaya Énergiya, Vol. 41, No. 6, pp. 440-441, December, 1976.

The 19th meeting discussed the state of the computer library of experimental neutron data in exchange format (EXFOR). At the present time this library contains more than 1,700,000 lines of information on magnetic tape – numerical results and brief descriptions of the conditions of many experiments on neutron physics. The meeting also considered problems pertaining to the completeness of the data library, data exchange, errors in the magnetic tape recordings, and the introduction of changes suggested earlier in the EXFOR format. Some problems of the SINDA bibliographic catalog were also considered (ensuring the completeness of the abstracts, the connection with the INIS system, the periodicity of publication, etc.).

The meeting recommended that all centers inform each other about the existence of evaluated data, descriptions of evaluations, and results of comparison of the evaluated data of the various libraries.

The results of the meeting showed that the international cooperation on the exchange of experimental neutron data is developing. The exchange of evaluated neutron data is increasing.

The next meeting of the four nuclear data centers will be held in Obninsk in April, 1977.

MEETINGS ON THE COMPILATION OF NUCLEAR DATA FROM REACTIONS WITH CHARGED PARTICLES AND DATA ON THE STRUCTURE OF THE ATOMIC NUCLEUS

L. L. Sokolovskii

The meeting of consultants on data from reactions with nuclear particles, organized by the Nuclear Data Section of the IAEA, was held in Vienna from April 28 to 30, 1976, with the participation of representatives of Gt. Britain, Poland, Rumania, the USSR, the USA, France, the Federal German Republic, and Japan. The agenda was purely technical: the index of bibliographical data, the range of compilation, computer file, keywords, dictionaries, improvement and coordination of dictionaries, and the principal rules of EXFOR for reactions with charged particles.

As a result of the work of the Meeting an international network was established of Centers and groups participating in the exchange of numerical, bibliographical, and evaluated material on data from reactions with charged particles.

It was decided that the next meeting on the compilation of data from reactions with charged particles would be held in the USSR after tha All-Union Conference on Neutron Physics and the Meeting of Four Neutron Centers in 1977.

The Meeting on Data on the Structure of the Atomic Nucleus and Radioactive Decay was also organized by the Nuclear Data Section of the IAEA and took place in Vienna from May 3 to 7, 1976. The meeting was attended by representatives of Austria, Belgium, the Federal German Republic, Gt. Britain, Holland, Hungary, Italy, Japan, Poland, Rumania, the USA, the USSR, and Sweden. Some of the subjects brought up for discussion were: definition of systems of exchange of nuclear data (bibliographical, numerical, and evaluated) and the format of the exchange, the general rules and terminology (dictionaries, methods of evaluation), the international file of evaluated data on the structure of the nucleus and decay (contents, structure, format, distribution), and international cooperation on data compilation and evaluation.

In the USA the work on the evaluation and compilation of data on the structure of the atomic nucleus and radioactive decay is concentrated in four laboratories (Brookhaven, Berkeley, Oak Ridge, and Idaho) and in the University of Pennsylvania. Work will be done here on all mass chains, except A = 21-44. That chain has been traditionally the domain of the State University of Utrecht (Holland). The United States plans to make a revision of the A-chains once every four years and invites other countries to participate in this so as to make the

Translated from Atomnaya Énergiya, Vol. 41, No. 6, p. 441, December, 1976.

analysis easier for themselves, on the one hand, and, on the other hand, to make the data file international. The US delegation reaffirmed the principle of free exchange of data of all forms.

Before the Vienna meeting, representatives of some West European countries got together to discuss some questions of the compilation and evaluation of nuclear data (April 27, 1976, in Belgium). At their meeting they pointed out the importance of international cooperation in the evaluation of nuclear data.

The Vienna meeting adopted as a recommendation the "Recent References" system of keywords as an international system for the exchange of bibliography on data on nuclear structure and decay. The format of the Oak Ridge Laboratory was recommended as a provisional one for the exchange of numerical and evaluated data.

The next meeting is planned for September or October, 1977. The site was not fixed definitely.

The proceedings of the meeting are in the Center of Data on Nuclear Structure and Nuclear Reactions (Moscow).

IAEA SYMPOSIUM ON THE DESIGN AND EQUIPMENT OF "HOT" LABORATORIES

B. I. Ryabov

Delegations from 32 countries and three international organizations participated in the Symposium which was held Aug. 2-6, 1976, in Finland. A total of 46 papers were presented in four main sections: safety in planning and design; systems of air transfer and purification; critically monitoring, fire protection, and waste handling; radiation protection and administrative measures; operating experience. Primary attention was paid to technical, structural, and organizational measures for increasing radiation safety during work with kilogram quantities of plutonium and with gram quantities of transuranium elements. Interest in these problems has been aroused by extension of fast reactor programs.

Increased radiation safety during work with irradiated fuel with a high plutonium content required additional safety measures. Comparatively few special laboratories are equipped for this purpose; mention was made of only two new facilities being built in Japan and projects for another two in the USA. In other countries, existing facilities are being reconstructed and modernized. Most laboratories for work with irradiated fuel incorporate large "hot" caves (up to 20 m long, 4-6 m wide, 7-10 m high) with a high degree of containment, biological shielding for activities up to 10^6 Ci, dismountable cover, bridge crane inside, and electromechanical manipulators. Besides large hot caves, ordinary-sized ones are used, but with dismountable shielding (or retractable wall) and boxes. Caves and boxes are equipped with critical-mass safety devices, a system for handling the product without affecting the air-tightness, an efficient system for decontaminating the exhaust air, and automatic fire-fighting installations employing liquid carbon dioxide or tetrafluorodibromomethane. Particular attention is paid to fire safety because the products are pyrophoric, which means that the possibility of a fire breaking out cannot be ruled out, and in such an event the filters go out of service and the ejection of a large quantity of activity is unavoidable.

In the United States the mean radiation dose allowed for personnel in "hot" laboratories is 1 rem/yr (0.5 mrem/h), the buildings and equipment are designed to withstand hurricane winds (tornadoes) and seismic activity of up to 9 points, which makes the construction about 10% more expensive but guarantees that dangerous contaminants are not dispersed in the event of natural disasters. When new laboratories are designed and old ones rebuilt, measures are planned for the well-timed shutdown of plants when breakdowns occur, and for the deactivation, dismantling, and evacuation of the equipment.

Much consideration is given to the standardization of the basic equipment and its subassemblies; this is a means not only of cutting the cost of radiation safety but also of increasing it since this makes it possible to

Translated from Atomnaya Énergiya, Vol. 41, No. 6, pp. 442-443, December, 1976.

introduce into practice equipment that is well designed, tried and tested, and therefore reliable. This purpose is also served by the use of high-quality materials. Standardized equipment and subassemblies is manufactured on an industrial scale in France and is sold not only on the home market. Another aspect of increased safety is that of automation of frequently recurring operations, such as analysis of fuel composition, γ spectrometry, and photometry. The operations are carried out using a computer. To automate auxiliary operations, France has developed a new manipulator, the MM-8, with programmed control and feedback, the program being recorded in the computer automatically when the operator makes the required movements manually. A shortcoming of the manipulator is that all the slave motors are inside the cave and this cannot ensure a long period of operation with a high level of γ-ray activity. The air from the α- and γ-contaminated drive mechanisms, shielded by a sheath with forced air, is expelled through a filter.

Stringent requirements are put on the ventilation systems of hot laboratories. Caves and boxes are kept at a vacuum of 25 to 40 mm H_2O (or even more) and the pressure drop between a cave and the repair zone is 6-25 mm H_2O. Most caves and boxes have a vent system for inflow ventilation which maintains the specified parameters of air interchange if the vacuum drops because of a leak (rupture of a glove, broken glass, etc.); in this case an alarm system is actuated and a sound signal is sounded. The inflowing air is purified by filters, and the exhaust from hot caves and boxes is, as a rule, in many stages. ^{131}I is trapped with high-quality carbon filters, designed with a frame compressed by a screw mechanism which ensures uniform density of the powdered carbon. A sophisticated air purification system is used when fuel elements are taken apart. Behind the carbon filters are scrubbing columns which are irrigated with sulfate compounds, mercury nitrates, and other solutions. After purification, the air is treated on filters of diodide or silver nitrate and on a monitoring filter. The coefficient of air purification with such a system is 10^5. It was particularly noted that there are as yet no filters resistant to high temperature (more than 200°C); consequently, in a fire the purification systems cease to function.

Major accidents can be caused by violation of the critical-mass safety. Data were presented at the symposium about the force of the bang in a box during a spontaneous reaction in terms of exploding TNT: with $2 \cdot 10^{17}$ fissions per second the force of the bang is that of 25 g TNT, and at $7 \cdot 10^{18}$ fissions/sec, 1000 g TNT. The most likely minimum accident is with $2 \cdot 10^{17}$ fissions/sec, but even in this case boxes are destroyed. A possible accident is prevented by critical-mass-safety devices as well as the limitation of the quantity of plutonium in the apparatuses. Particular difficulty is presented by the monitoring of critical-mass safety. Under development are new two-stage scintillation detectors which begin operating at the beginning of the reaction and give an alarm signal at a dose of 0.6 R/sec.

Organizational and technical measures enabling safe operating conditions to be maintained in "hot" laboratories found an important place in the discussion. This includes the development of new sanitary regulations, detailed reports by existing enterprises on the safety measures in plants, on a concrete radiation facility, statistics, etc. After considering and approving these reports, the competent state organs give permission to continue operations. Reports are resubmitted if the technology at the plant is altered or if the basic equipment is changed (France). In many countries, permission for work with plutonium is renewed each year with an indication of the maximum quantity allowed the given laboratory. The personnel undergoes the requisite training and should have high qualifications, and the basic equipment is subjected to a prophylactic examination and maintenance at least every 18 months.

Considerable interest was aroused among foreign delegations by the USSR delegation report which presented the main directions taken in solving the safety problems in designing "hot" laboratories and experimental facilities in our country. The symposium proceedings will be published by the IAEA.

SECOND SEMINAR ON COMPUTER SIMULATION OF RADIATION AND OTHER DEFECTS

Yu. V. Trushin

The seminar, which was held in the M. I. Kalinin Polytechnic Institute in Leningrad, June 22-24, 1976, was devoted primarily to radiation defects. The seminar was opened with a review by A. N. Orlov (A. F. Ioffe Physicotechnical Institute, Academy of Sciences of the USSR) who analyzed publications on "Radiation effects and the nuclear power industry" in the light of requirements put upon the material of thermonuclear reactor walls. Computer simulation can be used to solve some problems and in individual cases is as yet the only accessible method of investigation.

A paper by V. Ya. Migalena (Physicotechnical Institute of the Academy of Sciences of the USSR, Kharkov), based on the results of original papers by research teams, presented methods of calculating the spectra of primary knock-on atoms (PKA), taking account of elastic and inelastic nuclear processes during the scattering of nucleons of intermediate energy (up to 50 MeV). At this energy there is a significant anisotropy during scattering of primary particles and, consequently, an attendant anisotropy in the spatial distribution of the PKAs. A set of programs has been created for calculating the energy and spatial characteristics of PKAs during the interaction of protons, neutrons, and heavy ions with an energy of the order of 1 MeV/nucleon with different materials. The elastic scattering cross sections are determined from the optical model; inelastic processes at energies exceeding 10 MeV are described within the framework of the exciton model, taking account of the contribution of the pre-equilibrium and equilibrium components in the nuclear decay. In the interaction of heavy ions, allowance is made for the nuclear charge being screened by electrons. Calculated results were given for spectra of PKAs from protons with an energy of 5-25 MeV and heavy ions for some structural materials. In the case of light elements with $A < 40$, when elastic nuclear scattering is included the total number of PKAs is increased by a factor of 5-10 in comparison with calculations without account for nuclear interactions. Consideration is being given to the possibility of using protons and heavy ions to simulate radiation damage from fast and superfast neutrons.

A paper by V. V. Ogorodnik (Institute of Problems of Materials Science, the Academy of Sciences of the Ukrainian SSR) was devoted to computer simulation of radiation defects by the Vineyard method for binary crystals. The investigations are carried out on the model of the TiC crystal which has NaCl structure. Morse potential was used as the interaction potential. The equilibrium configuration was calculated for an ideal crystal of 125 atoms in the free state (without imposing boundary conditions at the surface). Practically uniform compression of the crystal was achieved under the action of surface tension forces and it amounted to 4%. Similar calculations were carried out for crystals with specified defects (vacancies in metal and carbon sublattices, metal and carbon interstitials). The energy released when a vacancy moves from a center to the surface is 2.4 eV, which in this model can be assumed to be the formation energy of a metal vacancy. Significant displacements in the direction of the vacancies were experienced by nearest-neighbor carbon atoms (up to 0.25 lattice constant). The interstitial atoms take up a dumbbell position in the ⟨111⟩ direction.

In his paper, Yu. R. Kevorkyan (I. V. Kurchatov Institute of Atomic Energy) gave the results of work done by a group of researchers on the simulation of cascades of atomic collisions in α-Fe with allowance for inelastic losses, the interactions of moving atoms with defects formed earlier in the cascade, and annealing for 10^{-7} sec at 300 and 800°K. The displacement efficiency decreases with the PKA energy down to 15 keV. More than 70% of the vacancies are combined into complexes and more than 80% of the interstitials are individual. The annealing at 300°K recombines 90% of the defect pairs, and this rises to 80% at 800°K. Distributions of vacancy clusters were also obtained according to size before and after annealing and some other cascade characteristics.

Translated from Atomnaya Énergiya, Vol. 41, No. 6, pp. 443-444, December, 1976.

L. K. Kuznetsov (N. I. Lobachevskii State University, Gorki) discussed the simulation of different processes occurring in bcc metals (α-Fe, Mo, W). As a result of the calculation of cascades of displacements, it was found that (contrary to Biller's conclusions) their spatial configuration depends on the direction of displacement of the PKAs. The most stable planar clusters of vacancies are those lying in the (110) plane and having the maximum number of bonds of the ⟨111⟩ type, while the bulk clusters are complexes of octahedral form. The formation energy of a planar complex is proportional to the number of vacancies N in the complex, and that of bulk complexes is $N^{2/3}$. The motion of dislocations in a field of randomly distributed obstacles (in the Foreman–Mackean approximation) is due to kinks in dislocation segments. As the stress increases it becomes possible for segments to be stripped from the obstacles. At high stresses disolcations may advance because of bowing of unstable segments. Two models of swelling have been developed on the basis of the diffusion mechanism of pore growth. Helium atoms produced in (n, α) reactions are the pore nuclei. Calculations for stainless steel 304 yielded data about the size distribution of pores and about swelling and also made it possible to evaluate the effect of irradiation conditions on these parameters.

V. V. Kolomytkin (I. V. Kurchatov Institute of Atomic Energy) presented a paper on the simulation of certain mechanisms of radiation creep in the initial stage of reactor irradiation when depleted zones are the most significant obstacles to dislocations. Radiation strengthening of platinum was simulated by taking account of the experimental data, particularly those obtained with an ion projector. Assuming that the surface of the depleted zone, growing during intersection with a dislocation zone, is characterized by a surface energy of γ and that the displacement stress obtained by calculation according to the Foreman–Mackean model is equal to the stress necessary to increase the zone surface, the authors obtained $\gamma = 240$ ergs/cm^2. Two simultaneously operating mechanisms of radiation creep were considered: 1) pinning of glissile edge dislocations by depleted zones; and 2) irradiation-accelerated climbing of dislocations. The inhomogeneity of the long-range dislocation fields is taken into account. The results are equal to experiments for α-Zr.

In their paper, S. I. Zaitsev and É. M. Nadgorny (Institute of Solid State Physics, Academy of Sciences of the USSR) presented the results of simulating the motion of dislocations through point radiation defects and other defects. Studies have been made of the problem of dislocation motion in a plane with randomly distributed immobile obstacles possessing an intrinsic elastic field typical of impurity and radiation defects. An obstacle is simulated by a barrier with Fleischer–Gibbs type of potential with a critical bending angle of 150°. The motion of dislocation is considered as a consequence of instantaneous displacement from one equilibrium position to another after a waiting time. The activation site and the waiting time are found by the Monte Carlo method. The dislocation velocity is found as a function of the stress, temperature, and barrier heights, and the activation energy as a function of the stress. Calculations were carried out for 10^3 to 10^4 obstacles for different forms of area. It was shown that the activation process proceeds in correlated fashion through "weak" angles, and the onset and propagation of quasikinks are important for dislocation motions. At a low temperature and low stress the velocity of a dislocation depends on its length but with more than 100 obstacles per dislocation this dependence vanishes.

In addition to the papers enumerated, the seminar heard eight brief communications on computer simulation of dislocations, dislocation pile-ups, phase boundaries, and microcracks in solids. The seminar was attended by 75 representatives of 21 scientific institutions from ten cities of the USSR.

INTERNATIONAL CONFERENCE ON "ION-EXCHANGE THEORY AND PRACTICE"

V. V. Yakshin

The conference, which was held July 25-30, 1976, in Cambridge, England, was attended by 250 specialists from 26 countries. The considerable advances made in the practical application of ion-exchange processes since the previous conference in 1969 made it necessary to hold this meeting of scientists for an exchange of views.

The conference heard and discussed 41 papers in five principal areas: development of the synthesis of ion-exchange resins (7 papers), ion-exchange equilibrium and kinetics (10), water treatment and purification (10), processes of separation of organic and inorganic materials (5), and the hydrometallurgy of nonferrous, rare-earth, and radioactive elements (9). Thus the main attention was given to investigations on the equilibrium and kinetics of ion exchange, the use of ion-exchange resins in water treatment processes and waste processing, as well as in the hydrometallurgical industry.

Of the papers on the development of the synthesis of ion-exchange resins and the influence of their structure on reactivity, the following should be singled out: "The mechanism of the formation of a polymer network in styrene-divinyl benzol copolymers" (L. Rubinsk and D. Smith, Gt. Britain) and "The effect of resin structure on the mechanical strength of its grains" (L. Gollan and D. Irving, Gt. Britain). The first paper considered the mechanism of formation of a macromolecular skeleton during copolymerization of styrene with commercial divinyl benzol. It was established that in the process of copolymerization of these components there is tangling of chains and nonuniform distribution of side chains. The first polymerization products are enriched in divinyl benzol (compared with the average content of the initial components). However, the nonuniformity of the copolymer structure is obliterated by the tangling and interpenetration of the styrene and divinyl benzol chains. As a result, an extremely compact structure of ion-exchange resins is obtained.

The second paper compared the mechanical properties of ion-exchange resins obtained on the basis of the copolymers of styrene and acrylonitrile with divinyl benzol. It was found that the character and water content of the ion-exchange resin prove to significantly affect the mechanical strength and that helium ion-exchange resins based on styrene and divinyl benzol copolymers are harder than acryl-based resins and therefore split more readily. Macroporous structures are more stable in the osmosis respect, but deform more easily than the helium type. This should be taken into account when choosing the type of resin for practical application.

In the paper "Oxidation disintegration of ion-exchange resins and its prevention," the American specialist L. Goldring presented the results of studying the stability of cation-exchange resins of the sulfostyrene type, disintegrating under the action of hydrogen peroxide and oxygen in the presence of metal ions. Iron and copper prove to be the strongest catalysts of the process of oxidation disintegration of ion-exchange resins. In order to inhibit them, iron and copper are converted into inert complex compounds by the introduction of derivatives of ethylene-diaminotetraacetic acids.

Of the papers on ion-exchange equilibrium and kinetics, those devoted to the study of ion-exchange processes, complicated by complexing in the resin phase and in the solution, and those devoted to the study of multicomponent mixtures on model solutions may be cited as examples. Mention can be made of the communication "The kinetics of the reaction of the propagating layer in ion-exchange resins" (G. Schmukler et al., Israel) where the example of the absorption of hydrogen ions by the sodium form of carboxylsilicate cation-exchange resin is used to consider a model according to which the ion-exchange rate is determined by the velocity of propagation of the saturated layer into the ion-exchange grain. The paper "Investigating slowly diffused particles in ion-exchange resins" (K. Behu et al., Gt. Britain) presented the results of investigations on the kinetics of plutonium (IV) absorption from nitrate solutions on the vinylpyridine ion-exchange resin Ionac XAX 1284.

Translated from Atomnaya Énergiya, Vol. 41, No. 6, pp. 444-445, December, 1976.

The use of ion exchange to recover uranium was the subject of a paper (H. Gardner and R. Coonin, Gt. Britain) which considered the possibility of transition from strong-base anion-exchange resins to the weak-base resin Amberlite XE 229. Notwithstanding the lower capacity for uranium (by 15%), the weakly alkaline anion-exchange resin is more selective and desorbs uranium more readily, thus ensuring that high-quality uranium dioxide is obtained. A successful 4-yr trial operation of a technological flowsheet employing the weak-base anion-exchange resin Amberlite XE 229 confirms the conclusion made by the authors. The use of weak-base anion-exchange resins in the uranium industry was also the subject of the paper by D. Naden and G. Willie (Gt. Britain). On the basis of laboratory experiments and the results of pilot plant operation, the authors came to the conclusion that macroporous anion-exchange resins can be used effectively in apparatus with a liquefied sorbent layer, especially in obtaining high-purity uranium. Further improvement of the apparatus for ion-exchange was considered in a paper by A. Himsley and E. Farkas (Canada). A distinctive feature of anion-exchange equipment is the use of a plate-type contactor in the sorption operation; with an initial concentration of 1 g/liter uranium in the solution this enables the resin to be saturated to 78 g/liter with a discharge of less than 1 mg/liter into the filtrate and an eluate concentration of 35 g/liter uranium.

Two papers pointed to the feasibility of the practical application of ion-exchange processes for extraction and purification of relatively inexpensive nonferrous metals such as copper and nickel. The data of these papers confirm the promise held out by the ion-exchange technology in nonferrous metallurgy.

A feature of the conference were papers on a new area of ion-exchange technology, the use of impregnated polymer materials to separate organic and inorganic compounds. These materials are obtained by introducing liquid complexing agents (extractants) into the resin structure when the polymer matrix is formed or by impregnating the ready polymer base with extractant. A paper by H. Kaukzor and A. Meier (Federal Republic of Germany) described the physicochemical properties of impregnated macroporous styrene-divinyl-benzol copolymers (Levextrel) with tributyl phosphate (TBP) and di-(2-ethyl-hexyl)-phosphoric acid (D2EHPA) and considered the possibility of their being used to recover uranium and plutonium, to separate trace quantities of chromium and indium from concentrated solutions of heavy metals, to separate heavy lanthanides, and to purify them from radioactive contaminants. Levextrel TBP resin was successfully tested under pilot plant conditions. In the opinion of the authors, resins of this type combine the advantage of extractants and sorbents and can be used to extract metals from dense pulps or dilute solutions from the underground leaching of various ores. Other papers on this subject included "Hydrometallurgical applications of resins impregnated with hydroxyomine, hydroxyquinoline, and hydroxamic acid" (F. Vernon, and Ch. Aisles, France) and "Further development of metal extraction with impregnated resins" (A. Warszawski and A. Paczornik, Israel) which discuss various liquid complexing agents and polymer matrices for obtaining impregnated resins and possible ways of using them in hydrometallurgical processes.

The conference devoted considerable attention to ion-exchange treatment of water to remove contaminants of an organic and inorganic nature as well as processes of demineralization in the preparation of water for boilers and high-pressure turbines. At the present time ion-exchange technology has some indisputable advantages over other technological processes, as was convincingly demonstrated by the conference delegates with practical examples.

Among the papers on the application of ion-exchange resins to separate compounds, a communication of unquestionable interest was "Ion-chromatography, principles and applications" (H. Small and D. Salk, USA) which described a new analytic method for the analysis of anions and cations in solutions, a method which is based on ion-exchange principles and employs a solution-conductivity sensor as a detector. At the present time the USA has started manufacture of ion chromatographs which made for easy analysis in solutions of ions of alkali-earth metals, primary, secondary, and tertiary amines and ammonium bases, anions of halides, nitrates, nitrites, iodates, and others, with a sensitivity of 10^{-8}.

The work of the conference showed that ion-exchange processes all find great practical application in the most diverse areas of science and technology such as hydrometallurgy, protection of the environment, analytic chemistry, the atomic industry, water treatment, and separation and purification of organic and inorganic compounds. Further progress in these areas is bound up with the development of new ion-exchange resins, the construction of efficient ion-exchange equipment, and the development of efficient technological processes employing new ion-exchange materials and equipment.

A. M. Petros'yants FROM THE SCIENTIFIC QUEST TO THE ATOMIC INDUSTRY. CONTEMPORARY PROBLEMS OF ATOMIC SCIENCE AND ENGINEERING IN THE USSR*

Reviewed by Yu. I. Koryakin

The fact that the book under review has had three editions within a relatively short time (first edition in 1970, second in 1972) attests to the unflagging interest in it. The "publishing viability" of any scientific book is determined by a number of factors, two of which are perhaps the principal ones: the timeliness of the subject and the author's skill in presenting the material. This book boasts both qualities, and with each edition they have undergone a welcome evolution.

The timeliness of the subject is obvious and is growing continuously and rapidly. Atomic science and engineering of our country have now become one of its major productive forces and considerable intellectual and material resources of the national economy are already involved in this area and are continuing to become involved on an increasing scale with each year. It is precisely in the use of atomic energy that hopes lie for the solution of serious diverse problems of power engineering and technology which, as is known, provide the means for the functioning of the entire national economy.

In recent years, especially in the period covered by the three editions of the book, there has been an enormous qualitative and quantitative growth in the application of atomic energy in our country and elsewhere, and this has been reflected in part in the successive printings.

In speaking of the author's skill, one can scarcely fail to note that in his preface to the first edition he called the material of the book 'sketches of the history of atomic science and engineering.' But this is only one aspect of the style of the presentation. In the first place, to a significant degree the book stems from the author's extensive experience in the utilization of atomic energy (almost from the very beginning) and his knowledge. In the second place, it is more characteristic than previous publications when, naturally, the author wanted above all to share his personal observations and recollections with the reader. But as the range of application of atomic energy in the USSR grew, so did the store of scientific and technical information which the author had and which he wanted to, and indeed had to, take along with him on his "route of publication." And since it is impossible to put everything in a book, the sketch genre faded into the background in successive editions. The retrospective view proved to be subordinate to the view of the present state and the future applications of atomic energy, especially as the very title of the book called for (if not required) precisely such accentuation.

This does not, of course, lead to a question about which approach is preferred: the author has a sufficient mastery of both the methods of science journalism and the subject presented, which is equally important. Nevertheless, it seems that the contents of the latest edition corresponds to the title to a greater extent than the previous editions.

And here we must emphasize that the title "Contemporary Problems...," as in fact follows from the contents of the book, should not be taken literally. Consideration of problems taken to mean tasks, goals, endeavors, or hopes in the domain of the utilization atomic energy, is naturally given due attention. But, as a rule, this follows from the detailed description of the present state of the art or the level reached in scientific and technical development and the scale on which the areas of application of atomic energy have been introduced into the practice of the national economy. Usually these areas are called problems.

*Atomizdat, Moscow (1976).

Translated from Atomnaya Énergiya, Vol. 41, No. 6, pp. 446-447, December, 1976.

The range of problems (in the sense indicated above) elucidated by the author is wide: from fundamental research to what has become ordinary practice. An enumeration would take too much space, and the "assortment" of these areas has already begun to be canonized to a certain degree, especially since the author addresses his book in the main to the wide reading public. And in such a case the author is fully justified in wanting to give the reader only high-quality, verified material, and to avoid turning the book into a receptacle of unverified ideas and assumptions as if they were not enticing and logically founded. The author's reputation prompts necessary discretion with respect to this.

But one danger lurks in such a position by the author. The point is that in describing the areas of application which have developed and especially the research on atomic energy, it is easy to become categorical and to be tempted to "cross the t's and dot the i's." Yet it is known that in science and technology there are unexpected reversals, unforeseen courses of events, and even dead ends. Atomic science and technology are not an exception. And although the author in the main avoided the temptations to be categorical, this is true only in the main since there are some shortcomings in this respect. Speaking of shortcomings, mention should be made, e.g., of cases where the author converses with the reader as if in passing (although the topic requires detailed discussion), but these cases are rare. The shortcomings mentioned should, of course, be regarded as unavoidable in the author's advance and his amazing creative activity and operativeness. In respect of the latter, it is a very good thing, for example, that the edition under review already has information about the use of atomic energy that was reflected in the materials of the 25th Congress of the Communist Party of the Soviet Union. To be sure, the author must share the merit of operativeness with Atomizdat which, incidentally, saw to it that the book was well designed.

V. A. Zuev and V. I. Lomov

PLUTONIUM HEXAFLUORIDE*

Reviewed by N. P. Galkin

In the past two decades considerable progress has been made in the chemistry and technology of plutonium hexafluoride, especially in connection with the development of fluoride methods of regenerating irradiated uranium–plutonium oxide nuclear fuel. Consequently, the publication of this monograph is fully justified.

The monograph systematizes the disconnected information in the literature about methods of obtaining plutonium hexafluoride and its properties, published up to 1973. The monograph consists of six chapters. The introduction describes the history of the discovery of plutonium hexafluoride as well as some of its peculiarities as compared with other known hexafluorides; particular note is taken of the high reactivity of this compound as well as its thermal and radiation instability.

Chapter I presents laboratory methods of obtaining and purifying plutonium hexafluoride, going into a detailed consideration of the kinetics and mechanism of interaction of the various plutonium compounds with fluorine and halogen fluorides (ClF, ClF_3, BrF_3, and BrF_5). The rules for storing and handling plutonium hexafluoride are given.

Chapter II is devoted to the physical properties of plutonium hexafluoride. It gives the most reliable data on the melting point, boiling point, vapor pressure, and triple point of this compound. The known thermodynamic, optical, magnetic, mechanical, and other properties of plutonium hexafluoride are described.

The most interesting chapter, Chapter III, brings together all the known chemical properties of plutonium hexafluoride. The reactions of the hydrolysis of water, and interactions with reducing agents, metal fluorides, and structural materials are considered. The material of Chapters II and III makes it possible to predict the behavior of plutonium at various stages in the process of regeneration of irradiated uranium–plutonium nuclear fuel by fluoride methods.

*Atomizdat, Moscow (1975).

Translated from Atomnaya Énergiya, Vol. 41, No. 6, p. 447, December, 1976.

Chapters IV and V are devoted to the thermal and radiation instability of plutonium hexafluoride. These characteristics have a significant effect on the apparatus design of fluoride methods of fuel regeneration and should be taken into account when designing equipment.

Chapter VI sums up the results of research on the physical and chemical properties of plutonium hexafluoride from the point of view of their possible use in the technology for obtaining and purifying plutonium hexafluoride during processing of irradiated oxide nuclear fuel.

Fluoride methods of regenerating irradiated fuel elements are not yet in practical use. Therefore, the authors of the book confine themselves to describing the promising directions in this domain. They discuss problems of plutonium extraction from irradiated fuel and possible means of purifying it from fission products. Difficulty has been noted in purifying plutonium hexafluoride from ruthenium fluoride.

On the whole, the book under review quite fully reflects the state of research in the domain of the chemistry and technology of plutonium hexafluoride. It is based on the use of contemporary phycicochemical data. Among the virtues of the book is the fact that the authors link up the thermal investigations on the physical and chemical properties of plutonium hexafluoride with the possibility of their practical application in the processing of irradiated fuel.

Unfortunately, the book contains typographical errors and stylistic errors. Regardless of the shortcomings mentioned, the book is of great interest and can undoubtedly be recommended to engineering and scientific workers who specialize in the chemistry and technology of the fluorides of actinides.

INDEX

SOVIET ATOMIC ENERGY

Volumes 40-41, 1976

SOVIET ATOMIC ENERGY

Volumes 40-41, 1976

(A translation of Atomnaya Énergiya)

L

M

N

O

P

R

S

T

U

SOVIET ATOMIC ENERGY

Volumes 40-41, 1976

(A translation of Atomnaya Énergiya)

Volume 40, Number 1 January, 1976

Volume 40, Number 2 February, 1976

Volume 40, Number 3 March, 1976

Volume 40, Number 4 April, 1976

Engl./Russ.

Volume 40, Number 5 May, 1976

Volume 40, Number 6 June, 1976

Volume 41, Number 1 July, 1976

Volume 41, Number 2 August, 1976

DEPOSITED ARTICLES

LETTERS TO THE EDITOR

Volume 41, Number 3 September, 1976

Volume 41, Number 4 October, 1976

Volume 41, Number 5 November, 1976

Volume 41, Number 6 December, 1976

ARTICLES

DEPOSITED ARTICLES

engineering science

continued
from back cover

Title	# of Issues	Subscription Price
Metallurgist *Metallurg*	12	$225.00
Metal Science and Heat Treatment *Metallovedenie i termicheskaya obrabotka metallov*	12	$215.00
Polymer Mechanics *Mekhanika polimerov*	6	$195.00
Problems of Information Transmission *Problemy peredachi informatsii*	4	$175.00
Programming and Computer Software *Programmirovanie*	6	$95.00
Protection of Metals *Zashchita metallov*	6	$195.00
Radiophysics and Quantum Electronics (Formerly Soviet Radiophysics) *Izvestiya VUZ. radiofizika*	12	$225.00
Refractories *Ogneupory*	12	$195.00
Soil Mechanics and Foundation Engineering *Osnovaniya, fundamenty i mekhanika gruntov*	6	$195.00
Soviet Applied Mechanics *Prikladnaya mekhanika*	12	$225.00
Soviet Atomic Energy *Atomnaya energiya*	12 (2 vols./yr. 6 issues ea.)	$235.00
Soviet Journal of Glass Physics and Chemistry *Fizika i khimiya stekla*	6	$ 95.00
Soviet Journal of Nondestructive Testing (Formerly Defectoscopy) *Defektoskopiya*	6	$225.00
Soviet Materials Science *Fiziko-khimicheskaya mekhanika materialov*	6	$195.00
Soviet Microelectronics *Mikroélektronika*	6	$135.00
Soviet Mining Science *Fiziko-tekhnicheskie problemy razrabotki poleznykh iskopaemykh*	6	$225.00
Soviet Powder Metallurgy and Metal Ceramics *Poroshkovaya metallurgiya*	12	$245.00
Strength of Materials *Problemy prochnosti*	12	$295.00
Theoretical Foundations of Chemical Engineering *Teoreticheskie osnovy khimicheskoi tekhnologii*	6	$195.00
Water Resources *Vodnye Resursy*	6	$190.00

SEND FOR YOUR
FREE EXAMINATION COPIES

Plenum Publishing Corporation

Plenum Press • Consultants Bureau
• IFI/Plenum Data Corporation
227 WEST 17th STREET
NEW YORK, N. Y. 10011

United Kingdom: Black Arrow House
2 Chandos Road, London NW10 6NR England

Back volumes are available. For further information, please contact the Publishers.

breaking the language barrier

WITH COVER-TO-COVER ENGLISH TRANSLATIONS OF SOVIET JOURNALS

in engineering science

Title	# of Issues	Subscription Price
Automation and Remote Control *Avtomatika i telemekhanika*	24	$260.00
Biomedical Engineering *Meditsinskaya tekhnika*	6	$195.00
Chemical and Petroleum Engineering *Khimicheskoe i neftyanoe mashinostroenie*	12	$275.00
Chemistry and Technology of Fuels and Oils *Khimiya i tekhnologiya topliv i masel*	12	$275.00
Combustion, Explosion, and Shock Waves *Fizika goreniya i vzryva*	6	$195.00
Cosmic Research (Formerly Artificial Earth Satellites) *Kosmicheskie issledovaniya*	6	$215.00
Cybernetics *Kibernetika*	6	$195.00
Doklady Chemical Technology *Doklady Akademii Nauk SSSR*	2	$65.00
Fibre Chemistry *Khimicheskie volokna*	6	$175.00
Fluid Dynamics *Izvestiya Akademii Nauk SSSR mekhanika zhidkosti i gaza*	6	$225.00
Functional Analysis and Its Applications *Funktsional'nyi analiz i ego prilozheniya*	4	$150.00
Glass and Ceramics *Steklo i keramika*	12	$245.00
High Temperature *Teplofizika vysokikh temperatur*	6	$195.00
Industrial Laboratory *Zavodskaya laboratoriya*	12	$215.00
Inorganic Materials *Izvestiya Akademii Nauk SSSR, Seriya neorganicheskie materialy*	12	$275.00
Instruments and Experimental Techniques *Pribory i tekhnika eksperimenta*	12	$265.00
Journal of Applied Mechanics and Technical Physics *Zhurnal prikladnoi mekhaniki i tekhnicheskoi fiziki*	6	$225.00
Journal of Engineering Physics *Inzhenerno-fizicheskii zhurnal*	12 (2 vols./yr. 6 issues ea.)	$225.00
Magnetohydrodynamics *Magnitnaya gidrodinamika*	4	$175.00
Measurement Techniques *Izmeritel'naya tekhnika*	12	$195.00

SEND FOR YOUR FREE EXAMINATION COPIES

Back volumes are available. For further information, please contact the Publishers.

continued on inside back cover

Declassified and Approved For Release 2013/09/23 : CIA-RDP10-02196R000700080005-5